Deep-Learning Based Optimization Framework for Wireless Powered Communication Networks

by

Aysun Gurur Önalan Köprü

A Dissertation Submitted to the
Graduate School of Sciences and Engineering
in Partial Fulfillment of the Requirements for
the Degree of

Doctor of Philosophy

in

Electrical and Electronics Engineering

KOÇ ÜNİVERSİTESİ

September 6, 2023

Deep-Learning Based Optimization Framework for Wireless Powered Communication Networks

Koç University

Graduate School of Sciences and Engineering

This is to certify that I have examined this copy of a doctoral dissertation by

Aysun Gurur Önalan Köprü

and have found that it is complete and satisfactory in all respects,

and that any and all revisions required by the final

examining committee have been made.

Committee Members:

Prof. Sinem Çöleri

Assoc. Prof. Ertuğrul Başar

Prof. Ceyda Oğuz

Prof. Özgür Gürbüz

Prof. İbrahim Altunbaş

Date:

To my dearest Berkay,

who has been my anchor throughout this journey

ABSTRACT

Deep-Learning Based Optimization Framework for Wireless Powered Communication Networks
Aysun Gurur Önalan Köprü
Doctor of Philosophy in Electrical and Electronics Engineering
September 6, 2023

Net-zero-energy networks enable communication when the connection to the electric grid or changing batteries is not feasible for the information sources by balancing harvested and consumed energy. Radio Frequency Energy Harvesting (RF-EH) is a key enabler for net-zero-energy networks as RF signals are independent from climate conditions, more predictable, and controllable. This thesis focuses on low-complexity resource allocation and optimization for RF-EH networks. In particular, the joint relay selection, scheduling, and power control problem in multiple-source-multiple-relay RF-EH network is formulated with the objective of minimizing the total schedule length and the constraints on data demand, energy causality, and maximum transmit power. The formulated problem is a mixed-integer non-linear problem and proven to be NP-hard. As a solution strategy, a bottom-up approach is followed by starting from a simpler scheduling and power control subproblem, then extending the problem with additional relay selection variables. First, the iterative algorithms for optimal and suboptimal solutions to the problem based on conventional optimization theory techniques are proposed. To address runtime concerns inherent in iterative algorithms, then, this thesis presents a novel approach integrating deep learning methods with established optimization principles. Feed-forward Deep Neural Network (DNN) architectures are presented to solve the scheduling and power control subproblem while leveraging optimality analysis for feature set extension and output layer simplification in the proposed DNN models. The remaining relay selection problem is reformulated as a classification task, successfully addressed through deep learning models, including a feed-forward DNN and two Convolutional Neural Network (CNN) based architectures. This thesis further introduces teacher-student learning, a process that transfers knowledge from a complex teacher network to a simpler student network, for an even lower complexity solution to the relay selection problem. A novel dichotomous-based neural architecture search algorithm designs the student network architecture. The results demonstrate the noteworthy reduction in runtime complexity achieved through deep learning models while maintaining optimality for the solution of resource allocation problems in RF-EH networks.

ÖZETÇE

Enerji Hasadı Yapan Kablosuz Ağlar için Derin Öğrenme Tabanlı Eniyilme
Aysun Gurur Önalan Köprü
Elektrik ve Elektronik Mühendisliği, Doktora
6 Eylül 2023

Net sıfır enerjili haberleşme ağları, elektrik şebekesine bağlanmanın veya batarya değiştirmenin mümkün olmadığı durumlarda toplanan ve tüketilen enerjiyi dengeleyerek haberleşmenin devamını mümkün kılar. Radyo Frekansı Enerji Hasadı (RF-EH), RF sinyallerinin iklim koşullarından bağımsız, daha tahmin edilebilir ve kontrol edilebilir olmasından ötürü net sıfır enerjili haberleşme için tercih edilir.Bu tez, RF-EH ağları için düşük karmaşıklıklı kaynak tahsisi ve optimizasyonuna odaklanmaktadır. Bu tez kapsamında özellikle çoklu-gönderici-çoklu-röle RF-EH ağları için ortak röle seçimi, zamanlama ve güç kontrolü problemi çalışılmıştır. Bu problem veri talebi, enerji korunumu ve maksimum iletim gücü kısıtlamalarını göz önünde bulundurarak, toplam enerji hasatlama süresi ve veri iletim zamanını en aza indirgemeyi hedefler. Formüle edilen problem, karışık tamsayılı lineer olmayan bir problemdir ve NP-zor olduğu kanıtlanmıştır. Çözüm stratejisi olarak, problem basitten karmaşığa doğru ele alınmıştır. Öncelikle, önceden belirlenmiş röle seçimi için zamanlama ve güç kontrolü altproblemi çözülmüş, sonra, probleme ek röle seçimi değişkenleri eklenerek ana problemin çözümüne ulaşılmıştır. Problem çözümü için optimizasyon teorisi tekniklerine dayalı özyinelemeli optimal ve buluşsal algoritmalar önerilir. Bu algoritmaların karmaşıklığı yüksek ve çalışma süreleri uzun olduğundan, derin öğrenme yöntemlerini optimizasyon prensipleriyle entegre eden yeni bir yaklaşım sunulur. İleri beslemeli yapay sinir ağları (YSA) mimarileri, zamanlama ve güç kontrolü altproblemini çözmek için sunulurken, önerilen YSA modellerinde özellik kümesini genişletmek ve çıktı katmanını basitleştirmek için optimalite analizi kullanılır. Röle seçimi problemi, bir sınıflandırma problemi olarak yeniden formüle edilir ve çözümü derin öğrenme modelleri aracılığıyla ele alınır. Röle seçimi problemi için ileri beslemeli bir YSA mimarisi ve evrişimli sinir ağları tabanlı iki mimari önerilir.

Bu tez ayrıca öğretmen-öğrenci öğrenme prensibini röle seçimi problemini daha hızlı çözmek içi kullanmaktadır. Bu prensip daha karmaşık bir öğretmen ağından daha basit bir öğrenci ağına bilgi aktaran bir süreçtir. Öğrenci ağının tasarımı için ikili arama yönetimi kullanışmıştır. Sonuçlar,RF-EH ağlarındaki kaynak tahsisi problemlerinde derin öğrenme modellerinin düşük karmaşıklıkta çözümleri optimalitaden ödün vermeden sunduğunu göstermektedir.

ACKNOWLEDGMENTS

I want to express my heartfelt gratitude to the following individuals whose unwavering support and contributions have been instrumental in completing this Ph.D. thesis.

First and foremost, I extend my most profound appreciation to my advisor, Prof. Sinem Çöleri. Her guidance, expertise, and patience have been invaluable throughout this research journey. I am genuinely thankful for her understanding and support, especially during challenging times when balancing a full-time job with my Ph.D. pursuits. I feel fortunate to have had the opportunity to learn from her wisdom and experience.

I am deeply grateful to Eren Soyak, who has been more of a mentor than a boss to me, for his support and belief in my research journey in industry and academia. His understanding during the most demanding and stressful phases of my Ph.D. research, unwavering trust in my abilities, and constant encouragement during self-doubt have been the pillars of my success. Under his guidance, I not only developed essential skills for industry but also cultivated personal and professional growth, supporting my Ph.D. journey and future research career.

I would like to thank my friend and colleague Elif Dilek Salık for valuable research collaboration in the first years of my Ph.D. I hope we continue to work together, accompanied by her cheerful conversations, for many more years.

I am fortunate to have sincere friends from Lifemote who cheer me up and applaud me. A simple "How are you?" is all you need in stressful times. Special thanks go to Tuğçe Duman, Özge Koyuncu, and Nur Kılıçlı.

I would also like to thank the Graduate School of Sciences and Engineering administrative office, especially Emine Büyükdurmuş, who welcomes me kindly and helps me happily whenever I have a question or problem regarding administrative issues.

I want to express my appreciation to my thesis committee members, Assoc Prof. Ertuğrul Başar, Prof. Ceyda Oğuz, Prof. Özgür Gürbüz, and Prof. İbrahim Altunbaş, for their time and valuable feedback.

I am indebted to my parents for providing the solid education my Ph.D. has been built upon. I also would like to thank my mother for caring for me during busy times, my sister for cheering me up, and my grandparents for praying for my success.

I owe the deepest gratitude to Berkay Köprü, whose tireless support has been the cornerstone of my six-year odyssey toward a Ph.D. In challenging times when I was trying to balance a full-time job with my Ph.D., he ensured my mental and physical well-being, reminding me to eat properly and exercise when my research and job consumed every waking moment. His ability to calm my nerves during moments of overwhelming stress and frustration was a constant source of solace. Together, we embarked on this academic adventure, attending classes, studying for the Ph.D. qualification exam, and engaging in endless, fruitful brainstorming sessions. His insights and ideas improved my work and elevated it to new heights. This thesis is not just a reflection of my own achievement but a testament to the unwavering support, love, and intellectual partnership that Berkay has provided. His belief in me has been the driving force behind my achievement, and for that, I am eternally grateful. I dedicate my thesis to Berkay.

Aysun

September 2023

TABLE OF CONTENTS

LIST OF TABLES

LIST OF FIGURES

Chapter 1

INTRODUCTION

One of the main challenges for today's communication networks is enabling networking operations when connecting to the electric grid or changing batteries is not feasible for the information sources. The solution here would be the key enabler for many use cases, such as massive IoT applications, emergency communication in disaster areas, and in/on-body networks [Viswanathan and Mogensen, 2020, Saif et al., 2021, Akhtar and Rehmani, 2017]. Energy Harvesting (EH) provides sustainable power sources to information sources by enabling them to scavenge energy from their surroundings. Hence, it has drawn significant research attention with the aim of integrating and jointly optimizing wireless networks with renewable energy sources or radiated energy harvesting and establishing performance benchmarks for wireless power and information distribution. Compared to natural energy sources such as vibration and sun, inductive and magnetic coupling, radio frequency energy harvesting (RF-EH) is preferred due to its independence from climate conditions, higher charging range, more predictable and controllable nature of RF signals, and the recent advancements on efficient RF-EH hardware design [Xie et al., 2013, Lu et al., 2015].

RF-EH has broadened the research on energy harvesting network designs as the RF signals can carry both energy and information. In the literature, two main RF-EH network designs are proposed: Simultaneous Information and Power Transfer (SWIPT) [Varshney, 2008, Grover and Sahai, 2010, Zhang and Ho, 2013, Perera et al., 2018], and Wireless Powered Communication Networks (WPCN) [Ju and Zhang, 2014, Liu et al., 2014, Kang et al., 2015, Hadzi-Velkov et al., 2017a]. In SWIPT, information and energy are sent through the same frequency band from a source to a destination. At the destination, a part of the received signal is used to harvest energy, and the remaining is consumed to decode information. In WPCN, a source harvests energy from broadcasted signals by an Access Point (AP) in down-link (DL), and then sends its message to the AP by exerting the harvested energy in up-link (UL).

As the number of sources and connected areas have been increasing, a single AP is not enough to cover and serve the expected high amount of connected devices. Multi-cell RF-EH networks with multiple APs are designed for common and sum throughput maximization in orthogonal frequency division multiplexing (OFDM) [Yu et al., 2019], minimum and sum throughput maximization with load coupling and long-term average interference [He et al., 2019], weighted sum-rate maximization with asynchronous time allocation for EH and IT [Kim et al., 2018].

Relay nodes have been considered in RF-EH networks for further improvement of network performance in terms of efficiency and reliability [Lu et al., 2015]. In conventional networks, relaying is a promising strategy to increase system throughput, network coverage, and energy efficiency by assisting information transmission of source nodes [Nosratinia et al., 2004]. In RF-EH networks, apart from information forwarding, relays can also broadcast more energy to the sources [Mishra et al., 2017, Ammar and Reynolds, 2018]. This requires balancing the trade-off in using relays for energy and information transmission. The three node model, consisting of a source, a relay, and a destination, is widely studied relay based for SWIPT [Nasir et al., 2015, Gu and Aissa, 2015] and WPCNs [Chen et al., 2015, Gu et al., 2015]. SWIPT is extended for relay selection in single-source-multiple-relay networks in [Krikidis, 2014, Gu et al., 2018, Wang et al., 2018, Zhao et al., 2016, Sui et al., 2018] and multiple-source-multiple-relay networks in [Ding et al., 2014]. The relay selection problem for WPCCN is addressed in [Chen et al., 2015]. Numerical results from these studies demonstrate the positive effect of relays on the outage and throughput of RF-EH Networks and compare the performance of various relay selection schemes.

Recently, the line of research on EH networks has been directed to short packet transmissions. Ultra reliable low latency communication (URLLC) aimed by 5G and beyond networks requires short packet length transmissions for which Shannon's channel capacity formulation does not apply. The EH networks, especially in IoT applications, also feature short packets due to their small data payloads, low latency requirements, and limited energy sources for longer IT. Save-then-transmit protocol with short packets is characterized for the cases where there exist single and multiple power beacons [Khan et al., 2017]. [López et al., 2017] derives a closed-form approximation of error probability in short packet transmission as a function of channel uses in WPCNs. This work is extended for WPCCNs with EH relays in [Alcaraz López et al., 2018].

This thesis focuses on the design and optimization of communication protocols for WPCNs. The resulting optimization problems are often mixed-integer non-convex problems for which polynomial-time solutions do not exist. In this thesis, we aim to solve such complex problems with deep learning techniques. Deep Neural Networks (DNNs) are universal function estimators that are successfully used in various application areas such as image classification, speech recognition, and language translation. They promise low-complexity solutions for complex problems. Recently, DNNs have also been considered in wireless communications [Elsayed and Erol-Kantarci, 2019]. They have become promising solutions for complex communication problems, such as channel coding, channel estimation, radio signal classification, etc.

DNNs have also been applied for resource allocation and optimization, which is crucial to ensure guaranteed performance for each user in wireless networks. With supervised training based on the ground truth obtained by optimal and/or other heuristic algorithms, researchers aim to achieve lower-complexity solutions. In [Cui et al., 2018], the scheduling problem over wireless interference links is solved by Convolutional Neural Networks (CNNs), where training input is the geographical locations of the users, and ground truth is obtained by a traditional scheduling algorithm. On the other hand, in unsupervised training approaches, the objective function of the optimization problem is utilized as a loss function of DNNs. researchers aim to achieve better performance with lower complexity by using. In

[Liang et al., 2020], the power control problem is solved by combining DNNs with ensemble learning techniques and utilizing unsupervised learning by directly maximizing the sum rate during training.

Moreover, model-based DNNs aim to benefit from mathematical models that have been developed for years in the wireless communications domain [Zappone et al., 2019]. By merging model-based and data-driven approaches, DNNs are promising tools in resource allocation and optimization, especially when an accurate but intractable theoretical model or tractable but inaccurate theoretical model is available. Energy efficiency maximization problems in multi-user networks, in non-Poisson cellular networks, and in cellular networks with unknown power consumption models are efficiently solved via model-based DNNs.

Inspired by the recent work on applications of DNNs in wireless communications, this thesis proposes a deep learning-based optimization framework for WPCNs.

1.1 Thesis Contributions

In particular, this thesis studies multiple-source-multiple-relay WPCCN, where relays and sources harvest energy from the RF signals broadcast by an AP in downlink for the information transmission from the sources with destination AP in uplink. In the system, each source can use a single relay to convey its message to the AP; whereas a relay can assist more than one source. Throughout this thesis, the system model with linear and non-linear EH models; and finite and infinite packet length regimes are considered.

A novel joint relay selection, scheduling, and power control problem is formulated for multiple-source-multiple-relay WPCCN first time in the literature. The formulated problem is proven to be NP-hard. The problem is first solved by optimization theory techniques. Iterative algorithms for optimal and sub-optimal solutions are proposed based on a bottom-up approach starting from a simpler sub-problem of scheduling and power control, and then, extending the problem with additional relay selection variables.

Since iterative algorithms raise runtime concerns, this thesis proposes deep learning techniques combined with the rules from optimization theory to improve algorithm complexity. First, feed-forward DNN architectures are studied for the low-complexity solution to the scheduling and power control subproblem. Optimality analysis of the problem is utilized to enrich the input features and simplify the output layers of the proposed DNN architectures. Then, the relay selection problem is defined as a classification problem and solved by supervised deep learning models. A feed-forward DNN and two CNN-based architectures are proposed for the solution of the classification problem. To reduce runtime further, teacher-student learning, which transfers knowledge from a complex teacher network to a simple student network, and which is supported by a novel dichotomous-based neural architecture search algorithm, is proposed. This thesis applies teacher-student learning for the first time in the literature in the low-complexity resource allocation and optimization of wireless networks.

The results of this thesis indicate the significant improvement brought by the relay nodes to the performance of the WPCCNs and the significant reduction in runtime complexity without sacrificing optimality provided by deep learning models for the solution of the resource allocation problems in WPCCNs.

1.2 Thesis Structure

This thesis is organized as follows. Chapter 2 presents the novel joint relay selection, scheduling, and power control problem for multiple-source-multiple-relay network and optimization theory-based solution of the problem. Chapter 3 focuses on the scheduling, and power control subproblem and proposes the deep learning-based framework for a low-complexity solution. Chapter 4 extends the scheduling and power control problem for short packet communications and proposes optimization theory and deep learning based solutions. Chapter 5 defines the relay selection problem as a classification problem and designs a feed-forward DNN architecture for the solution. Chapter 6 presents two CNN-based architectures for the relay selection problem, and then, employs teacher-student learning to reduce runtime further by shrinking the CNN architecture. Finally, Chapter 7 concludes this thesis.

Chapter 2

RELAY SELECTION, SCHEDULING, AND POWER CONTROL IN WIRELESS POWERED COOPERATIVE COMMUNICATION NETWORKS

2.1 Introduction

Radio frequency energy harvesting (RF-EH) has drawn significant attention as an alternative to fixed power supplies (e.g. batteries) [Lu et al., 2015]. RF-EH has also broadened the research on energy harvesting network designs as the RF signals can carry both energy and information. In the literature, two main RF-EH network designs are proposed: Simultaneous Information and Power Transfer (SWIPT) [Perera et al., 2018], and Wireless Powered Communication Networks (WPCN) [Kang et al., 2015, Hadzi-Velkov et al., 2017b, Chen et al., 2019, Li et al., 2019]. In SWIPT, information and energy are sent simultaneously from the access point (AP) to multiple network nodes. In WPCN, nodes harvest energy from signals broadcast by the AP in downlink (DL), and then send their message to the AP in uplink (UL) by exerting this harvested energy.

Recently, relay nodes have been considered in RF-EH networks for further improvement of network performance in terms of efficiency and reliability [Lu et al., 2015]. In conventional networks, relaying is a promising strategy to increase system throughput, network coverage and energy efficiency by assisting information transmission of source nodes [Nosratinia et al., 2004]. In RF-EH networks, apart from information forwarding, relays can also broadcast more energy to the sources [Mishra et al., 2017, Ammar and Reynolds, 2018]. This requires balancing the trade-off in the usage of relays for energy and information transmission.

The first widely studied relay based energy harvesting network is the three node model, consisting of a source, a relay and a destination. [Nasir et al., 2015, Gu and Aissa, 2015] consider an EH relay in SWIPT where the source and the destination have an unlimited power source. In these studies, the EH relay uses part of the information signal sent by the source for energy harvesting; while the remaining part of the signal is used to forward information to the destination. In three node WPCN model, which is also referred as Wireless Powered Cooperative Communication Network (WPCCN), both relay and source need to harvest energy [Chen et al., 2015, Gu et al., 2015]. In the DL, AP broadcasts RF signals for energy harvesting at the relay and source. Then, in the first half of the information transmission (IT) period, the source broadcasts the information to the relay, or both the relay and AP. In the second half, the relay conveys the information to the AP. For both SWIPT and WPCCN, average throughput and outage probability of the network are derived under different conditions (e.g. amplify or decode and forward relaying, with/without direct link between source and destination). Numerical results demonstrate the positive effect of relays on the outage and throughput of RF-EH networks.

SWIPT is extended for relay selection in a network containing one source, one destination, and multiple EH relays [Krikidis, 2014, Gu et al., 2018, Wang et al., 2018, Zhao et al., 2016, Sui et al., 2018]. After a relay is selected, simultaneous energy and data transmission is performed as in the three node model. A straightforward approach to the relay selection problem is to choose the relay randomly inside a circular sector with a central angle in direction of the destination [Krikidis, 2014]. The relay selection schemes are also designed based on the remaining energies in relay batteries (for the cases where EH relays are equipped with batteries) [Gu et al., 2018, Wang et al., 2018], or channel state information (CSI) either between source-and-relay, relay-and-destination or both [Zhao et al., 2016, Sui et al., 2018]. Outage probability and average throughput of the networks are analyzed as performance indicator.

The relay selection problem for WPCCN is only addressed in [Chen et al., 2015]. In this work, the network consists of an AP, an EH source, and multiple EH relays.

The first part of a time block is allocated for power transfer from the AP to the source and relays. The remaining is further divided into two equal length slots for IT in which the source first broadcasts the information towards the AP and relays, and then the selected relay amplifies and forwards the signal to the AP. The performance of the aforementioned CSI based relay selection criteria is evaluated in terms of outage probability and throughput for fixed transmission rate. Although the optimal fraction of the time block between EH and IT to maximize throughput is discussed through simulation results, durations of the IT slots were not optimized but assumed equal. However, this optimization can bring significant improvement, especially for time critical network applications, such as real-time surveillance and networked control systems [Sadi and Coleri Ergen, 2014, Hou and Kumar, 2012]. Furthermore, optimization of power control and rate adaption were not studied.

RF-EH networks with multiple source-destination pairs require separate study for the relay selection problem since individually optimum relays do not guarantee the best relay selection for the entire network. To the best of our knowledge, the multiple source relay selection problem is considered only in [Ding et al., 2014] for SWIPT and has not been analyzed for WPCCN in the literature. In SWIPT, relay selection is performed by employing a game theoretic approach, where the sources are competing for the help of relays.

Joint relay selection and resource allocation problem on information transmission is extensively studied in various contexts in the literature. In three node model, rate maximization and power allocation problem under sum power constraints and individual power constraints are studied for orthogonal frequency division multiplexing (OFDM) transmission [Vandendorpe et al., 2009]. In single-source-multiple-relay networks, a relay selection and power allocation scheme is proposed with the aim of balancing the energy usage of the network nodes[Ke et al., 2010]. In multiple-source-multiple-relay networks, a stable matching algorithm is used to solve joint relay selection and energy efficient power allocation problem for multiple-cell non-orthogonal multiple access (NOMA) networks [Baidas et al., 2019]. The solution strategies of these works cannot be applied in WPCCN as the corresponding problems do not consider EH constraints, which change the nature of the problem.

In this paper, we study multiple-source-multiple-relay WPCCN, where relays and sources harvest energy from the RF signals broadcast by an AP for the information transmission from the sources with destination AP, for the first time in the literature. We extend previous studies on single-source-single/multiple-relay WPPCN by formulating the interactions among the sources for relay selection while considering their energy harvesting capabilities. In the system, each source can use a single relay to convey its message to the AP; whereas a relay can assist more than one source. Our goal is to determine the optimal relay selection, power control, and scheduling for energy harvesting and information transmission under perfectly known channel state information (CSI) and linear energy harvesting model assumptions. The major contributions of the paper are listed as follows:

- We consider multiple-source-multiple-relay WPCCN; whereas the earlier work in the literature is limited to the single-source-single/multiple-relay WPCCN.

- A novel optimization problem is formulated for joint relay selection, scheduling and power control. Besides the usual energy and data causality constraints, we include maximum transmission power constraints. The objective is to minimize the duration of the schedule for wireless power transfer and data transmission. The formulated problem is a non-convex mixed integer non-linear problem (MINLP).

- The formulated problem is proven to be NP-hard, so, as a solution strategy, we propose a bottom-up approach starting from a simpler sub-problem of scheduling and power control, then, extending the problem with additional relay selection variables.

- A novel scheduling and power control problem is formulated where the objective is to minimize the schedule length for the energy and data transmission and the constraints concern energy, data, and maximum transmit power requirements. An efficient globally optimum and a faster sub-optimal algorithm are proposed for the solution of the problem. In the optimal algorithm, by proving the convexity of the individual optimal IT lengths of sources with respect to the given EH length, we transform the scheduling and power control problem into a bi-level optimization problem where each subproblem obtains individual IT lengths of single-source networks for a fixed EH length and the master problem performs a bi-section search on optimal EH length. On the other hand, the sub-optimal algorithm computes the IT duration of the sources for a sub-optimal EH length, which is derived based on the optimal solution of single-source network.

- Extending scheduling and power control problem with relay selection variables requires the search over all possible source-relay combinations. We adapt Branch-and-Bound to the solution of our problem so that we propose a globally optimum and two heuristic algorithms. The optimal algorithm systematically searches for relay-source combinations by following the nodes of a BB-tree. A node is pruned if it is not promising to provide better feasible solution than the one obtained at the previous nodes. For pruning decision, problem specific lower and upper bounds are developed based on the mathematical analysis of the problem. The heuristic approaches either limit the number of branches generated from each node or completely remove the branching to obtain solutions in polynomial time. After any relay assignment is completed, the scheduling and power control problem is solved to obtain the schedule length.

- Although the BB-based heuristics operate in polynomial time, their run-time still rapidly increases with the number of the nodes of the WPCCN. For better time complexity, an improvement type heuristic approach is also proposed. The heuristic starts with an initial solution determined by CSI-based relay selection criterion, and then, alters the selected relay for a source in each iteration until there is no improvement in schedule length. To determine the CSI-based criterion, we derive the necessary condition on the relay selection for three node WPCCN, and then, generalize this condition to multiple-source-multiple-relay WPCCN.

- We derive and compare the complexity of the proposed algorithms. Further, we illustrate the superiority of the proposed algorithms to previously proposed conventional harvest-then-cooperate protocol [Chen et al., 2015] in terms of schedule length and run-time for various network sizes and transmit power levels.

The rest of the paper is organized as follows. Section 2.2 describes the system model and assumptions used throughout the paper. In Section 2.3, the joint relay selection, scheduling, and power control problem is formulated. Section 2.4 introduces and solves the sub-problem on scheduling and power control. The BB based optimal and heuristic algorithms are proposed in Sections 2.5 and 2.6, respectively. Section 2.7 provides a relay selection criterion based heuristic algorithm. Section 2.8 presents the simulation results. Finally, Section 2.9 concludes the paper.

2.2 System Model

We consider a WPCCN containing one AP, N sources, denoted by S_i, $i = 1, 2, \ldots, N$, and K decode-and-forward (DF) relays, denoted by R_j, $j = 1, 2, \ldots K$. The AP, all the sources and relays are equipped with a single antenna and operate in the same frequency band. TDMA protocol is used as medium access control protocol. The time is divided into time blocks, which are further divided into 3 time slots for EH, IT of sources, and IT of relays, respectively. In the first time slot, relays and sources harvest energy from the AP during τ_0 amount of time. With the harvested energy, each source communicates directly to the AP, or information is transferred from the source to the relay and then from the relay to the AP. Accordingly, IT time slots are further divided into sub-slots corresponding to each source and relay. Assume that the j^{th} relay is selected by the i^{th} source for cooperation. Then, a sub-slot is allocated for the IT from source S_i to relay R_j with duration $\tau_{S_i}^{R_j}$ and another sub-slot is allocated for the IT from R_j to AP with duration $\tau_{R_j}^{AP}$ for $i =$

$1, 2, \ldots, N$ and $j = 0, 1, 2, \ldots K$, where R_0 refers to AP. If the i^{th} source prefers direct communication with the AP, information transfer is completed in the first IT block in $\tau_{S_i}^{R_0}$ amount of time and $\tau_{R_0}^{AP}$ is obviously zero. In a time block, each source S_i needs to send $D_{S_i} > 0$ amount of data to the AP for $i = 1, 2, \ldots, N$. For IT, each source can use a single relay [Chen et al., 2015, Krikidis, 2014, Wang et al., 2018, Ding et al., 2014]. However, the relays can assist multiple sources and must convey all the information they receive from the sources to the AP.

The AP is assumed to have an unlimited power source. The transmission power of the AP is assumed to be constant and denoted by P_A. The sources and relays do not have any embedded energy supplies so they have to replenish energy from the RF signals broadcast by the AP for IT. They possess rechargeable batteries with low energy storage and high self discharge rate, e.g. super-capacitors [Kaus et al., 2010]. Therefore, the harvested energy cannot be stored for further use. Super-capacitors have a wide variety of applications, in hybrid energy storage systems, automotive industry, wireless sensor networks [Sengupta et al., 2018], thus, the corresponding model is widely used in the literature, e.g. [Kang et al., 2015, Hadzi-Velkov et al., 2017b]. The battery capacity of the sources and relays are assumed to be larger than the maximum amount of energy that can be harvested in a time block[Luo et al., 2016]. Moreover, the relays that are not selected by any of the sources in a time block are assumed to be in sleep state until the end of that time block, so, do not waste energy.

We consider a centralized network architecture where the AP runs all the proposed algorithms. The AP maintains the synchronization of the network and informs the sources and relays about the schedule, relay selection, and power allocation at the beginning of each time block.

Block fading channels are assumed, where the channel gains remain constant during each transmission block but change independently from one block to another. Let h_X^Y and g_X^Y be the channel gains between X and Y for DL and UL, respectively, where $X, Y \in \{AP, S_i, R_j\}$, $i = 1, 2, \ldots, N$ and $j = 1, 2, \ldots K$ (e.g. $h_{AP}^{S_i}$ is the DL channel gain between AP and S_i). All the channel gains are assumed to be known by the AP at the beginning of each time block, similar to the previous works, e.g., [Zhao et al., 2016, Kang et al., 2015, Chen et al., 2019, Li et al., 2019]. With this assumption, we focus on the relay selection, scheduling and power control problem and obtain the performance limits of the investigated network [Chen et al., 2019]. Note that, CSI can be obtained through a training process at the start of each time block, and then, can be fed back to the AP together. Compared to the time and energy cost of the information transmissions, the time and energy spent in the training can be considered negligible for a low mobility network [Li et al., 2019].

We assume that P_A is large enough to ignore AWGN noise component during EH phase and all the sources and relays have constant harvesting efficiency. Thus, the energy harvested at the i^{th} source and j^{th} relay, for $i = 1, \ldots, N$ and $j = 1, \ldots, K$, can be expressed as

$$E_{S_i} = \zeta_{S_i} \tau_0 P_A h_{AP}^{S_i} \text{ and } E_{R_j} = \zeta_{R_j} \tau_0 P_A h_{AP}^{R_j}, \tag{2.1}$$

respectively, where ζ_{S_i} and ζ_{R_j} are the energy harvesting efficiency of S_i and R_j, respectively. This model is valid if the energy harvesting circuit is designed such that the energy harvesting efficiency is flat over desired receive power range [Choi et al., 2018] and is widely used in the literature on energy harvesting networks [Kang et al., 2015, Hadzi-Velkov et al., 2017b, Nasir et al., 2015, Gu and Aissa, 2015, Chen et al., 2015, Gu et al., 2015, Gu et al., 2018, Sui et al., 2018, Li et al., 2019]. In IT phase, we consider continuous power model, which is a commonly used model in the literature [Zhang et al., 2016, Sadi and Coleri Ergen, 2014], so the transmit power takes any value below a maximum level P^{max}. The transmit power is further limited by the amount of the harvested energy given in Eq. (2.1). The required energy for decoding the received message at relays is negligible compared to the energy consumption for IT [Gu and Aissa, 2015]. Thus, $P_{S_i}^{R_j} \leq E_{S_i}/\tau_{S_i}^{R_j}$ and $P_{R_j}^{AP} \leq E_{R_j}/\tau_{R_j}^{AP}$, where $P_{S_i}^{R_j}$ and $P_{R_j}^{AP}$ are the average transmit power of S_i and R_j during IT, respectively. We use continuous transmission rate model and Shannon's channel capacity formula for AWGN channels to determine maximum achievable rate. We ignore interference as all sources and relays use separate time slots for IT. Hence, the instantaneous UL transmission rates $T_{S_i}^{R_j}$ from S_i to R_j and $T_{R_j}^{AP}$ from R_j to AP are given by

$$T_{S_i}^{R_j} = W \log_2 \left(1 + P_{S_i}^{R_j} g_{S_i}^{R_j}/(WN_0)\right), \tag{2.2}$$

$$T_{R_j}^{AP} = W \log_2 \left(1 + P_{R_j}^{AP} g_{R_j}^{AP}/(WN_0)\right). \tag{2.3}$$

2.3 Problem Formulation

We consider a multiple-source-multiple-relay WPCCN, where each source S_i needs to send D_{S_i} amount of data by using its harvested energy with or without help of a relay for $i = 1, \dots, N$. Let b_i^j be the relay selection parameter taking value 1 if the j^{th} relay is selected for the i^{th} source and 0 otherwise, for $i = 1, \dots, N$ and $j = 0, \dots, K$. Then, a joint relay selection, time allocation and power control problem with the objective of total time minimization subject to demand, energy and power constraints is formulated as follows:

$$\min \quad \tau_0 + \sum_{i=1}^{N} \sum_{j=0}^{K} \tau_{S_i}^{R_j} + \sum_{j=1}^{K} \tau_{R_i}^{AP} \tag{2.4a}$$

$$\text{s.t.} \quad \sum_{j=0}^{K} b_i^j = 1, \qquad i = 1, \dots, N, \tag{2.4b}$$

$$P_{S_i}^{R_j} \leq P^{max} b_i^j, \quad i = 1, \dots, N,\ j = 0, \dots, K, \tag{2.4c}$$

$$P_{R_j}^{AP} \leq \min \left\{ P^{max}, P^{max} \sum_{i=1}^{N} b_i^j \right\}, \quad j = 0, \dots, K, \tag{2.4d}$$

$$P_{S_i}^{R_j} \tau_{S_i}^{R_j} \leq \zeta_{S_i} P_A h_{AP}^{S_i} \tau_0, \qquad i = 1, \dots, N, \quad j = 0, \dots, K, \tag{2.4e}$$

$$P_{R_j}^{AP} \tau_{R_j}^{AP} \leq \zeta_{R_j} P_A h_{AP}^{R_j} \tau_0, \qquad j = 1, \dots, K, \tag{2.4f}$$

$$\tau_{S_i}^{R_j} W \log_2 \left(1 + \frac{P_{S_i}^{R_j} g_{S_i}^{R_j}}{WN_0}\right) \geq D_{S_i} b_i^j, \quad i = 1, \dots, N,\ j = 0, \dots, K, \tag{2.4g}$$

$$\tau_{R_j}^{AP} W \log_2 \left(1 + \frac{P_{R_j}^{AP} g_{R_j}^{AP}}{WN_0}\right) \geq \sum_{i=1}^{N} D_{S_i} b_i^j, \quad j = 0, \dots, K, \tag{2.4h}$$

$$\tau_0, \tau_{R_j}^{AP}, P_{R_j}^{AP}, \tau_{S_i}^{R_j}, P_{S_i}^{R_j} \geq 0, \quad i = 1, \ldots, N,$$
$$j = 1, \ldots, K, \tag{2.4i}$$

$$b_i^j \in \{0, 1\}, \quad i = 1, \ldots, N, \ j = 1, \ldots, K. \tag{2.4j}$$

The variables of the optimization problem are τ_0, EH duration; $\tau_{S_i}^{R_j}$, IT duration from the i^{th} source to the j^{th} relay; $\tau_{R_j}^{AP}$, IT duration from the j^{th} relay to the AP; $P_{S_i}^{R_j}$, transmit power of the i^{th} source when it transmits to the j^{th} relay; $P_{R_j}^{AP}$, transmit power of the j^{th} relay when it transmits to the AP; and b_i^j, the relay selection parameter.

The objective of the optimization problem is to minimize the duration of the schedule for energy harvesting and data transmission. Eq. (2.4b) guarantees that one and only one relay is selected for each source. Note that a relay can be chosen for more than one source. Eqs. (2.4c) and (2.4d) determine the maximum allowable transmit power of the sources and relays, respectively. If R_j is not selected for S_i, $P_{S_i}^{R_j}$ is forced to be zero in Eq. (2.4c). If R_j is not selected for any source, then $P_{R_j}^{AP}$ is set to zero by Eq. (2.4d). Eqs. (2.4e) and (2.4f) represent the limit on the transmit power of sources and relays imposed by the harvested energy amount. Demand constraint Eq. (2.4g) requires that each source S_i conveys a certain amount D_{S_i} of data to the AP with/without the help of a relay. Relays need to convey all data they gather from sources. Accordingly, demand requirement of a relay is given in Eq. (2.4h). Lastly, Eq. (2.4i) and (2.4j) represent non-negativity and integrality constraints, respectively.

The described problem is a non-convex MINLP as all equations except Eqs. (2.4b) - (2.4d) are non-linear and Eqs. (2.4e) - (2.4h) are non-convex. Next, we show the NP-hardness of the problem.

2.3.1 NP-Hardness

Theorem 1. *The joint relay selection, time allocation and power control problem in Eq. (2.4) is NP-hard.*

Proof. We reduce the NP-hard minimum Makespan Scheduling Problem (MSP) on identical machines to an instance of Problem (2.4). MSP aims to find an assignment of the N jobs with processing times $t_i, i = 1, \ldots, N$, to K identical machines such that the makespan, which is the time elapsed until all jobs completed, is minimized.

Let us define a problem instance where UL channels gains are equal to each other as DL gains, i.e., $g_X^Y = g$ and $h_X^Y = h$, where $X, Y \in \{AP, S_i, R_j\}, \forall i = 1, \ldots, N,\ j = 0, \ldots, K$. In this condition, the relays become identical. Any relay brings same amount of improvement in IT duration of a source node, which removes the effect of the relay selection on IT durations. As the channel gains are same, the required energy for D_{S_i} amount of data transmission from S_i to R_j is same for any j, i.e., not affected by the relay assignment. However, a relay assisting many sources necessitates more energy for IT which results in longer EH duration. For the minimum EH duration, the data amount forwarded by the relays should be balanced. Consider that D_{S_i} as processing time for $S_i, \forall i, j$ as IT lengths and required energy are directly related to the data amount. Hence, the problem instance turns into an MSP which asks for an assignment of N sources with different data demands D_i to K identical relays such that the maximum of total data amount forwarded by a relay is minimized. Since MSP is NP-hard and reduced to an instance of the problem, Problem (2.4) is NP-hard. $\square$

2.3.2 Solution Strategy

For the solution of Problem (2.4), we first formulate a sub-problem on scheduling and power control for WPCN with multiple source-destination pairs and an AP as energy source, which is the reduced form of the original problem for a given relay selection. A preliminary version of this problem and the solution algorithms has previously appeared in [Salik et al., 2019]. Then, the best relay selection is searched either by BB based techniques or an improvement type heuristic approach.

2.4 Scheduling and Power Control Problem

This section discusses the scheduling and power control problem for WPCN with multiple source-destination pairs. Each source has a destination, which is either the selected relay targeting the AP or the AP if no relay is chosen for that source. Since relays have to convey the information gathered from the sources to the AP, they act like sources. Thus, in this section, the term source covers both the sources and the selected relays, the total number of which is denoted by N.

During τ_0 amount of time, sources harvest energy from the signals broadcast by the AP in DL. Then, the i-th source transmits D_{S_i} amount of data to the corresponding destination during τ_{S_i} amount of time in UL, for $i = 1, 2, \ldots, N$. Accordingly, the scheduling and power control problem is given as follows:

$$\min \quad \tau_0 + \sum_{i=1}^{N} \tau_{S_i} \tag{2.5a}$$

$$\text{s.t.} \quad P_{S_i}\tau_{S_i} \leq \zeta_{S_i} P_A h_{S_i} \tau_0, \quad i = 1, 2, \ldots, N, \tag{2.5b}$$

$$\tau_{S_i} W \log_2\left(1 + \frac{P_{S_i} g_{S_i}}{W N_0}\right) \geq D_{S_i},\ i = 1, 2, \ldots, N, \tag{2.5c}$$

$$P_{S_i} \leq P^{max}, \quad i = 1, 2, \ldots, N, \tag{2.5d}$$

$$\tau_0, \tau_{S_i}, P_{S_i} \geq 0, \quad i = 1, 2, \ldots, N, \tag{2.5e}$$

where h_{S_i} is the DL channel gain between S_i and AP, g_{S_i} is the UL channel gain between S_i and its destination, P_{S_i} is the transmit power of S_i, for $i = 1, \ldots, N$.

Problem (2.5) is a non-convex non-linear optimization problem due to the non-convexity of Eqs. (2.5b) and (2.5c). We first give the optimal solution of the single source scenario. Then, we extend our solution strategy to the multiple-source scenario by modeling the system as multiple single-source networks and designing a bisection search for a mutual EH duration of such networks. Moreover, single source solutions will be used in the sub-optimal algorithm, where optimum EH lengths of each individual source are computed and the maximum of them is set as mutual EH duration.

2.4.1 Single Source

In this subsection, we consider a single source WPCN, i.e., $N = 1$. We first analyze Problem (2.5) without Eq. (2.5d), and then provide the optimal solution by additionally considering Eq. (2.5d) in Theorem 2. When there is a single source in the network, EH duration τ_0 should be adjusted just to meet S_1's power requirement, i.e., Eq. (2.5b) holds with equality. Therefore, we can combine Eqs. (2.5b) and (2.5c) as

$$\tau_{S_1} W \log_2\left(1 + \frac{\zeta_{S_1} P_A h_{S_1} \tau_0 g_{S_1}}{\tau_{S_1} W N_0}\right) \geq D_{S_1}, \tag{2.6}$$

which represents a convex set. Before Theorem 2, we present the following lemmas and definitions that are used in the proof of the theorem.

Lemma 1. *Let us rewrite Eq. (2.6) such that τ_0 is a function of τ_{S_1}, i.e.*

$$\tau_0 \geq V(\tau_{S_1}) \triangleq \frac{\tau_{S_1}}{\gamma_{S_1}}(2^{\frac{D_{S_1}}{W\tau_{S_1}}} - 1), \tag{2.7}$$

where $\gamma_{S_1} = \frac{g_{S_1}\zeta_{S_1} P_A h_{S_1}}{W N_0}$. $V(\tau_{S_1})$ is strictly decreasing with respect to τ_{S_1}.

Proof. We show that the first order derivative of $V(\tau_{S_1})$ is negative to prove the strictly decreasing behavior of $V(\tau_{S_1})$ with respect to τ_{S_1}.

$$\frac{dV(\tau_{S_1})}{d\tau_{S_1}} = \frac{2^{\frac{D_{S_1}}{W\tau_{S_1}}} - 2^{\frac{D_{S_1}}{W\tau_{S_1}}} \frac{D_{S_1}}{W\tau_{S_1}} \ln 2 - 1}{\gamma_{S_1}}. \tag{2.8}$$

As the denominator of Eq. (2.8) is always positive, we need to show that the numerator of Eq. (2.8) is negative. Let us denote $\frac{D_{S_1}}{W\tau_{S_1}}$ by x and the numerator of Eq. (2.8) by $f(x)$. Note that τ_{S_1} is strictly positive so as to serve the strictly positive D_{S_1}, so, $x > 0$. $f(x) = 2^x - 2^x x \ln 2 - 1$ is a decreasing function of x, since $\frac{df(x)}{dx} = -2^x x(ln2)^2 < 0$. $f(x)$ takes its maximum value as x goes to 0, which is $\lim_{x\to 0} f(x) = 0$. Therefore, $f(x) < 0$ for $x > 0$ and, as a result, $\frac{dV(\tau_{S_1})}{d\tau_1} < 0$. □

Lemma 2. *The solution to Problem (2.5) without Eq. (2.5d) is given by*

$$\dot{\tau}_{S_1} = \frac{D\ln(2)}{W\alpha_{S_1}}, \tag{2.9}$$

$$\dot{\tau}_0 = \frac{D\ln(2)}{W\alpha_{S_1}\gamma_{S_1}}\left(2^{\alpha_{S_1}/\ln(2)} - 1\right), \tag{2.10}$$

where $\gamma_{S_1} = \frac{g_{S_1}\zeta_{S_1} P_A h_{S_1}}{W N_0}$, $\alpha_{S_1} = \mathbb{L}_0\left(\frac{\gamma_{S_1}-1}{e}\right) + 1$, and $\mathbb{L}_0(.)$ is the Lambert W-function in 0 branch.

Proof. Let us think of the objective function in the slope-intercept form, e.g., $\tau_0 = -\tau_{S_1} + C_1$, where C_1 is the total transmission time to be minimized. We illustrate the graphical relationship between the curve $V(\tau_{S_1}) = \frac{\tau_{S_1}}{\gamma_{S_1}}(2^{\frac{D_{S_1}}{W\tau_{S_1}}} - 1)$ and the line $\tau_0 = -\tau_{S_1} + C_1$ in Fig. 2.1 (a) The area above the curve $V(\tau_{S_1})$ represents the feasible region. The parallel lines represent the different values of C_1. There are three possible cases: The line intersects with the curve at two points, at one unique point, i.e., tangent line, and does not intersect at all.

The intersection point with the tangent line is the optimal solution of the problem. τ_{S_1} and τ_0 values at this unique tangent point are given by Eqs. (2.9) and (2.10), respectively. For the details of this proof, please refer to [Salik et al., 2019]. □

Definition 1. *$\ddot{\tau}_{S_1}$ and $\ddot{\tau}_0$ are defined as the values of τ_{S_1} and τ_0, respectively, in the solution of the system, when Eqs. (2.5b)-(2.5d) hold with equality. If the equality of Eq. (2.5d), i.e., $P_{S_i} = P^{max}$, is considered in Eqs. (2.5c) and (2.5b), which also hold with equality, $\ddot{\tau}_{S_1}$ and $\ddot{\tau}_0$ are expressed, respectively, by*

$$\ddot{\tau}_{S_1} = \frac{D_{S_1}}{W \log_2\left(1 + \frac{P^{max} g_{S_1}}{W N_0}\right)} \tag{2.11}$$

and

$$\ddot{\tau}_0 = \frac{P^{max} \ddot{\tau}_{S_1}}{\zeta_{S_1} P_A h_{S_1}}. \tag{2.12}$$

Theorem 2. *If the solution $(\dot{\tau}_{S_1}, \dot{\tau}_0)$ given in Eqs. (2.9) and (2.10) satisfies Eq. (2.5d) with $P_{S_1} \leq P^{max}$, i.e., $(\dot{\tau}_{S_1}, \dot{\tau}_0)$ is feasible, it is optimal to Problem (2.5). Otherwise, the optimal solutions are $\ddot{\tau}_{S_1}$ and $\ddot{\tau}_0$ given in Eqs. (2.11) and (2.12), respectively.*

Proof. We prove the theorem by again using the graphical approach. Fig. 2.1 (b) extends the graphical representation in Fig. 2.1 (a) by additionally including the maximum power constraint (2.5d). Two possible realizations of (2.5d) are depicted by orange lines. The feasible region is the intersection of the area above the blue curve and the area below the orange line.

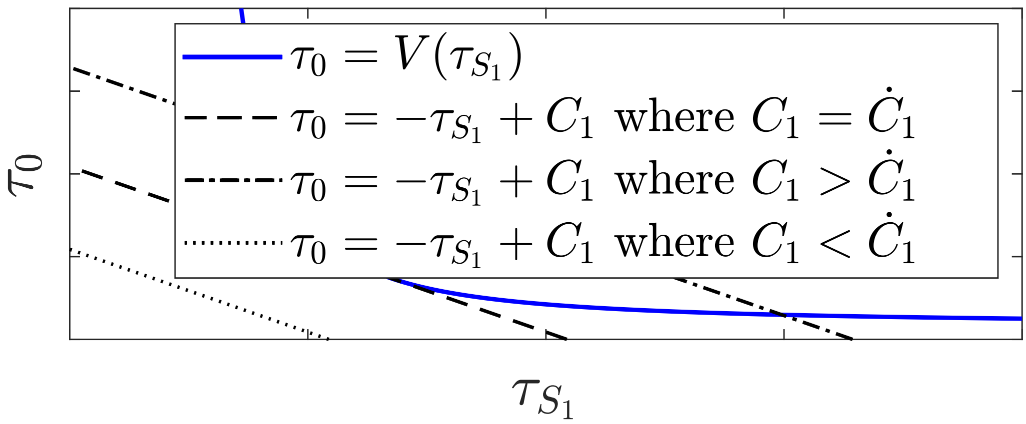

(a)

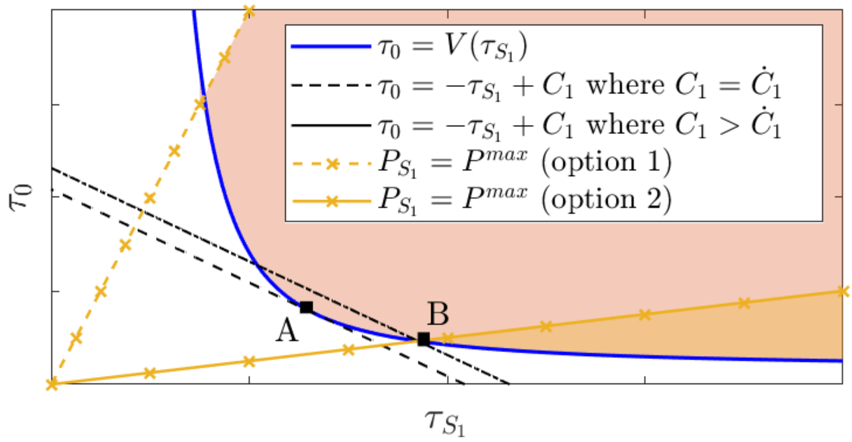

(b)

Figure 2.1: (a) Graphical representation of the constraints given in Eqs. (2.5b) and (2.5c) for single source WPCN. (b) Graphical representation of the constraints given in Eqs. (2.5b), (2.5c), and (2.5d) for single source WPCN.

Let us consider first that Eq. (2.5d) lies as in option 1, where the feasible region is the union of red and orange shaded areas. By Lemma 2, $\dot{\tau}_{S_1}$ and $\dot{\tau}_0$, indicated by point A, minimize the total EH and IT time. Since they also satisfy $P_{S_1} \leq P^{max}$, as seen in Fig. 2.1 (b) , they are optimal.

Now, let us consider that Eq. (2.5d) lies as in option 2, where the feasible region is only the orange shaded area and Point A is not feasible. The optimal solution lies on the boundary of the feasible region [Hillier and Lieberman, 2010] as the problem is convex and the objective is linear. Thus, the intersection of the blue curve and the orange line, point B, minimizes the total schedule length. At point B, the source adjusts its transmit power as $P_{S_1} = P^{max}$, which gives the solution $\ddot{\tau}_{S_1}$ and $\ddot{\tau}_0$ provided in Definition 1. □

2.4.2 Multiple Source

This subsection analyzes a multiple-source WPCN, i.e., $N > 1$. To solve Problem (2.5) optimally for $N > 1$, we transform it into a bi-level optimization problem, in which for a fixed EH duration, the individual IT durations of the sources are solved first, and then, the optimal EH time that minimizes the total schedule length is searched. For the former, we derive the optimal solution for the given EH length; while for the latter, we develop a bi-section search benefiting from the convexity of the total IT times with respect to the EH time. This search obtains a near-optimal solution; and its complexity depends on the gap between the optimal and near-optimal solutions.

In the following, we first give the mathematical foundations of this transformation into bi-level optimization in Section 2.4.2, and then, present the resulting algorithm in Section 2.4.2. Further, a sub-optimal algorithm based on the solution of the single source case is proposed in Section 2.4.2 to obtain solutions with a lower time-complexity.

Bi-level Transformation

This subsection provides the mathematical background on the transformation of Problem (2.5) into bi-level optimization. The idea is to decompose the original problem into smaller sub-problems, which are then coordinated by a master problem. For a fixed τ_0, Problem (2.5) is separable into N *easy* and convex sub-problems regarding each S_i with the aim of minimizing corresponding τ_{S_i}. τ_0 is a variable of master problem and couples the sub-problems. The objective of the master problem is to minimize the sum of τ_0 and the objectives of the sub-problems. The optimal solution to the master problem is optimal for the original Problem (2.5) [Chiang et al., 2007].

We first formulate the sub-problems and derive the solutions with Lemma 3. Theorem 3 proves that the objective of the master problem is a convex function of τ_0, which allows us to apply bi-section search on τ_0 for the optimal solution. For this search, the lower and upper bounds on τ_0 are given by Lemmas 4 and 5.

Sub-problems: All of the sub-problems are in the same reduced form of Problem (2.5) for $N = 1$ and fixed $\tau_0 = \overline{\tau_0}$, which is given as

$$\begin{aligned}
\overline{\tau_{S_1}}(\overline{\tau_0}) = \min \quad & \tau_{S_1} && (2.13a)\\
\text{s.t.} \quad & P_{S_1}\tau_{S_1} \leq \zeta_{S_1} P_A h_{S_1} \overline{\tau_0}, && (2.13b)\\
& \tau_{S_1} W \log_2\left(1 + \frac{P_{S_1} g_{S_1}}{W N_0}\right) \geq D_{S_1}, && (2.13c)\\
& P_{S_1} \leq P^{max}, && (2.13d)\\
& \tau_{S_1}, P_{S_1} \geq 0, && (2.13e)
\end{aligned}$$

where $\overline{\tau_{S_1}}(\overline{\tau_0})$ represents the optimal solution. Problem (2.13) is non-convex due to the non-convexity of Eqs. (2.13b) and (2.13c).

Lemma 3. *The optimal solution to Problem (2.13) is obtained as follows. For $\overline{\tau_0} > \ddot{\tau}_0$, where $\ddot{\tau}_0$ is obtained by Eq. (2.12), the optimal IT duration $\overline{\tau_{S_1}} = \ddot{\tau}_{S_1}$, given by Eq. (2.11). Otherwise, $\overline{\tau_{S_1}}$ is derived as a solution of the nonlinear equation*

$$\overline{\tau_0} = V(\overline{\tau_{S_1}}) = \frac{\overline{\tau_{S_1}}}{\gamma_{S_1}}\left(2^{\frac{D}{W\overline{\tau_{S_1}}}} - 1\right). \tag{2.14}$$

Proof. To prove the lemma, we first derive an equivalent convex formulation of Problem (2.13), then, solve the resulting problem via a graphical approach.

For the convex reformulation, let us define η as the ratio of the consumed energy in UL to the harvested energy in DL. By using η, we can rewrite Eq. (2.13b) as $P_{S_1}\tau_{S_1} = \eta\zeta_{S_1} P_A h_{S_1}\overline{\tau_0}$ and combine it with Eq. (2.13c) as

$$\tau_{S_1} W \log_2\left(1 + \frac{\eta\zeta_{S_1} P_A h_{S_1}\overline{\tau_0} g_{S_1}}{\tau_{S_1} W N_0}\right) \geq D_{S_1}. \tag{2.15}$$

Hence, equivalently, we solve the problem with objective Eq. (2.13a) and constraints Eqs. (2.15), (2.13d), and (2.13e). Note that Eq. (2.15) represents a convex

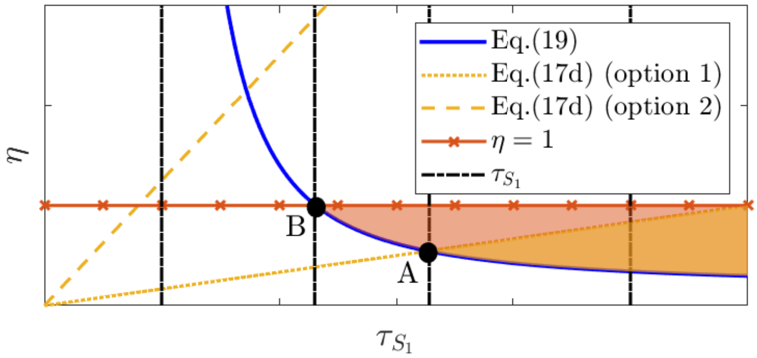

Figure 2.2: Graphical representation of the feasible region for Problem (2.13).

set for fixed $\overline{\tau_0}$. Moreover, the objective function, Eq. (2.13a), and Eqs. (2.13d)-(2.13e) are linear. Therefore, Problem (2.13) turns into a non-linear convex problem.

Fig. 2.2 indicates the feasible region for the problem with the possible values of the objective function τ_{S_1} (black vertical dotted lines). The blue solid curve represents the left-hand side of the demand constraint Eq. (2.15) for fixed D_{S_1} and varying η and τ_{S_1}. To satisfy the minimum demand amount D_{S_1}, the solution must lie above the curve. On the other hand, due to the energy causality constraint $\eta \leq 1$, a feasible solution must be under the red horizontal dotted line. Depending on maximum UL power constraint Eq. (2.13d) (two possibilities are indicated with orange lines) feasible region is either orange area, or both orange and red areas.

In Fig. 2.2, we observe that the feasible region is intersected by $\tau_{S_1} = c$, where c is a constant, with minimum c at either Point A or B depending on Eq. (2.13d). The optimal solution is at Point A, the intersection of Eqs. (2.13d) and (2.15), if the feasible region is restricted by Eq. (2.13d) (option 1). By Definition 1, at Point A, where the source transmits at P_{max}, the transmission necessitates $\ddot{\tau}_{S_1}$ amount of IT and $\ddot{\tau}_0$ amount of EH duration. Even though $\tau_0 > \ddot{\tau}_0$, the source transmits at P_{max} by exhausting only a part of the harvested energy to satisfy the constraint Eq. (2.13d).

When τ_0 is set to a value that the source cannot harvest enough energy to transmit at P_{max}, i.e., $\tau_0 < \ddot{\tau}_0$, Eq. (2.13d) does not affect the feasible region (option

2). The region is bounded by $\eta = 1$, where the source uses all the harvested energy for D_{S_1} amount of data transmission. The optimal solution can be derived by solving Eq. (2.15) for $\eta = 1$ at equality, which results in the solution of Eq. (2.14). □

Master Problem: After finding an expression for the individual IT times of the sources for fixed EH length, we now prove that the objective of the master problem, i.e., the total EH and derived IT durations, is convex over EH time, which allows us to search the optimal EH time with bisection method.

Theorem 3. *Let $g(\overline{\tau_0})$ be the objective function of the master problem, i.e., $g(\overline{\tau_0}) = \overline{\tau_0} + \sum_i \overline{\tau_{S_i}}(\overline{\tau_0})$. $g(\overline{\tau_0})$ is convex over $\overline{\tau_0}$.*

Proof. We show that $\overline{\tau_{S_1}}(\overline{\tau_0})$ is convex. Then, $g(\overline{\tau_0})$ is also convex since $\overline{\tau_{S_i}}(\overline{\tau_0})$'s are all in the same form and the convexity is closed under sum. To prove the convexity of the $\overline{\tau_{S_1}}(\overline{\tau_0})$, we showed in [Salik et al., 2019] that (a) $\overline{\tau_{S_1}}(\overline{\tau_0})$ is proper, i.e., the domain of the function denoted by $dom\overline{\tau_{S_1}}$ is not empty, (b) $dom\overline{\tau_{S_1}}$ is convex and (c) $\overline{\tau_{S_1}}(\overline{\tau_0})$ is sub-differentiable at every $\overline{\tau_0} \in dom\overline{\tau_{S_1}}$. Then, by Theorem 2.4.1(iii) in [Zalinescu, 2002], $\overline{\tau_{S_1}}(\overline{\tau_0})$ is convex. □

Lemma 4. *Let $\{\hat{\tau}_0^i, \hat{\tau}_{S_i}\}$ denote the solution pair of the single source problem corresponding to S_i by Theorem 2, for $i = 1, \ldots, N$. $\max_{i=1,\ldots,N} \hat{\tau}_0^i$ gives a lower bound for the optimum τ_0 of Problem (2.5).*

Proof. To prove the statement, we discuss that further decrease of τ_0 below the value of $\max_{i=1,\ldots,N} \hat{\tau}_0^i$ would increase the total schedule length, i.e., $\tau_0 + \sum_{i=1}^{N} \tau_{S_i}(\tau_0)$. Note that by Lemma 1, τ_0 is a decreasing function of τ_{S_i}. Then, by inverse function theorem [Trench, 2013], $\tau_{S_i}(\tau_0)$ is a decreasing function of τ_0. Suppose $\hat{\tau}_0^1 \geq \hat{\tau}_0^i, \forall i, i \neq 1$. Let us set τ_0 to $\hat{\tau}_0^1$. The pair of $\{\hat{\tau}_0^1, \hat{\tau}_{S_1}\}$ minimizes $\tau_0 + \tau_{S_1}(\tau_0)$ by Theorem 2. Since $\hat{\tau}_0^1 \geq \hat{\tau}_0^i$ and $\tau_{S_i}(\tau_0)$ is decreasing function of τ_0; picking $\tau_0 < \hat{\tau}_0^1$ would increase the term $\tau_0 + \tau_{S_1}(\tau_0)$ (by definition) and $\tau_{S_i}(\tau_0), \forall i, i \neq 1$ (as $\tau_{S_i}(\hat{\tau}_0^1) \leq \hat{\tau}_{S_i} = \tau_{S_i}(\hat{\tau}_0^i), \forall i$). Hence, the total schedule length increases if $\tau_0 < \hat{\tau}_0^1$. If $\tau_0 > \hat{\tau}_0^1$, despite the increase in the term $\tau_0 + \tau_{S_1}(\tau_0)$, τ_{S_i} decreases for $\forall i, i \neq 1$, which may result in a decrease of the total schedule length. Hence, $\max_{i=1,\ldots,N} \hat{\tau}_0^i$ gives a lower bound on the optimal value of τ_0. □

Lemma 5. *Let $\ddot{\tau}_0^i$ be the solution of single source network when Eqs. (2.5b)-(2.5d) hold with equality with the only source S_i, for $i = 1, \ldots, N$. Define $\ddot{\tau}_0^{max} = \max_{i \in \{1,\ldots,N\}}\{\ddot{\tau}_0^i\}$. Then, $\ddot{\tau}_0^{max}$ is the upper bound for the optimum τ_0 of Problem (2.5).*

Proof. When $\overline{\tau_0} > \ddot{\tau}_0^i$, τ_{S_i} is constant for all i, i.e., $\tau_{S_i} = \ddot{\tau}_{S_i}$, by Lemma 3. Then, further increase of $\overline{\tau_0}$ greater than $\ddot{\tau}_0^{max}$ does not improve τ_{S_i} for any i. Since the objective function is minimizing total EH and IT times $\tau_0 + \sum_i \tau_{S_i}$, $\ddot{\tau}_0^{max}$ gives the upper bound on the optimal τ_0. □

Optimal Algorithm

Algorithm 1 Power Constrained Multiple User Time Minimization Algorithm (POWMU)

1: **Input:** P^{max}, P_A, h_{S_i}, ζ_{S_i}, D_{S_i}, for $i = 1, \ldots, N$
2: **Output:** $\overline{\tau_0}$, $\overline{\tau_{S_i}}(\overline{\tau_0})$, $g(\overline{\tau_0})$, P_{S_i} for $i = 1, \ldots, N$
3: **for all** $i = 1, \ldots, N$ **do**
4: Compute $\dot{\tau}_{S_i}$ and $\dot{\tau}_0^i$ by Eqs. (2.9) and (2.10) for source S_i.
5: Compute $\ddot{\tau}_0^i$ by Eq. (2.12) for source S_i.
6: **if** $\zeta_{S_i} P_A h_{S_i} \dot{\tau}_0^i / \dot{\tau}_{S_i} \le P^{max}$, **then** $\hat{\tau}_0^i \leftarrow \dot{\tau}_0^i$;
7: **else** $\hat{\tau}_0^i \leftarrow \ddot{\tau}_0^i$.
8: $lb \leftarrow \max_{i \in \{1,\ldots,N\}} \hat{\tau}_0^i$
9: $ub \leftarrow \max_{i \in \{1,\ldots,N\}} \ddot{\tau}_0^i$
10: **while** $ub - lb > 2\epsilon$ **do**
11: $\tau_0^{'} = \frac{lb+ub}{2}$
12: **if** $\frac{dg(\overline{\tau_0})}{d(\overline{\tau_0})}|_{\overline{\tau_0}=\tau_0^{'}} \ge 0$, **then** $ub \leftarrow \tau_0^{'}$.
13: **if** $\frac{dg(\overline{\tau_0})}{d(\overline{\tau_0})}|_{\overline{\tau_0}=\tau_0^{'}} \le 0$, **then** $lb \leftarrow \tau_0^{'}$.
14: Evaluate and return P_{S_i}, $\overline{\tau_{S_i}}(\overline{\tau_0})$, $g(\overline{\tau_0})$ where $\overline{\tau_0} = \tau_0^{'}$ for $i = 1, \ldots, N$

Based on the bi-level transformation, POWMU, given in Algorithm 1, obtains the globally optimal solution as follows. The for loop (Lines 3-7) computes $\hat{\tau}_0^i$ and $\ddot{\tau}_0^i$ for all $i = 1, \ldots, N$ by following Theorem 2 and Definition 1, respectively. Then, the lower (lb) and upper (ub) bounds on τ_0 are set as maximum of $\hat{\tau}_0^i$'s and $\ddot{\tau}_0^i$'s based on Lemmas 4 and 5, respectively (Lines 8-9). The algorithm continues with the bisection search on τ_0 based on Lemma 3 and Theorem 3. In each iteration, the current solution, $\tau_0^{'}$, is set to the mean of the lb and ub (Line 11). If the first derivative of $g(\overline{\tau_0})$ calculated at $\tau_0^{'}$ is non-negative, meaning that the function increases at that point, then the ub is set to $\tau_0^{'}$ (Line 12). If the derivative is non-positive, the function is decreasing at that point, the lb is set to $\tau_0^{'}$ (Line 13). Note that if the derivative is 0, which means the optimal solution is found, both ub and lb are set to $\tau_0^{'}$, so, the algorithm terminates. This procedure continues until the difference between ub and lb is lower than 2ϵ, where $\epsilon > 0$ is a small constant determining the accuracy of the solution (Line 10). The last computed $\tau_0^{'}$ is set as the optimal EH time and the objective of the master problem, $g(\overline{\tau_0})$, and power allocation P_{S_i} for $i = 1, \ldots, N$, are evaluated at $\tau_0^{'}$ and returned (line 14).

Remark 1. *Given the initial lb and ub, by bisection search method, to obtain an optimal solution in the error bound, ϵ, the number of iterations, k, should be at least as large as $log_2(\frac{ub-lb}{\epsilon})$ [Salik et al., 2019]. The smaller the chosen ϵ value, the better the accuracy of the solution by POWMU but at the cost of higher number iterations, so, complexity.*

The overall complexity of POWMU is $\mathcal{O}(Nlog_2(\frac{ub-lb}{\epsilon}))$, with the derivative calculations, $\mathcal{O}(N)$, at each iteration and by Remark 1.

Algorithm 2 MAX-EH

1: **Input:** P^{max}, P_A, h_{S_i}, ζ_{S_i}, D_{S_i}, for $i = 1, \ldots, N$

2: **Output:** $\hat{\tau}_0^{max}$, τ_{S_i}, $\hat{\tau}_0^{max} + \sum_{i=1}^{N} \tau_{S_i}$, P_{S_i} for $i = 1, \ldots, N$

3: **for all** $i = 1, \ldots, N$ **do**

4: Compute $\dot{\tau}_{S_i}$ and $\dot{\tau}_0^i$ by Eqs. (2.9) and (2.10) for source S_i.

5: Compute $\ddot{\tau}_0^i$ by Eq. (2.12) for source S_i.

6: **if** $\zeta_{S_i} P_A h_{S_i} \dot{\tau}_0^i / \dot{\tau}_{S_i} \leq P_{max}$, **then** $\hat{\tau}_0^i \leftarrow \dot{\tau}_0^i$;

7: **else** $\hat{\tau}_0^i \leftarrow \ddot{\tau}_0^i$.

8: $\hat{\tau}_0^{max} = \max_{i=1,\ldots,N}\{\hat{\tau}_0^i\}$

9: **for all** $i = 1, \ldots, N$ **do**

10: **if** $\max_{i=1,\ldots,N}\{\hat{\tau}_0^i\} > \ddot{\tau}_0^i$, **then** $\tau_{S_i} \leftarrow \ddot{\tau}_{S_i}$ by Eq. (2.11)

11: **else** Obtain τ_{S_i} by Eq. (2.14).

12: Compute and return: $\hat{\tau}_0^{max} + \sum_{i=1}^{N} \tau_{S_i}$ and P_{S_i} for $i = 1, \ldots, N$.

Sub-optimal Algorithm

In this subsection, we present a sub-optimal algorithm to obtain solutions in lower time-complexity. The sub-optimal algorithm MAX-EH, given in Algorithm 2, provides a solution to the multiple source problem by exploiting the optimality conditions of single source network. After individual optimum schedule lengths of the sources are obtained, the EH duration of the entire network is set to the maximum of the individual EH durations.

The algorithm is described as follows. Individual optimal EH length of each source S_i, expressed as $\hat{\tau}_0^i$, is calculated by Theorem 2 (Lines 3-7). Maximum of these solutions, denoted by $\hat{\tau}_0^{max}$, is computed (Line 8). Then, IT durations, τ_{S_i}, for fixed $\tau_0 = \hat{\tau}_0^{max}$, are obtained for all i by following Lemma 3 (Lines 9-11). The objective function value, i.e., $\hat{\tau}_0^{max} + \sum_{i=1}^{N} \tau_{S_i}$, and power allocations P_{S_i}, for $i = 1, \ldots, N$, are computed and returned (Line 12).

The time complexity of the algorithm is $\mathcal{O}(N)$ as obtaining $\hat{\tau}_0^i$s and finding the maximum require N iterations.

Remark 2. *The solution obtained by MAX-EH provides a tight upper bound on the*

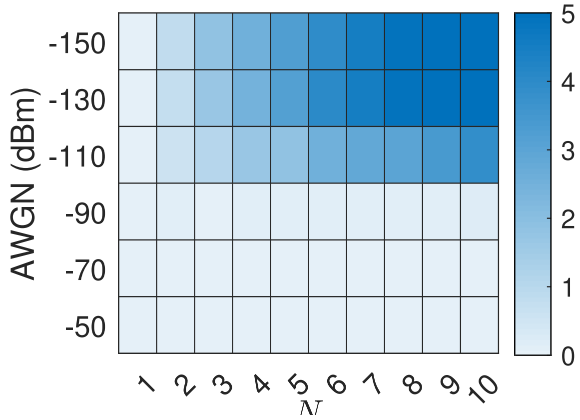

Figure 2.3: Optimality gap (%) of MAH-EH for varying number of sources (N) and AWGN power spectral density (N_0)

optimal solution of Problem (2.5) for moderate and high AWGN levels. We show the tightness of this upper bound by numerical simulations. The detailed simulation parameters are given in Section 2.8. The optimality gap of the algorithm, versus varying number of sources (N) and AWGN spectral density (N_0), is depicted in Fig. 2.3. In general, the gap is lower than 5%; whereas it is lower for the small number of sources and 0 for single source network. For $N_0 \geq -90$ dBm, moderate and high noise level, the optimality gap is lower than 0.2%. This is because the prolonged IT durations due to the higher noise level become dominant in the total schedule length.

2.5 Branch and Bound Based Algorithm

In this section, we develop a Branch-and-Bound based Algorithm (BBA) for the globally optimal solution of Problem (2.4). Branch-and-Bound (BB) is a tree based search algorithm and BB based techniques are commonly used for the solution of non-convex MINLPs [Belotti et al., 2012]. They systematically explore the solution space by dividing it into smaller sub-spaces, i.e., branching. The entire solution space is represented by the root of the BB-tree and each resulting sub-space after partitioning is represented by a BB-tree node. Before creating new branches, the current BB-tree node is checked against lower and upper bounds on the optimal solution and is discarded if a better solution than the incumbent solution cannot be obtained, i.e, pruning. We adapt BB for our problem by developing problem specific lower and upper bound generation methods and integrating it with POWMU.

BBA starts with the MINLP formulation given in Problem (2.4). The relaxation of the problem is obtained and solved. If b_i^js in the solution of the relaxed problem are fractional, BBA continues with branching. A source is selected by $i' = \arg\max_{i,j,i\in\{1,\ldots,N\},j\in\{0,\ldots,K\}} b_i^j$. Then, branching is performed by assigning one of the relays $R_j, j = 0, \ldots, K$ to the i'^{th} source at each new branch. As a result, $K+1$ new nodes are created, where each new node corresponds to the j^{th}, $j = 0, \ldots, K$, relay selected for the i'^{th} source. This selection is forced by setting $b_{i'}^j$ to 1 if the j^{th} relay is selected, and 0 otherwise. It is possible to continue branching on other variables, but, this is not necessary as after relays are selected, the problem can be solved by POWMU.

During the BB-search, the solution of the relaxed problem is used in the branching decision and the objective value of the relaxed problem is considered as a lower bound on the objective of the original problem. We derive the relaxed problem and the lower bound of Problem (2.4) in Section 2.5.1. Moreover, an incumbent solution is stored. To update the incumbent solution, in each node to be branched, an upper bound is calculated. The upper bound can be any feasible solution in the sub-space. If the upper bound of a node is lower than the incumbent, then it is set as the incumbent. We present the upper bound generation for Problem (2.4) in Section 2.5.2.

A BB-tree node is pruned, if the further search of the corresponding sub-space is not necessary. We prune a node if a feasible solution cannot be found at that node; the lower bound of the node is greater than the incumbent solution, as the node cannot provide a better solution than the current one; or all b_i^js of the solution are integers, as we call POWMU to obtain the minimum schedule length for the determined relay selection, and this is the optimum solution in the corresponding sub-space. The algorithm continues until all BB-nodes are pruned.

2.5.1 Lower Bound Generation

A convex relaxation of the sub-problem is solved to optimality to find a lower bound on the objective. The relaxation of Problem (2.4) is obtained as follows. The integrality constraint Eq. (2.4j) of Problem (2.4) is relaxed as $0 \leq b_i^j \leq 1$. This relaxation allows b_i^j to take fractional values for $i = 1, \ldots, N$ and $j = 0, \ldots, K$. In Problem (2.4), $P_{S_i}^{R_j} \tau_{S_i}^{R_j}$ and $P_{R_j}^{AP} \tau_{R_j}^{AP}$ are replaced by new variables $A_{S_i}^{R_j}$ and $A_{R_j}^{AP}$, respectively, so that constraints (2.4e)-(2.4h) represent convex sets. After the replacement, Eqs. (2.4c) and (2.4d) include a product of two variables (e.g., $b_i^j \tau_{S_i}^{R_j}$ and $b_i^j \tau_{R_j}^{AP}$), which causes the non-convexity. Instead of these products, we define their convex/concave envelopes, lower and upper bounding constraints, which is a common relaxation technique proposed in [Belotti et al., 2012]. Now, the relaxed problem can be solved by a convex optimization tool, e.g., CVX [Grant and Boyd, 2014].

2.5.2 Upper Bound Generation

For each node, any feasible solution to the problem in the corresponding sub-space can be an upper bound. The initial upper bound, also the initial incumbent solution, is obtained by assigning all sources directly to AP, which is the simplest feasible solution. In other BB-tree nodes, we obtain the upper bound as follows. The relaxed problem is already solved for lower bound generation and the resulting b_i^js are known. For each source S_i, the relay with the maximum b_i^j is selected, i.e., $R_j = \arg\max_{j \in \{0,1,\ldots,K\}} b_i^j,\ i = 1, \ldots, N$. Then, POWMU acquires a feasible solution resulting in the minimum schedule length for the determined relay selection.

2.6 Branch-and-Bound Based Heuristics

BBA searches for all possible relay selection options, K^N nodes, in the worst case, which results in an exponential run-time. BBA generates the lower and upper bounds by solving the relaxed problem and using POWMU, respectively. The complexity of solving the relaxed problem depends on the solver and is ambiguous. It is highly dependent on the number of variables, so rapidly increases with increasing number of sources or relays. Let us denote this complexity with $\mathcal{O}(C)$. The complexity of POWMU is $(N+K)log_2(\frac{ub-lb}{\epsilon})$ as given in Section 2.4.2. Then, the worst case complexity of BBA is $\mathcal{O}((K^N(C+(N+K)log_2(\frac{ub-lb}{\epsilon})))$. We now propose the BB-based heuristic algorithms for better time complexity.

One Branch Heuristic (OBH)

OBH explores only one branch of the Branch-and-Bound tree. It starts by obtaining the relaxation of Problem (2.4), as described in Section 2.5.1. The relaxed problem is solved to obtain initial fractional values of b_i^js. Among the fractional b_i^js, the maximum one is selected and it is forced to be 1 in the next iteration. OBH repeatedly solves the relaxed problem containing b_i^j values set to 1 in the previous iterations, finds the maximum of the fractional b_i^j in the optimal solution of the resulting problem and forces it to be 1. This continues until the relay selection of all the source nodes. Finally, POWMU provides the solution for the resulting relay selection.

In OBH, $N-1$ relaxed problems are solved and POWMU is called only once. Thus, the overall complexity is $\mathcal{O}((N-1)C+(N+K)log_2(\frac{ub-lb}{\epsilon}))$.

Relaxed Problem Based Heuristic (RPH)

RPH considers only the relaxed problem and does not perform branching. It obtains and solves the relaxation of Problem (2.4) as in Section 2.5.1. This solution gives fractional b_i^j values. Then, the relay R_j with $\max_{j\in\{0,\ldots,K\}} b_i^j$ is assigned to each source S_i, for $i=1,\ldots,N$. After relay selection, the total EH and IT times is obtained by POWMU. Note that this is the same approach that we use to determine upper bounds of each node in BBA.

RPH solves only one relaxed problem and calls POWMU once. The overall complexity is $\mathcal{O}(C+(N+K)log_2(\frac{ub-lb}{\epsilon}))$.

2.7 Relay Criterion Based Heuristic Algorithm

The ultimate aim of this section is to propose a heuristic algorithm of lower complexity for the solution of Problem (2.4). Although the BB-based heuristic approaches have polynomial time-complexity, their runtime rapidly increases with the number of variables as they must solve the relaxed problem. For large size networks, the need for another heuristic approach with lower time-complexity arises.

We first analyze the simpler problem instances to derive a CSI-based relay selection condition of three node WPCCN in Section 2.7.1. In Section 2.7.2, we extend the condition for a single-source-multiple-relay network for relay selection, and then, present the heuristic algorithm, which initializes relay assignment based on this condition and iteratively updates the relay assignment as long as there is an improvement in the schedule length.

2.7.1 Optimality Conditions

In three node WPCCN, the condition on whether a relay assistance is beneficial or not is established by comparing the total schedule lengths of cases where IT is performed with and without a relay. Obviously, the network benefits from the relay if the total schedule length with relay assistance is lower than that of direct source-to-AP communication.

For the following Lemma 6 and Claim 1, we assume that P^{max} is sufficiently high so that the power constraints Eqs. (2.4c) and (2.4d) are not effective to ease the mathematical comparisons. Later, we will discuss the effect of P^{max} over an example scenario.

Lemma 6. *Let $\{\hat{\tau}_0^i, \hat{\tau}_{S_i}^{AP}\}$ be the solution pair of the single source problem corresponding to S_i for direct transmission to AP by Theorem 2 for $i = 1, \ldots, N$. $\hat{\tau}_0^i$ and $\hat{\tau}_{S_i}^{AP}$ are decreasing functions of $g_{S_i}^{AP} h_{AP}^{S_i}$.*

Proof. We prove the lemma by showing that the first derivatives of $\hat{\tau}_0^i$ and $\hat{\tau}_{S_i}^{AP}$ with respect to $g_{S_i}^{AP} h_{AP}^{S_i}$ are negative. Due to the assumption on P^{max}, Eqs. (2.9) and (2.10) determine $\{\hat{\tau}_0^i, \hat{\tau}_{S_i}^{AP}\}$. Note that $g_{S_i}^{AP} h_{AP}^{S_i}$ is proportional to γ_{S_i}, as $\gamma_{S_i} =$

$\frac{g_{S_i}^{AP}\zeta_{S_i}P_A h_{AP}^{S_i}}{WN_0}$. The first derivative of Eq. (2.9) is

$$\frac{d\hat{\tau}_{S_i}^{AP}}{d\gamma_{S_i}} = -\frac{\mathbb{L}_0\left(\frac{\gamma_{S_i}-1}{e}\right)}{(-1+\gamma_{S_i})\left(1+\mathbb{L}_0\left(\frac{\gamma_{S_i}-1}{e}\right)\right)^3}, \tag{2.16}$$

where $\mathbb{L}_0(.)$ is the Lambert W-function in 0 branch. If $\gamma_{S_i} > 1$, then $(-1+\gamma_{S_i}) > 0$ and $\mathbb{L}_0\left(\frac{\gamma_{S_i}-1}{e}\right) > 0$. Thus, $d\bar{\tau}_{S_i}^{AP}/d\gamma_{S_i} < 0$. If $0 < \gamma_{S_i} < 1$, then $(-1+\gamma_{S_i}) < 0$ and $\mathbb{L}_0\left(\frac{\gamma_{S_i}-1}{e}\right) < 0$. Also, $-1 < \mathbb{L}_0\left(\frac{\gamma_{S_i}-1}{e}\right) < 0$, since $-1/e < (-1+\gamma_{S_i})/e < 0$. Thus, $d\hat{\tau}_{S_i}^{AP}/d\gamma_{S_i} < 0$. As a result, $\hat{\tau}_{S_i}^{AP}$ is a decreasing function of $g_{S_i}^{AP}h_{AP}^{S_i}$.

To ease the calculations, the first derivative of Eq. (2.7) is derived instead of Eq. (2.10).

$$\frac{d\hat{\tau}_0}{d\gamma_{S_i}} = \frac{\hat{\tau}_{S_i}}{\gamma_{S_i}^2}\left(1 - 2^{\frac{D}{W\hat{\tau}_{S_i}}}\right) < 0, \tag{2.17}$$

since $\frac{D}{W\tau_{S_i}} > 0$ so $2^{\frac{D}{W\tau_{S_i}}} > 1$. As a result, $\hat{\tau}_0^i$ is a decreasing function of $g_{S_i}^{AP}h_{AP}^{S_i}$. □

Claim 1. *Under the moderate and high AWGN, the necessary condition for relay selection R_1 at source S_1 is*

$$\min\left(g_{S_1}^{R_1}h_{AP}^{S_1}, g_{R_1}^{AP}h_{AP}^{R_1}\right) > g_{S_1}^{AP}h_{AP}^{S_1}. \tag{2.18}$$

Proof. We prove the lemma by comparing the total schedule length of the cases with and without relay assistance. To compute the schedule lengths, we benefit from the heuristic algorithm MAX-EH instead of optimal algorithm POWMU based on Remark 2.

By following MAX-EH solution strategy, the schedule lengths are calculated as follows. If there is no relay assistance, the solution for the direct transmission, $\{\hat{\tau}_0, \hat{\tau}_{S_1}^{AP}\}$, is obtained by Eqs. (2.9) and (2.10). We denote the solution of three node WPCCN by $\{\tau_0', \tau_{S_1}'^{R_1}, \tau_{R_1}'^{AP}\}$. Let $\bar{\tau}_0^{S_1}$ [$\bar{\tau}_0^{R_1}$] be the optimal EH length when S_1 [R_1] is the single source targeting the R_1 [the AP] of the network. τ_0' is set to the maximum of $\{\bar{\tau}_0^{S_1}, \bar{\tau}_0^{R_1}\}$; and $\tau_{S_1}'^{R_1}$ and $\tau_{R_1}'^{AP}$ are calculated for given τ_0' by Eq (2.14).

Now, we show the condition where $\tau_0' + \tau_{S_1}'^{R_1} + \tau_{R_1}'^{AP} < \hat{\tau}_0 + \hat{\tau}_{S_1}^{AP}$. Let us first consider the case where the source needs more energy than the relay, i.e., $\bar{\tau}_0^{S_1} > \bar{\tau}_0^{R_1}$.

By Lemma 6, this refers to $g_{S_1}^{R_1} h_{AP}^{S_1} < g_{R_1}^{AP} h_{AP}^{R_1}$. τ_0' is set to $\bar{\tau}_0^{S_1}$ so it is a decreasing function of $g_{S_1}^{R_1} h_{AP}^{S_1}$. In direct transmission, $\hat{\tau}_0$ is a decreasing function of $g_{S_1}^{AP} h_{AP}^{S_1}$. Again based on Lemma 6, if $g_{S_1}^{AP} h_{AP}^{S_1} < g_{S_1}^{R_1} h_{AP}^{S_1}$, $\tau_0' < \tau_0$ and $\tau_{S_1}^{\prime R_1} < \tau_{S_1}^{AP}$ hold. Otherwise, relay cannot bring improvement since already $\tau_0 + \tau_{S_1}^{AP} < \tau_0' + \tau_{S_1}^{\prime R_1}$. As a result, in the case of $g_{S_1}^{R_1} h_{AP}^{S_1} < g_{R_1}^{AP} h_{AP}^{R_1}$, the necessary condition of relay selection is $g_{S_1}^{AP} h_{AP}^{S_1} < g_{S_1}^{R_1} h_{AP}^{S_1}$.

Next, we analyze the case where the source needs less energy than the relay, i.e., $\bar{\tau}_0^{S_1} < \bar{\tau}_0^{R_1}$. By Lemma 6, this refers to $g_{S_1}^{R_1} h_{AP}^{S_1} > g_{R_1}^{AP} h_{AP}^{R_1}$. Similar to the previous case, inequality $g_{S_1}^{AP} h_{AP}^{S_1} < g_{R_1}^{AP} h_{AP}^{R_1}$ is the necessary condition for relay selection. By considering both cases, the minimum of $\left(g_{S_1}^{R_1} h_{AP}^{S_1}, g_{R_1}^{AP} h_{AP}^{R_1}\right)$ must be greater than $g_{S_1}^{AP} h_{AP}^{S_1}$ for a relay to bring improvement. $\square$

Now, we exemplify the relay selection condition given in Eq. (2.18). In this example, an AP and a source are located at $(0, 0)$ and $(4, 0)$ in a gridded area, respectively. The relay is moved on the horizontal axis from $(-2, 2)$ to $(5, 2)$. We assume that the channels gains are only dependent on the distance. The rest of the simulation parameters are given in Section 2.8. Under moderate noise level, variation of the total transmission time as relay moves is depicted in Fig. 2.4 (a) The dashed blue line is the total time when information is transferred without the relay; whereas the solid blue line is the total time when information is transferred via the relay. By comparing blue lines, it is observed that transmission with the relay's help results in lower total time when relay is in between $x = 0.53592$ and $x = 3.46408$. The shaded area is the relaying region determined by Eq. (2.18). The distance between the intersection point of blue lines and the closest edge to that point of the shaded area is only 2×10^{-5}m. This demonstrates that Eq. (2.18) gives the necessary condition for relay selection at moderate noise level.

In Fig. 2.4 (a) the orange and red lines correspond to the results for different P^{max} values. As P_{max} decreases, the error in the shaded area increases, however, we observe that in realistic power levels such as 10 mW, the error is negligible, e.g., 0.4%.

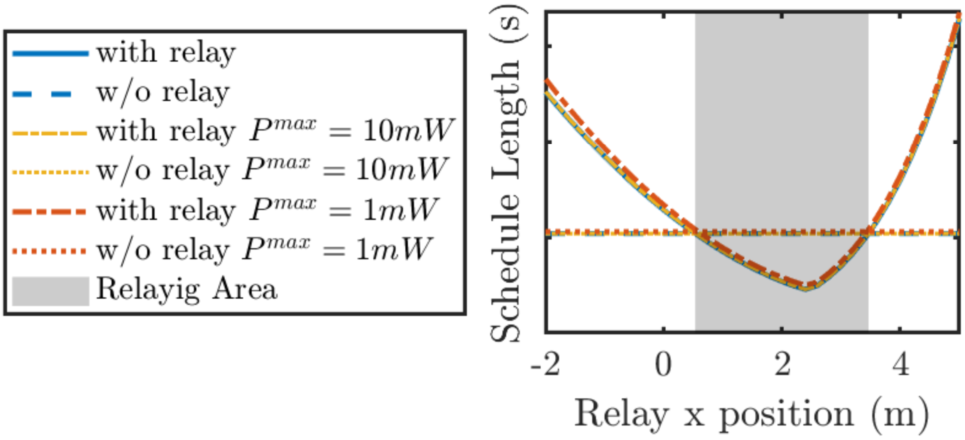

(a)

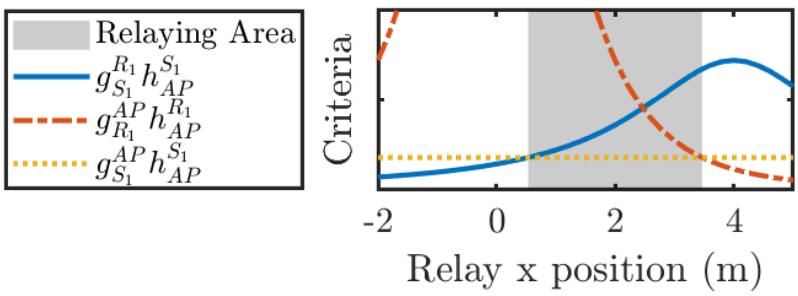

(b)

Figure 2.4: Example to validate Eq. (2.18) as a relay selection criterion. (a) Schedule length vs. the relay position in three node WPCCN. (b) Components of the criterion given by Eq. (2.18) vs. the relay position.

2.7.2 Heuristic Algorithm

The straightforward approach to determine source-relay pairs for the solution of Problem (2.4) is choosing the individual best relay for each source. Then, the total schedule length can be calculated by POWMU. However, this is not necessarily the best selection for the entire network. If one specific relay is assigned to many sources, then the selected relay needs to forward many messages. This requires more EH time resulting in an increase in the schedule length of the network. Therefore, next, we develop a heuristic algorithm, called RSTMA, which starts with an initial solution obtained by individual relay selection and reassigns a source from a relay to another in each iteration as long as there is improvement in the total schedule length.

The individual relay selection is performed as follows. In Fig. 2.4 (b), the blue line indicates the criterion $g_{S_1}^{R_1} h_{AP}^{S_1}$; whereas the red line represents the criterion $g_{R_1}^{AP} h_{AP}^{R_1}$. We observe that the higher $\min\left(g_{S_i}^{R_j} h_{AP}^{S_i}, g_{R_j}^{AP} h_{AP}^{R_j}\right)$ value, the lower the total EH and IT time. Accordingly, the individual relay selection criterion can be defined as

$$\arg\max_{j} \min\left(g_{S_i}^{R_j} h_{AP}^{S_i}, g_{R_j}^{AP} h_{AP}^{R_j}\right) \tag{2.19}$$

for source S_i. Note that this criterion is same as the opportunistic relaying (OR) criterion proposed for outage performance in [Chen et al., 2015].

The detailed procedure for RSTMA is given in Algorithm 3. Initially, we match each S_i with R_{k_i} by using the criterion given in Eq. (2.19) (Line 3). POWMU finds the total schedule length τ and power allocation vector $\overline{P}$, containing $P_X^Y, X, Y \in \{AP, S_i, R_j\}$, for the given relay selection (Line 4). τ' is used to store a new schedule length and initially is set to τ (Line 5). The following procedure continues while there is an improvement in schedule length (Line 6). The sources assigned to relay R_j are grouped under G_j for all j (Line 7). The relay with the greatest number of the sources is most probably the one requiring more EH time. Thus, starting with the ones belonging to the group of such relay, the sources are reassigned to the other relays one by one (Lines 8-11). As the aim is to lower the burden of the relay assisting multiple sources, the relays assisting single source is not in the interest of the reassignment procedure (Line 8). Since the relay R_j with higher $\min\left(g_{S_i}^{R_j} h_{AP}^{S_i}, g_{R_j}^{AP} h_{AP}^{R_j}\right)$ is expected to provide lower schedule length based on Eq. (2.19), a source is first reassigned to such a relay. If this change does not bring an improvement, other relay options are tried (Lines 12-15). Whenever an improvement is observed, τ and $\overline{P}$ are updated by τ' and $\overline{P}'$ respectively; relay selection variables, b_i^j for $j = 0, \ldots, K$, are set; the cycle is broken for the sake of time complexity; the algorithm searches for another source-relay reassignment (Lines 16-19).

RSTMA calls POWMU for K^N possible source-relay combinations if it obtains an improvement at the last element of the set W for each group G_j and each source

Algorithm 3 Relay Selection and Time Minimization Algorithm (RSTMA)

Input: P^{max}, P_A, h_X^Y, g_X^Y, ζ_{S_i}, ζ_{R_j}, D_{S_i}, for $X, Y \in \{AP, S_i, R_j\}$, $i = 1, \ldots, N$, and $j = 1, \ldots, K$

Output: b_i^j, τ_0, τ_X^Y, P_X^Y, for $X, Y \in \{S_i, R_j\}$, $i = 1, \ldots, N$, and $j = 0, \ldots, K$

$k_i = \arg\max_{j \in \{0,\ldots,K\}} \min\left(g_{S_i}^{R_j} h_{AP}^{S_i}, g_{R_j}^{AP} h_{AP}^{R_j}\right)$, $\forall i = 1, \ldots, N$

$\tau, \overline{P} \leftarrow$ POWMU (S_i, R_{k_i}), $i = 1, \ldots, N$

$\tau' = \tau$ and $\overline{P}' = \overline{P}$

while $\tau' \leq \tau$ **do**

  $G_j = \{S_i : k_i = j, i = 1 \ldots, N\}, j = 0, 1, \ldots, K$

  $J = \text{sort}_j(|G_j| > 1, '\mathit{descend}')$

  if $J \neq \emptyset$ **then**

    for $j \in J$ **do**

      for $S_i \in G_j$ **do**

        $W = \textbf{sort}_j(\min\left(g_{S_i}^{R_j} h_{AP}^{S_i}, g_{R_j}^{AP} h_{AP}^{R_j}\right), \forall j, j \neq k_i, '\mathit{descend}')$

        for $w \in W$ **do**

          $k_i \leftarrow w$

          $\tau', \overline{P}' \leftarrow$ POWMU (S_i, R_{k_i}), $i = 1, \ldots, N$

          if $\tau' < \tau$ **then**

            $\tau = \tau'$ and $\overline{P} = \overline{P}'$

            $b_i^{k_i} = 1$ and $b_i^j = 0$ for $j \neq k_i$

            break

$S_i \in G_j$. Thus, the worst case complexity is $\mathcal{O}(K^N(N+K)log_2(\frac{ub-lb}{\epsilon}))$. Although this complexity is exponential, due to its initial point determined by Eq. (2.19) and sorting mechanisms (Lines 8 and 12), RSTMA terminates in less number of iterations, as demonstrated in Section 2.8.

2.8 Performance Evaluation

In this section, the performance of the proposed algorithms, BBA, OBH, RPH, and RSTMA, is evaluated via numerical simulations and compared with benchmark harvest-then-cooperate protocol (HTC) from [Chen et al., 2015], and the initial solution of RSTMA, denoted by OR+POWMU, as it uses OR criteria for relay selection and POWMU for schedule length calculation. HTC divides unit time block T into ρT for EH and $(1-\rho)T$ for IT. It considers single source network and equal length IT blocks $(1-\rho)T/2$ for source-to-relay and relay-to-AP communication. We adapt HTC scheme to multiple-source network by allocating $(1-\rho)T/2\psi_i$ time for IT from each source S_i to its selected relay R_j and from R_j to the AP, where ψ_i is a constant proportional to the bottleneck channel gain of source-to-AP transmission, i.e. $\psi_i = \min\left(g_{S_i}^{R_{ki}}, g_{R_{ki}}^{AP}\right) \sum_{i=1}^{N} \min\left(g_{S_i}^{R_{ki}}, g_{R_{ki}}^{AP}\right)^{-1}$, so that the source with worse channel condition is served with longer IT. The unit time block is assumed as 1 ms, i.e., $T = 1$ ms. ρ is set to 0.8, which is the best value for schedule length minimization according to our simulations. We additionally include the enforcement for obeying P^{max} limitation. For relay selection, OR criteria, corresponding to Eq. (2.19), is applied.

Simulations are conducted over 1000 independent random network realizations in MATLAB. Sources are uniformly distributed in a circular quadrant between radius $3-4$ m. The AP is located at the center of the circle. Relays are deterministically positioned between the sources and the AP at distance 2 m from the AP. 5-source 2-relay WPCCN is considered unless otherwise stated, as different sized networks behave similarly. The WPCCN is simulated at 915 MHz central frequency with 1 MHz bandwidth.

Large scale channel statistics are formulated as

$$PL(d) = PL(d_0) - 10\upsilon \log_{10}(d/d_0) + Z, \tag{2.20}$$

where $PL(d_0)$ is the free space path loss at unit distance d_0 in dB, d is the distance between the transmitter and receiver, $PL(d)$ is the path loss at distance d in dB, υ is the path-loss exponent, and Z is a zero-mean Gaussian random variable with standard deviation σ_Z. For small scale statistics, Rayleigh fading model is used with scale parameter Ω set to the mean power level determined by $PL(d)$ [Morsi et al., 2015]. The simulation parameters are chosen as $N_0 = -90$ dBm, $\zeta_{S_i} = \zeta_{R_j} = 50\%$ [Le et al., 2008], $PL(d_0) = 31.67$, $\sigma_Z = 2$ dB, and $\upsilon = 2$. The transmit power of the AP is chosen as 4 W, which is the maximum allowed power at 915 MHz band according to FCC regulations [Lu et al., 2015]. All sources are assumed to transmit equal amount of data, 50 bits, to the AP.

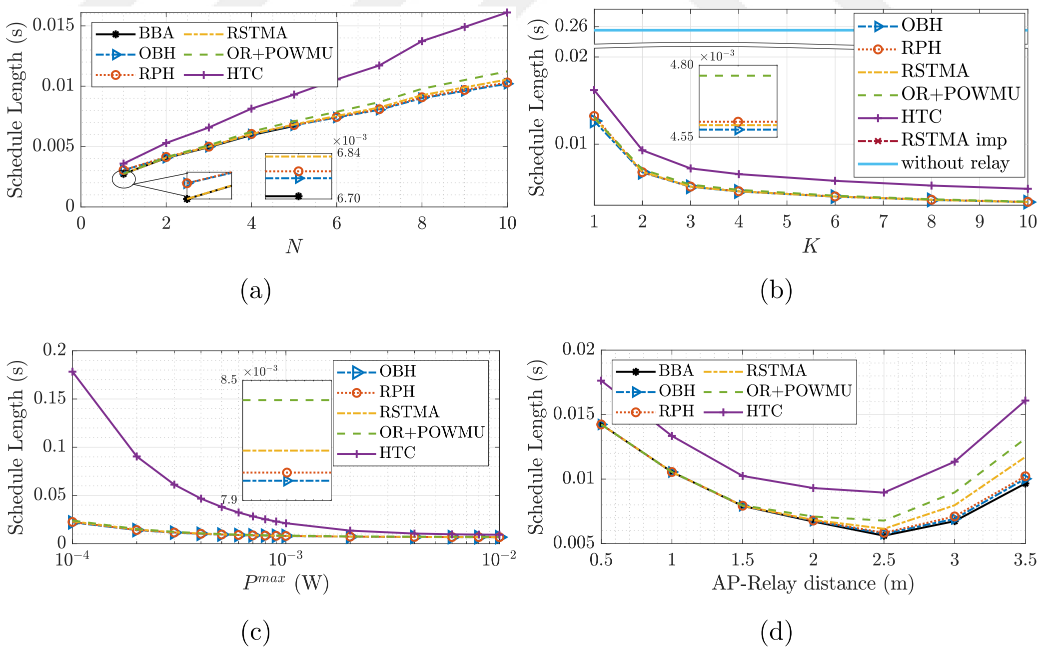

Figure 2.5: Schedule length vs. (a) number of sources, (b) number of relays, (c) maximum power limit of the sources and relays, and (d) relay position.

Figs. 2.5 (a) - 2.5 (d) depict the schedule length of the network obtained by different algorithms for varying number of sources, number of relays, maximum UL

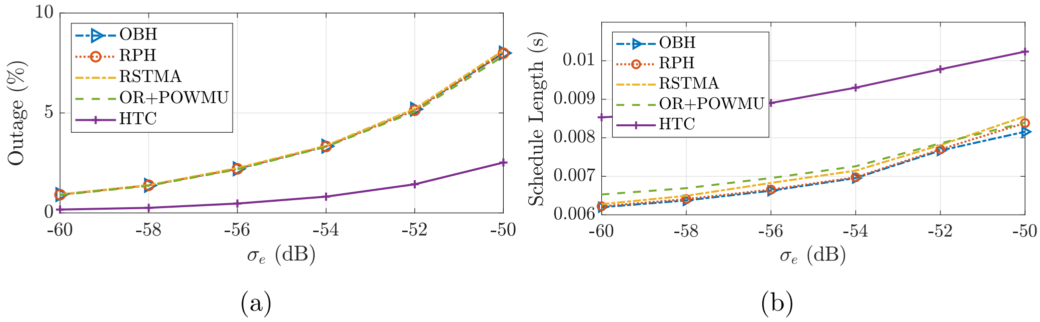

Figure 2.6: (a) Data outage vs. channel estimation error (b) Schedule length vs. channel estimation error.

transmit power limit, and relay position, respectively. BBA is only simulated for the first and fourth cases up to 5 sources due to its exponential time complexity. The proposed algorithms outperform the benchmark approach HTC; whereas the heuristic approaches, OBH, RPH, and RSTMA, perform very closely to the optimum algorithm BBA. The difference in the schedule length computed by the proposed heuristics results from the assignment of the relays, as POWMU obtains the optimum schedule length for given relay selection. OBH performs best, RPH is the second best, which is followed by RSTMA. Comparison of RSTMA with OR+POWMU indicates the significance of the further improvement by RSTMA from its initial point determined by OR+POWMU, especially for higher number of sources. This observation highlights the fact that the individual best relay selection is not necessarily the best for the entire network. The figures are further analyzed as follows.

In Fig. 2.5 (a), the schedule length increases with the increasing number of sources as expected. For $N = 3$, BBA outperforms HTC by 25%; whereas the gap between BBA and RSTMA is 0.88%, the gap between BBA and RPH is 0.77%, and the gap between BBA and OBH is 0.63%. For $N = 5$, BBA provides 28% lower schedule length than HTC; whereas the gap between BBA and RSTMA is 1.86%, the gap between BBA and RPH is 1.18%, and the gap between BBA and OBH is 0.85%. This demonstrates that the performance improvement of the optimal algorithm, BBA, over HTC increases as N increases. Moreover, slight increase is observed in the optimality gap between BBA and the proposed heuristic algorithms for large N values. For smaller number of sources, e.g., $N = 1$, RSTMA provides lower schedule length than RPH.

In Fig. 2.5 (b), the schedule length decreases with the increasing number of relays, which indicates the benefit of the relays. Compared to the non-relay case, for which the optimal time allocation and power control are obtained by POWMU, using 2 relays reduces the schedule length of the network by 97%; whereas using 10 relays decreases it by 98.6%. This demonstrates diminishing returns as the number of relays increases.

In Fig. 2.5 (c), the gap between the HTC and proposed algorithms is higher at lower P^{max} levels as HTC does not consider transmit power limitation, e.g., 87% gap for $P^{max} = 10^{-4}$ W. The gap closes as P^{max} increases, but, there is still 27% gap between HTC and OBH for $P^{max} = 10^{-2}$ W.

Fig. 2.5 (d) depicts the schedule length of the network for different relay positions, where the AP and sources stay at the same positions. The relays bring the highest improvement when they are located at 2.5 m, closer to the sources than the AP. Between $0.5 - 2.5$ m, all the proposed heuristics performs very close to BBA. After 2 m, the performance of RSTMA degrades.

Fig. 2.6 presents the performance of the algorithms under imperfect CSI, where channel estimation error is modelled as zero-mean complex Gaussian random variable with standard deviation σ_e [Chen and Tellambura, 2005]. Simulations are performed for σ_e up to -50 dB, since the maximum path loss value is -44 dB. Fig. 2.6 (a) depicts the data outage percentage, which is defined as the percentage of data that cannot be transmitted within the allocated time slots, for different σ_e values. The proposed algorithms have less than 5% outage until $\sigma_e = -52$ dB, which is considered tolerable [Cui et al., 2020]. As HTC does not obtain the minimum schedule length and the overestimated time can compensate the imperfect CSI, HTC has lower outage than the proposed algorithms. Fig. 2.6 (b) shows the schedule length for different σ_e values, for the case when the sources repeat EH and IT processes until they complete the required IT. $\sigma_e = -50$ dB causes $12\%, 10\%, 14\%, 11\%,$

Table 2.1: Algorithm Comparison

Name	Complexity	Performance
BBA	$\mathcal{O}((K^N(C+(N+K)log_2(\frac{ub-lb}{\epsilon})))$	globally optimal
OBH	$\mathcal{O}((N-1)C+(N+K)log_2(\frac{ub-lb}{\epsilon}))$	the best heuristic
RPH	$\mathcal{O}(C+(N+K)log_2(\frac{ub-lb}{\epsilon}))$	the second best heuristic for greater N
RSTMA	$\mathcal{O}(K^N(N+K)log_2(\frac{ub-lb}{\epsilon}))$	the second best heuristic for lower N
OR+POWMU	$\mathcal{O}(K+(N+K)log_2(\frac{ub-lb}{\epsilon}))$	worse than RSTMA
HTC	$\mathcal{O}(2K+N)$	the worst approach

and 7% longer schedule length for OBH, RPH, RSTMA, OR+POWMU, and HTC, respectively, compared to their corresponding schedule length at the perfect CSI. Although HTC is more robust against imperfect CSI, the proposed algorithms provide shorter schedule length than HTC.

Fig. 2.7 shows the run-time performance of the proposed algorithms. BBA has exponential complexity in practical simulations as well. The runtime of OBH quadratically increases with the increasing number of sources as it has to solve the relaxed problem $N-1$ times and the complexity of the relaxed problem also depends on N. The runtime of RPH increases linearly with the number of sources as it solves the relaxed problem just once. The runtime of RSTMA is up to 99.9% and 99.7% lower than that of OBH and RPH, respectively. RSTMA has higher runtime than OR+POWMU, as it improves the OR criteria with further iterations depending on the number of sources. For $N=5$, BBA, OBH, RPH, RSTMA, and OR+POWMU have 6.85×10^5, 2.66×10^5, 2.48×10^4, 52.75, and 7.88 times higher runtime than HTC, respectively.

The complexity and performance of all the algorithms are summarized in Table 2.1. The complexity of OR+POWMU is $\mathcal{O}(K+(N+K)log_2(\frac{ub-lb}{\epsilon}))$ as OR and POWMU requires K and $(N+K)log_2(\frac{ub-lb}{\epsilon})$ iterations respectively; whereas the complexity of HTC is $\mathcal{O}(2K+N)$ as it calls OR, and then, calculates the power allocation for all sources and relays in $N+K$ iterations.

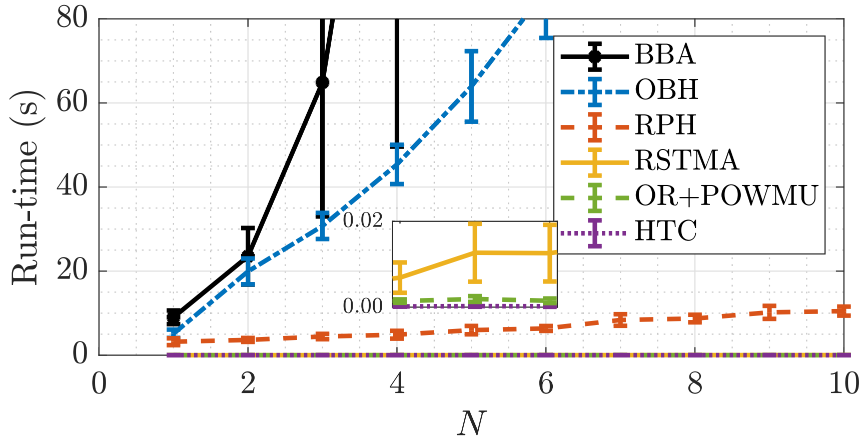

Figure 2.7: Run-time of the algorithms vs. number of sources.

2.9 Conclusion

We formulate a novel joint relay selection, scheduling and power control problem for multiple-source-multiple-relay WPCCN. The problem aims to minimize the total schedule duration of energy harvesting and information transmission, while satisfying data, energy causality, and maximum UL transmit power constraints. The problem is non-convex MINLP and proven to be NP-hard. Given the relay selection, we first formulate a scheduling and power control problem, and then propose an efficient optimal and a faster sub-optimal algorithm for the solution. To determine relay assignments, we first adapt an exponential-time branch-and-bound (BB) based algorithm for the optimal solution of the problem. Then, two BB-based heuristic approaches are proposed together with a lower complexity relay criterion based algorithm. We demonstrate via numerical simulations that our proposed approaches exhibit better performance than the conventional harvest-then-cooperate approaches with up to 87% lower schedule length for various network sizes and transmit power levels at the cost of higher algorithm complexity with at least 7.88 times higher runtime. The extension of this work for imperfect CSI, non-linear energy harvesting and battery model with long-term energy storage is subject to future work.

Chapter 3

DEEP LEARNING BASED MINIMUM LENGTH SCHEDULING FOR HALF DUPLEX WIRELESS POWERED COMMUNICATION NETWORKS

3.1 Introduction

Energy Harvesting (EH) has drawn significant attention as an alternative solution to the fixed power supplies (e.g., batteries) for energy constrained networks (e.g., wireless sensor networks). Compared to natural energy sources such as vibration and sun, inductive and magnetic coupling, radio frequency (RF) energy harvesting is preferred due to its independence from climate conditions, more predictable and controllable nature of RF signals [Liu et al., 2017], especially for time critical applications[Zheng et al., 2016], where the delay caused by the unpredictable power supply can have significant outcomes. Besides using RF signals as energy source for wireless powered communication networks (WPCNs), minimum length scheduling is used to ensure strict delay requirements of time critical applications. In the minimum length scheduling problem, the objective is to minimize the total time scheduled for EH and information transmission (IT). The common constraints of the problem are data demand, energy causality, and transmit power limitations.

Minimum length scheduling problem is studied in WPCNs for half-duplex systems with [Salik et al., 2019] and without [Chi et al., 2017] transmit power restrictions, for multiple-source-multiple-relay based half-duplex systems[Onalan et al., 2020], for full-duplex systems with [Iqbal et al., 2020] and without [Kang et al., 2015] transmit power restrictions, and for discrete rate full-duplex system[Iqbal et al., 2022a]. The aforementioned works propose iterative algorithms for optimal or sub-optimal solutions to the problems. The iterative algorithms that solve a complex mathematical equation in each iteration suffer from high run-time. However, algorithm run-time is as significant as total time minimization for time-critical applications. Non-iterative sub-optimal algorithms are only considered in [Kang et al., 2015], which do not always provide close-to-optimal solutions under varying network conditions.

Deep Neural Networks (DNNs), as universal function estimators, are advantageous for robust, low-complexity, and close-to-optimal solutions to the optimization problems in wireless communications [Zappone et al., 2019, Elsayed and Erol-Kantarci, 2019]. Therefore, DNN-based solutions have also proliferated for the optimization of WPCNs[Hameed et al., 2021, Lee et al., 2021, Khan and Coleri, 2021]. A DNN-based scheme is proposed for the joint optimization of the time and power allocations with energy beamforming design in MIMO WPCN [Hameed et al., 2021]. The network is trained offline with reference labels from a sequential parametric convex approximation (SPCA)-based iterative algorithm. In wireless powered two-way communication system, sum rate maximization of forward link with the minimum rate constraint for backward link is studied in [Lee et al., 2021]. The network's training is, first, performed in a supervised manner by using the sub-optimal solutions of the problem, then, continued in an unsupervised manner with a problem specific loss function. Joint minimum length scheduling and power allocation problem for full-duplex systems is solved with multiple DNNs in [Khan and Coleri, 2021]. The network is trained offline with optimal solutions obtained by an iterative algorithm. All mentioned DNN-based solutions provide lower complexity than iterative algorithms with very high accuracy.

This paper proposes two deep learning based approaches for robust and low-complexity solutions of the minimum length scheduling problem in WPCNs. We consider a half-duplex WPCN, where the users harvest energy from broadcasted signals from an access point (AP) in the downlink (DL) and transmit information to the AP with the harvested energy in the uplink (UL). The formulated minimum length scheduling problem with the joint optimization of power, EH, and IT time allocations[Salik et al., 2019] is hard to solve due to its non-convex and non-linear nature. The optimal solutions via iterative algorithms require high computational time; whereas the sub-optimal solutions lack robustness against changing network conditions. To overcome these issues, this paper proposes a feed forward DNN architecture trained with supervised and unsupervised techniques. The major contributions of this paper are listed as follows:

- Several feed-forward DNN architecture is proposed for the minimum length scheduling problem for half-duplex WPCNs. Inputs of the DNN are UL and DL channel state information (CSI), and two parameters derived from the optimality conditions of the problem. Outputs of the DNN are transmit powers of the users and the EH and IT time allocations.

- Both supervised and unsupervised techniques are applied for the offline training of the proposed architecture. We use the solutions from the optimal iterative algorithm as truth labels in the former. In the latter, we utilize the objective function of the problem and/or the data outage amount as a loss function.

- Simulation results indicate the superiority of the proposed DNN-based approaches in terms of run-time against the benchmark iterative algorithms. The DNN-based approaches are also shown to be robust under varying network conditions including the UL transmit power limit and the transmit power of the AP.

This paper is organized as follows: Section 3.2 describes the system model and the assumptions. Section 3.3 formulates the minimum length scheduling problem. Section 3.4 presents the DNN-based solutions to the problem. Section 3.5 evaluates the performance of the proposed DNN-based solutions against the benchmark algorithms. Section 3.6 concludes the paper.

3.2 System Model and Assumptions

We consider a half duplex WPCN with one AP, and N users, denoted by U_i, $i = 1, ..., N$. The AP and all users are equipped with single antenna and operate in the same frequency band. Harvest-then-Transmit protocol[Ju and Zhang, 2014] is applied as medium access protocol. In a transmission frame, users first harvest energy from the signals broadcast by AP in DL during τ_0 amount of time. Then, τ_i amount of time is assigned for the IT from each user U_i to the AP in UL. Each user U_i has to send $D_i > 0$ amount of data in a transmission frame. The AP maintains the synchronization of the network by informing the users about the current schedule in a fixed and negligible time at the beginning of each time frame.

The users only have rechargeable batteries with low energy storage and high self discharge rate, e.g. super-capacitors [Kaus et al., 2010]. Therefore, the harvested energy cannot be stored for further use[Kang et al., 2015, Salik et al., 2019, Chi et al., 2017]. The battery capacity is larger than the maximum amount of energy that can be harvested in a time frame. The AP has an unlimited power source and transmits with constant power P_A. P_A is large enough to ignore the receiver noise component in energy harvesting.

We assume block fading channels. The DL and UL channel gains between U_i and the AP are denoted by h_i and g_i, respectively. The channel gains are perfectly known by the AP at beginning of each transmission frame similar to the previous works, e.g., [Lee et al., 2021, Hameed et al., 2021, Khan and Coleri, 2021]. The energy spent to obtain channel gains at the AP is negligible.

The energy harvested at U_i is $E_i = \zeta_i P_A h_i \tau_0$, where $\zeta_i \in (0, 1)$ is the EH efficiency of U_i, and assumed to be constant. This model is valid if the energy harvesting circuit is designed such that the energy harvesting efficiency is flat over desired receive power range [Choi et al., 2018] and is widely used in the literature [Kang et al., 2015, Chi et al., 2017, Lee et al., 2021, Hameed et al., 2021]. We consider continuous power model [Salik et al., 2019, Khan and Coleri, 2021] for UL IT, so the transmit power takes any value below a maximum level P^{max}. The transmit power is further limited by the amount of the harvested energy. Thus, the average transmit power of U_i, denoted by P_i, $P_i \leq E_i/\tau_i$. We use continuous transmission rate model and Shannon's channel capacity formula for AWGN channels to determine maximum achievable rate. We assume interference-free IT. Then, the instantaneous UL transmission rate of U_i is given by $T_i = W \log_2(1 + P_i g_i/(WN_0))$, where W is the channel bandwidth and N_0 is the noise power spectral density.

3.3 Optimization Problem

This section, first, presents the mathematical formulation of the minimum length scheduling problem for HTT WPCNs. Then, two lemmas are provided by analyzing the optimality conditions of the problem, which will be exploited for the design of DNN-based solution in the next sections.

3.3.1 Formulation

The minimum length scheduling problem with the optimum time allocation and power control for a HTT WPCN is formulated as follows:

$$\min \quad \tau_0 + \sum_{i=1}^{N} \tau_i \tag{3.1a}$$

$$\text{s.t.} \quad P_i \tau_i \leq \zeta_i P_A h_i \tau_0, \quad i = 1, 2, \ldots, N, \tag{3.1b}$$

$$\tau_i W \log_2\left(1 + \frac{P_i g_i}{W N_0}\right) \geq D_i, \; i = 1, 2, \ldots, N, \tag{3.1c}$$

$$P_i \leq P^{max}, \quad i = 1, 2, \ldots, N, \tag{3.1d}$$

$$\tau_0, \tau_i, P_i \geq 0, \quad i = 1, 2, \ldots, N, \tag{3.1e}$$

The variables of the optimization problem are τ_0, EH duration; τ_i, IT duration of U_i; and P_i, transmit power of the i^{th} source. The goal of the problem is to minimize the total EH and IT times. Eq. (3.1b) guarantees that energy consumed for information transmission does not exceed the harvested energy at that time block for each user. Eq. (3.1c) necessitates the successful transmission of D_i bits from U_i to the AP. Eq. (3.1d) determines the maximum transmit power of users. Eq. (3.1e) gives the non-negativity constraints.

The problem (3.1) is a non-convex non-linear optimization problem due to the non-convexity of Eqs. (3.1b) and (3.1c).

3.3.2 Analysis of Optimality Conditions

Lemma 7. *For a given set of transmit powers* $[P'_1, \ldots, P'_i, \ldots, P'_N]$*, where* $P'_i \leq P^{max}, \forall i = 1, 2, \ldots, N$*, the feasible solution set* $[\tau'_0, \tau'_1, \ldots, \tau'_i, \ldots, \tau'_N]$ *of the problem (3.1) attaining minimum schedule length is expressed by*

$$\tau'_i = \frac{D_i}{W \log_2 \left(1 + \frac{P'_i g_i}{W N_0}\right)} \tag{3.2}$$

$$\tau'_0 = \max_i \left\{ \frac{P'_i \tau'_i}{\zeta_i P_A h_i} \right\} \tag{3.3}$$

Proof. For a given set of transmit powers $[P'_1, \ldots, P'_i, \ldots, P'_N]$, where $P'_i \leq P^{max}, \forall i = 1, 2, \ldots, N$, minimum IT times can be reached by satisfying data requirement constraint in Eq. (3.1c) with equality. Then, τ'_i is obtained as in Eq. (3.2).

To transmit with P'_i in τ'_i amount of time, each user U_i requires $P'_i \tau'_i$ amount of energy, which can be harvested in $(P'_i \tau'_i)/(\zeta_i P_A h_i)$ amount of time. Since all users' energy requirement needs to be satisfied for a feasible solution, the feasible EH time τ'_0 is the maximum of all individually required EH times as in Eq. (3.3). □

Lemma 8. *Consider a single-user WPCN where* U_i *is the only user. Let* $\dot{\tau}_i$ *and* $\dot{\tau}_0$ *denote the optimal solution to the optimization problem (3.1) without Eq. (3.1d).*

Let

$$\gamma_i = \frac{g_i \zeta_i P_A h_i}{W N_0} \tag{3.4}$$

and

$$\alpha_i = \mathbb{L}_0 \left(\frac{\gamma_i - 1}{e} \right) + 1, \tag{3.5}$$

where $\mathbb{L}_0(.)$ *is the Lambert W-function in 0 branch. Then,* $\dot{\tau}_i$ *is inversely proportional to* α_i*.* $\dot{\tau}_0$ *is proportional to* α_i *while it is inversely proportional to* γ_i*.*

Proof. The optimal solution to the problem (3.1) without Eq. (3.1d) for single-user network is given by [Salik et al., 2019]

$$\dot{\tau}_i = \frac{D \ln(2)}{W \alpha_i}, \tag{3.6}$$

$$\dot{\tau}_0 = \frac{D \ln(2)}{W \alpha_i \gamma_i} \left(2^{\alpha_i / \ln(2)} - 1\right). \tag{3.7}$$

This mathematical formulation proves the proportionality claims given in Lemma 8. □

3.4 Deep Neural Network based Robust and Low-complexity Framework

This section presents several deep-learning approaches for the minimum length scheduling problem. We first direct apply feed-forward DNNs between the inputs and outputs of the problem. We, then, extend our framework by using explainable AI (XAI) techniques; and exploiting optimization theory-based solutions by Lemma 1 and Lemma 2. We also study the impact of employing deep learning as an inner block of iterative algorithms. We also adopt rule-based deep learning and deep-unfolding approaches from the literature to the minimum length scheduling problem.

The optimization problem (3.1) defines a non-linear mapping from the DL and UL channel gains to optimal transmit powers and schedule lengths as follows:

$$\mathcal{P} : \{\mathbf{h}, \mathbf{g}\} \rightarrow \{\mathbf{P}, \tau\}$$

where $\mathbf{h}[\mathbf{g}] \in \mathbb{R}^{N \times 1}$ is the input vector whose i^{th} element corresponds to the DL[UL] channel gain $h_i[g_i]$ of U_i; $\mathbf{P} \in \mathbb{R}^{N \times 1}$ is the output vector with the i^{th} entry containing the transmit power P_i of U_i; $\tau \in \mathbb{R}^{(N+1) \times 1}$ is the output vector with the i^{th} entry representing the IT time τ_i of U_i for $i > 0$ and EH time for $i = 0$. $\mathcal{P}$ is a continuous non-linear approximation function mapping channel gains to the transmit powers and schedule lengths.

Another representation $\mathcal{P}'$ of the problem 3.1 can be defined as follows: As Lemma 7 provides the function $\mathcal{F}$ to obtain feasible EH and IT times for a given power allocation,

$$\mathcal{F} : \{\mathbf{P}\} \in \mathbb{R}^{N\times 1} \rightarrow \{\tau\} \in \mathbb{R}^{(N+1)\times 1},$$

a non-linear mapping from the DL and UL channel gains to optimal power allocations is adequate to represent the problem (3.1). Further, γ_i, α_i by Eqs. (3.4)-(3.5) can be exploited as inputs of a mapping to the optimal solution since Lemma 8 indicates the correlation among α_i, γ_i, and the optimal solutions. Then,

$$\mathcal{P}' : \{\mathbf{h}, \mathbf{g}, \alpha, \gamma\} \in \mathbb{R}^{4N\times 1} \rightarrow \{\mathbf{P}\} \in \mathbb{R}^{(N+1)\times 1},$$

where $\gamma[\alpha] \in \mathbb{R}^{N\times 1}$ is the input vector whose i^{th} element corresponds to $\gamma_i[\alpha_i]$ of U_i. The advantage brought by α and γ as inputs of the network is decreasing training and validation losses.

This representation allows us to design multi-input, multi-output deep neural network architecture to obtain the approximation function $\mathcal{P}'$ for a robust, low-complexity and feasible solution of the problem (3.1). Next, we describe the proposed DNN architecture in Section 3.4.1, data generation in Section 3.4.2 and training process in Section 3.4.3.

3.4.1 Deep Learning Architectures

Fig. 3.1b depicts the block diagram of the data-driven deep learning approach, which learns the approximation function $\mathcal{P}$. We consider two DNN architectures, one for EH and IT lengths, and the other for transmit powers. Both DNNs are multi-input, multi-output, feed-forward, fully connected; consist of five hidden layers; and use h_i and g_i for each user U_i, $i = 1, \ldots, N$ as inputs. In both DNNs, the five hidden layers are of the size $8 \times N$, $8 \times N$, $8 \times N$, $4 \times N$, and $4 \times N$. The output layer of the first DNN consists of N nodes corresponding to the transmit power P_i of each user U_i, $i = 1, \ldots, N$; whereas The output layer of the second DNN consists of $N + 1$ nodes corresponding to the EH duration τ_0, and IT duration τ_i of each user U_i, $i = 1, \ldots, N$. We utilize RelU activation function in each hidden layer. We define a customized activation function $P^{max}S(x)$, where $S(x) = 1/(1+\exp^x)$ is the sigmoid

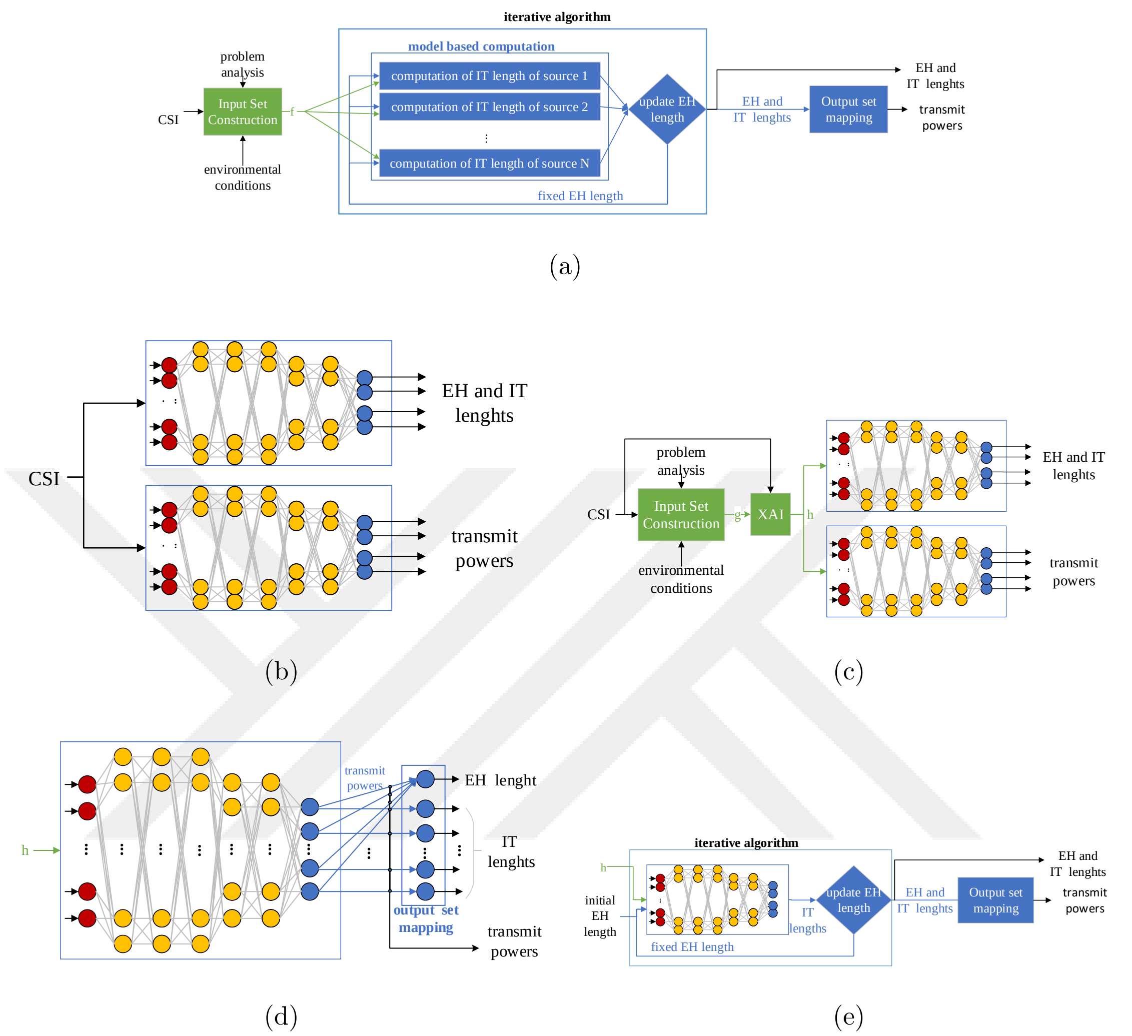

Figure 3.1: The block diagrams of a) POWMU b) DNN c) XAI+DNN d) MIN-NET and MIN-US-NET e) SB-DNN

function, in the first output layer, to ensure maximum transmit power constraint in Eq. (3.1d). This approach is referred simply as DNN from now on and provides a sub-optimal solution.

Fig. 3.1c shows the block diagram of the DNN architecture extended by the inclusion of the additional features at the input by exploiting Lemma 8 and then the selection of the most impactful inputs by using XAI techniques. Additional input parameters, α, γ, based on the optimality conditions of the problem, can improve the accuracy of the aforementioned DNN architecture. The most impactful features, among $\alpha, \gamma, \mathbf{h}$ and $\mathbf{g}$ are then selected based on the mutual information (MI) between all possible inputs and the schedule length in XAI. This approach is named as XAI+DNN.

Figure 3.1d depicts the optimization theory-based deep learning architecture which is constructed by exploiting Lemma 7 to ensure the feasible solution at the output of the network and Lemma 8 to determine the inputs of the network. The proposed architecture is again fully connected, feed-forward, and with five hidden layers. h_i, g_i, α_i, and γ_i for each user U_i, $i = 1, \ldots, N$, are the inputs of the proposed DNN. The five hidden layers are of the size $8 \times N$, $8 \times N$, $8 \times N$, $4 \times N$, and $4 \times N$. The first output layer consist of N nodes corresponding to the transmit power P_i of each user U_i, $i = 1, \ldots, N$. The second output layer consist of $N + 1$ nodes corresponding to the EH duration τ_0, and IT duration τ_i of each user U_i, $i = 1, \ldots, N$. There is a deterministic output set mapping (OSM) between two output layers based on Eqs. (3.2) and (3.3). We utilize RelU activation function in each hidden layer. We define a customized activation function $P^{max} S(x)$, where $S(x) = 1/(1 + \exp^x)$ is the sigmoid function, in the first output layer, to ensure maximum transmit power constraint in Eq. (3.1d). The supervised DNN proposed for solution of the minimum length scheduling problem is called MIN-NET; whereas the unsupervised DNN is called MIN-US-NET.

Fig. 3.1e shows how a DNN can replace the inner workings of the iterative optimal algorithm. The optimal solution of the problem is Power Constrained Multiple User Time Minimization (POWMU) algorithm presented in Fig. 3.1a. POWMU finds the optimal solution to the minimum length scheduling problem by transforming it into a bi-level optimization problem. It first obtains an expression for the individual IT times for N networks with a single user for a fixed EH duration. Then, the optimal EH time is searched with the bisection method. POWMU derives individual IT lengths by employing numerical analysis techniques to solve complex mathematical equations for a given EH length in each sub-problem. Here, deep learning architecture, called SB-DNN, replaces these derivations. The SB-DNN uses again a feed-forward, fully connected architecture with five hidden layers to estimate the individual IT times for fixed EH length. The inputs of the DNN are the vector h and fixed EH length; whereas the outputs are the IT lengths of each source. We utilize RelU activation function in each hidden layer.

3.4.2 Data Generation

DL and UL channel gains, i.e., **h** and **g**, are generated for users uniformly distributed within a circular area of radius 1 m where the AP is located at the center. The channel attenuation is determined considering both large and small scale statistics. The attenuation due to the large scale statistics is modeled as $PL(d) = PL(d_0) + 10\upsilon log(d/d_0) + Z$, where d is the distance between the user and the AP, $PL(d)$ is the path loss at distance d in decibels, $PL(d_0)$ is the path loss at reference distance $d_0 = 1$ m, υ is the path loss exponent and Z is a Gaussian random variable with zero mean and standard deviation σ_z. The small-scale fading is modeled by Rayleigh fading with scale parameter Ω set to the mean power level determined by $PL(d)$. For generated **h** and **g**, α and γ are calculated by Eqs. (3.5) and (3.4), respectively.

3.4.3 Training

We employ both supervised and unsupervised learning for the training of the DNN. For supervised training, we obtain the optimal solution of the problem with POWMU algorithms proposed in [Salik et al., 2019]. For unsupervised training, either the objective function of the problem or the data outage amoıunt is employed as a loss function. Data outage refers to the unmatched amount of data demand when sources transmit with the predicted powers during predicted times.

For DNN and XAI+DNN, both architectures predicting power and time allocations are trained with joint loss function, which is the weighted sum of mean square error (MSE) and data outage amount. For MSE calculation, the truth labels are obtained by POWMU.

For the supervised training of MIN-NET, we use the MSE between the optimal and predicted EH and IT times as a loss function. For the unsupervised training of MIN-US-NET, the objective function Eq. (3.1a) is utilized as the loss function.

The SB-DNN is trained with a loss function as data outage amount. Then, the optimal EH length is again searched by the bisection method, whose outputs are EH and IT lengths and are mapped to transmit powers as in OPT. Although the training is unsupervised, we benefit from OPT to obtain observed EH lengths throughout the iterations, which are direct inputs of the sub-block DNN.

3.4.4 Benchmark Deep Learning Architectures

DeepCTRL couples data representations with rules of physical worlds by introducing separate data and rule encoders and a decision encoder to merge their outputs [Seo et al., 2021]. Fig.3.2a depicts DeepCTRL approach adapted to the minimum length scheduling problem in WPCNs by combining a problem-specific rule encoder which is trained to prevent data outage with a data encoder which is trained to minimize the MSE loss.

Deep unfolding is another problem-driven method that unfolds the repeated iterations into T number of blocks boosted by DNNs [Balatsoukas-Stimming and Studer, 2019]. Typically T is much smaller than the required number of iterations by optimization theory-based approaches. Fig.3.2b depicts our adaptation of deep-unfolding for the minimum length scheduling problem in WPCNs. Instead of replacing problem-specific mathematical derivations with DNNs as in SB-DNN, the update state of the iterative algorithm is replaced by a DNN, which helps to reduce the required number of blocks to find a sub-optimal/optimal solution. In each block of the unfolding, IT lengths are calculated by formulations derived from the optimality conditions of the problem for the given EH length. Then, the next EH length is determined by a DNN. We set T as half of the number of sources plus one. We apply end-to-end supervised training.

The main difference between deep unfolding and SB-DNN is which inner block of OPT is replaced by a DNN. Deep unfolding replaces the update state of OPT to reduce the number of iterations. SB-DNN replaces the model-based computations but uses the number of iterations as in OPT.

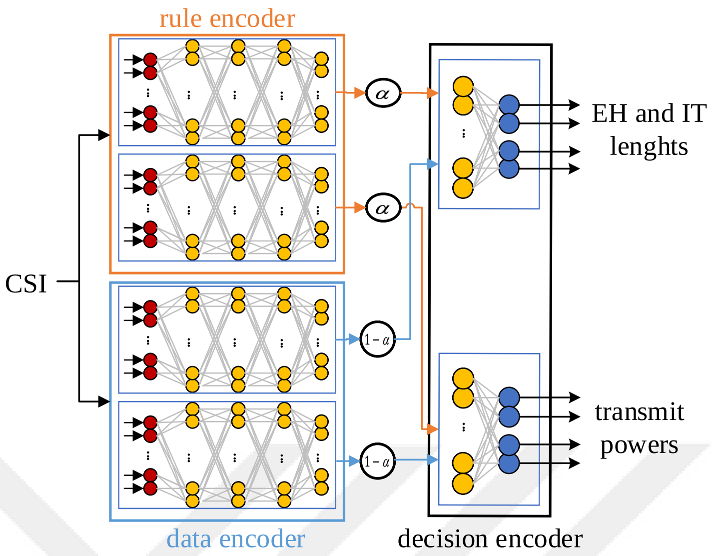

(a)

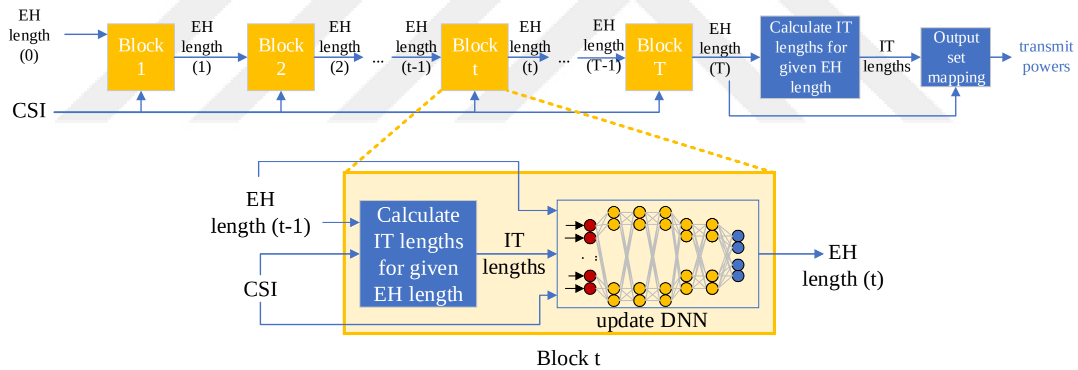

(b)

Figure 3.2: The block diagram of benchmark algorithms: a) DeepCTRL b) Deep unfolding

3.5 Performance Evaluation

In this section, we compare the performances of our proposed deep neural network solutions, to the benchmark algorithms POWMU[Salik et al., 2019], MAX-EH[Salik et al., 2019] and Transmission Completion Time-minimized (TCT) Algorithm [Chi et al., 2017], DEEP-CTRL, and deep unfolding via numerical simulations. POWMU is the algorithm we use to obtain optimal solutions for the supervised training of the

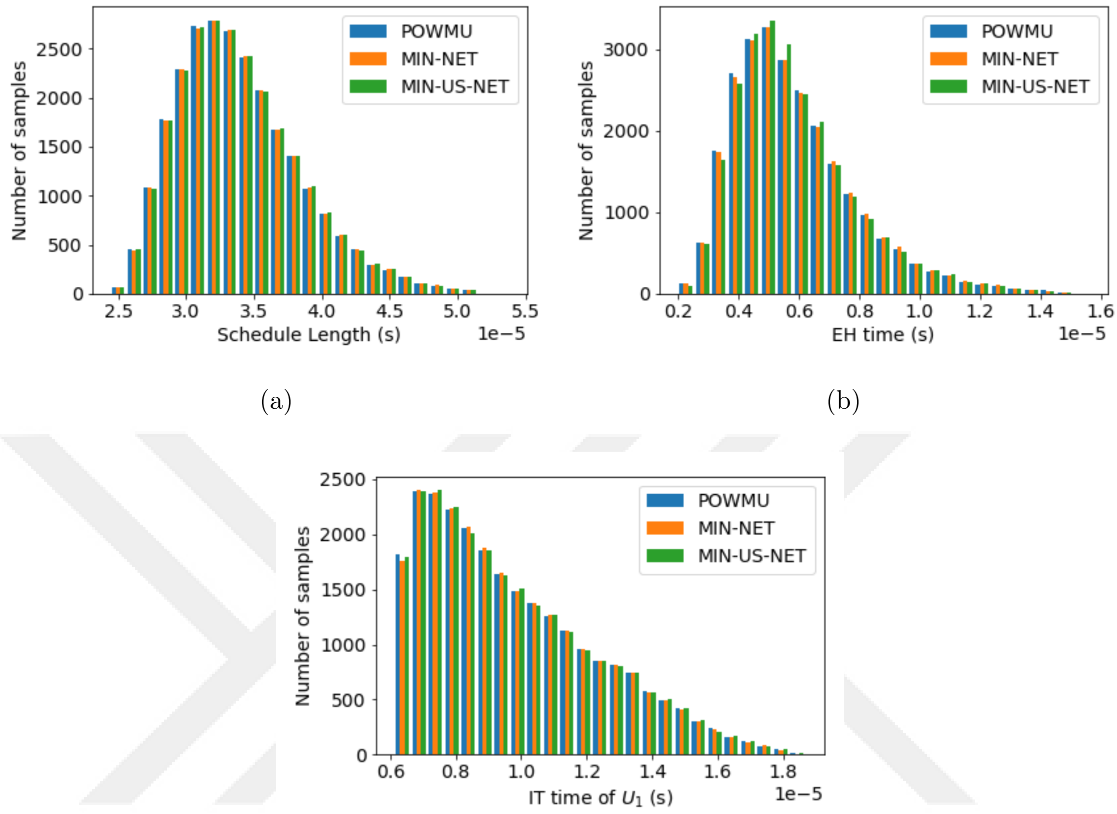

(a) (b)

(c)

Figure 3.3: Distribution of optimal and predicted (a) schedule length, (b) EH time, and (c) IT Time of U_1 in 4-user network.

proposed DNN architecture. MAX-EH obtains a sub-optimal solution by transforming N-user networks into N single user networks. TCT finds the optimal schedule length for HTT WPCN where the users are free to transmit at any power. In our simulations, we force TCT to obey P_{max} limitation, i.e., for any user allocated to transmit at a power level greater than P^{max}, its transmit power is adjusted to P^{max}. Hence, TCT also provides a sub-optimal solution.

All deep learning approaches are implemented in PyTorch. Adam optimizer with batch size 32 and learning rate 10^{-4} is utilized to optimize the network weights. 250,000 independent random network realizations are generated as described in Section 3.4.2 for each simulated N-user network under different network conditions.

Generated data is divided into train, validation and test sets with 80%, 10%, 10% ratios, respectively. The performance of the benchmark algorithms are also measured over the test data. Thus, the simulations results are presented as average of the performance over 25,000 independent random network realizations. All simulations are performed by a laptop with Windows 64-bit OS, 8GB RAM, Intel i7-7600U dual core processor.

We consider an indoor environment operating at a center frequency of $f_c = 915$ with the following simulation parameters: $W = 1$ MHz, $N_0 = -110$ dBm, $\sigma_Z = 2$ dB, $PL(d_0) = 31.7$ dB, $\upsilon = 2$, $\zeta_i = 0.5 \forall i$, $D_i = 50$ bits $\forall i$, $P_{AP} = 2$ W, and $P^{max} = 1$ mW.

Figure 3.3 illustrates the distribution of optimal and predicted schedule length, EH time, and IT time of the 1^{st} user in a 4-user network over the entire test set. Similar IT time distributions are observed for other users of the network. The DNN based solutions, MIN-NET and MIN-US-NET, very well approximate the optimal solution of the problem (3.1).

Figure 3.4 indicates the gain, provided by α and γ as inputs of the network, in training and validation losses of the supervised learning. Feeding α and γ into the network provides 30% lower loss.

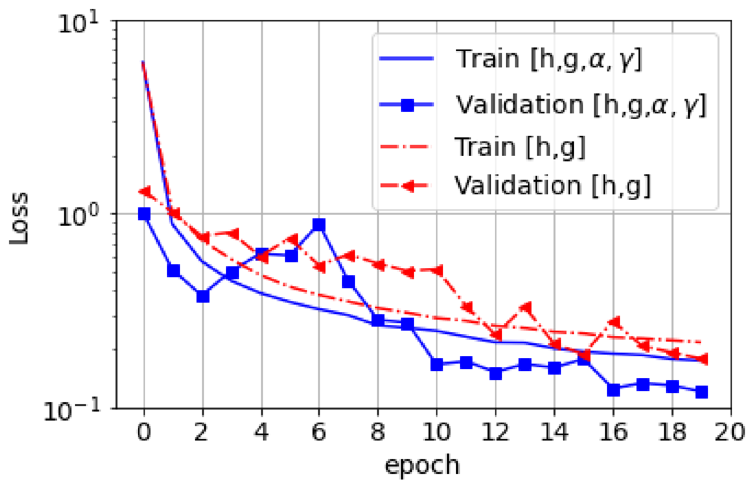

Figure 3.4: Train and validation losses for 4-user network for different input sets.

Figure 3.5 depicts the schedule length for increasing number of users from 10 to 20. TCT performs worse than all other algorithms since it does not take UL transmit power limitation into account. The neural network based solutions MIN-NET and MIN-US-NET outperforms MAXEH. MIN-NET performs very closely to the optimal algorithm POWMU. The maximum optimality gap for MIN-NET, MIN-US-NET, MAXEH, and TCT are 0.12%, 0.82%, 1.05%, and 3.36%, respectively.

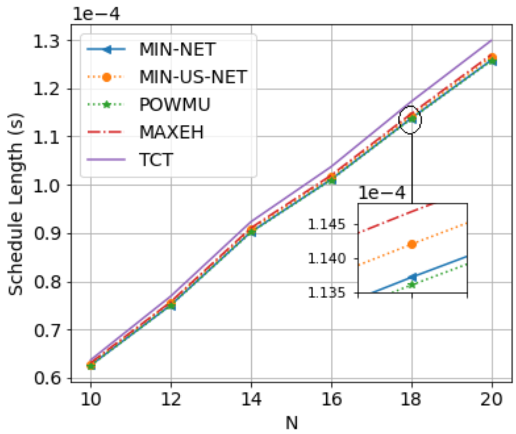

Figure 3.5: Schedule length for different number of users.

Figure 3.6 presents the schedule length of 4-user network for different P^{max}. TCT converges to the optimal solution as P^{max} increasing; whereas MAXEH performs better for lower P^{max}, as expected. On the other hand, the DNN based solutions are robust against changing P^{max} as they perform very closely to the optimum for each P^{max}. The supervised approach MIN-NET slightly outperforms the unsupervised approach MIN-US-NET for lower P^{max}; while the opposite is true for higher P^{max}.

Figure 3.7 shows the schedule length of 4-user network for varying P_{AP}. TCT is outperformed by all algorithms. MIN-NET,MIN-US-NET and MAXEH converge to the optimum as P_{AP} increasing. The optimality gap of MAXEH increases as P_{AP} decreasing so MIN-NET and MIN-US-NET easily outperform MAXEH for lower P_{AP}.

Figure 3.8 indicates the run-time performance of the algorithms for different number of users ranging from 2 to 20 where error-bars represent the standard de-

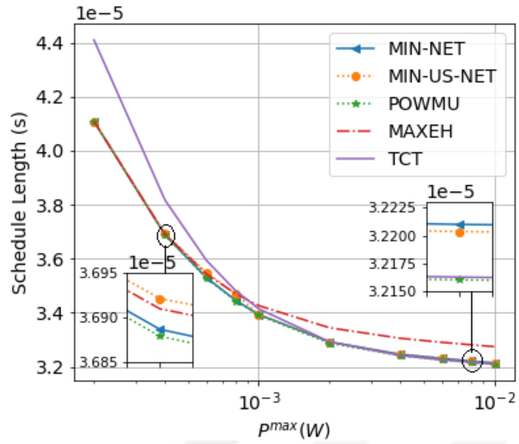

Figure 3.6: Schedule length vs. the maximum transmit power of users for 4-user network.

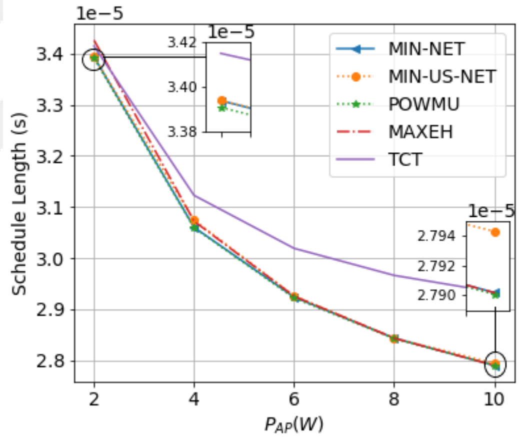

Figure 3.7: Schedule length vs. transmit power of AP for a 4-user network.

viation in run-time. For a fair comparison, MATLAB implementations of all the algorithms are used for run-time evaluation. The forward propagation phase of DNN based approaches are implemented in MATLAB as of matrix multiplications and activation functions for which the matrix weights are exported from PyTorch models. The run-times of MIN-NET and MIN-US-NET are very close since they use the same network architecture for which the number of matrix calculations in the forward propagation is the same. Note that the DNN training is offline so the

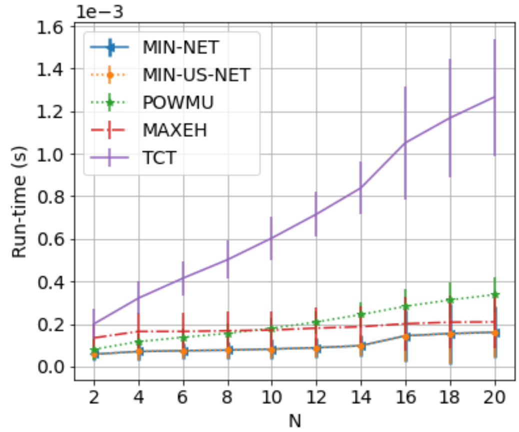

Figure 3.8: Run-times of the algorithms for different number of users.

training times are not taken into account here. MIN-NET and MIN-US-NET are up to 8.5, 2.3, 2.5 times faster than TCT, MAXEH, and POWMU, respectively. For $N = 10$, the run-times of MIN-NET and MIN-US-NET is lower than 0.1ms.

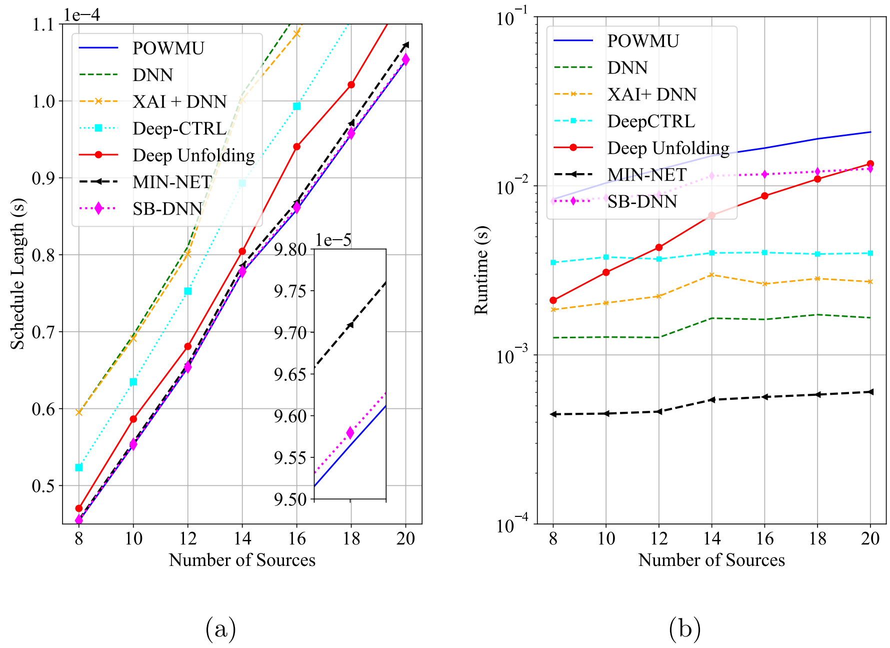

Figure 3.9: a) Schedule length vs. number of sources b) Runtime vs. number of sources

Figs. 3.9a and 3.9b show the schedule length and the runtime for different number of sources, respectively. POWMU reaches the minimum schedule length with the highest runtime, as expected. The runtime of solving sub-problems, e.g., via fixed point iterations, rapidly increases with the number of sources. SB-DNN performs very close to POWMU with runtime improvement due to the usage of DNN in the solution of the sub-problems. The difference in the runtime of POWMU and SB-DNN increases as the network size increases. In DNN and XAI+DNN, the outputs may not satisfy the data demands due to the prediction errors despite the loss function enforcing the minimization of data outage amount. In such cases, to ensure a feasible solution, scheduling is repeated for sources with remaining information to send. This repetition causes a longer schedule length than the optimum. XAI+DNN utilizes additional features compared to DNN, resulting in lower schedule length but higher runtime than DNN. DeepCTRL provides higher accuracy since it also benefits from the rule encoder. The disadvantage of the additional rule encoder is additional runtime compared to DNN. MIN-NET provides close to optimum solutions with up to 2% gap as OSM simplifies the learning process during training and ensures a feasible solution. MIN-NET also results with the lowest runtime since it uses only one DNN architecture, thanks to OSM. Deep unfolding provides competitive results in terms of schedule length; whereas its runtime increases as T increases with number of sources. In runtime vs. optimality trade-off, MIN-NET provides the lowest runtime; whereas SB-DNN provides the highest accuracy.

In general, deep unfolding is advantageous for the problems where the optimization theory based algorithms have exponential runtime so obtaining labels or inner iteration parameters becomes infeasible even for offline training with increasing network sizes. For the minimum length scheduling problem considered in this work, optimal algorithm POWMU has polynomial runtime so we can train SB-DNN in single block based on EH length updates of POWMU which brings an advantage in runtime for larger size networks.

3.6 Conclusion

This paper proposes two DNN-based approaches for the minimum length scheduling problem in half-duplex WPCNs. The original problem is formulated for single antenna AP, and multiple single antenna users with energy harvesting capability. The problem aims to optimize EH and IT times, and UL transmit powers for minimum scheduling length under minimum data and maximum transmit power limitations of the users. The problem is hard to solve through iterative algorithms due to its non-convexity and non-linearity. For a low complexity and robust solution, we purpose several deep learning architectures whose inputs are the channel gains and parameters derived from these gains; and outputs are power, EH, and IT time allocations. The best DNN-based approach provides up to 2.3, 2.5, and 8.5 times lower run-time than three different iterative benchmark algorithms. This approach also outperforms benchmark heuristic algorithms with high accuracy with only 0.12% optimality gap and robustness against varying network conditions.

Chapter 4

OPTIMIZATION THEORY AND DEEP LEARNING BASED RESOURCE ALLOCATION IN NET-ZERO-ENERGY NETWORKS WITH SHORT PACKETS

4.1 Introduction

Low latency and net-zero energy communication are the key requirements of 6G for massive Internet of Things (IoT) deployments [Viswanathan and Mogensen, 2020]. Low latency can be addressed by minimum length scheduling; whereas RF energy harvesting (EH) networks enable net-zero energy communication for the information sources. Furthermore, short packets are typical forms of traffic generated by IoT systems and require incorporating the short blocklength constraint into information theoretic analysis [Durisi et al., 2016]. Thus, the study on the minimum length scheduling for net zero energy networks with short packets is essential.

RF-EH networks with short packet transmissions are recently studied for energy efficiency in UAV systems [Xie et al., 2023a], packet error rate minimization in cognitive IoT [Vu et al., 2022], and throughput maximization in multihop networks [Nguyen et al., 2023]. These works present polynomial time iterative algorithms for the sub-optimal or near-optimal solutions to the problems. In [Nguyen et al., 2023], additionally, a convolutional neural network is trained with the solutions of the iterative algorithm to obtain a low-complexity solution. None of these works optimize the schedule length or latency.

The minimum length scheduling problem is widely considered in RF-EH networks but without short packets. For instance, the problem is formulated for full-duplex systems in [Iqbal et al., 2022b] and half-duplex systems in [Onalan et al., 2020, Onalan et al., 2022]. [Iqbal et al., 2022b] and [Onalan et al., 2020] propose polynomial time iterative algorithms for optimal and sub-optimal solutions; whereas [Onalan et al., 2022] presents a deep learning based low-complexity sub-optimal solution.

In RF-EH networks, the minimum length scheduling with short packets is only studied in [Chen et al., 2019] by jointly optimizing information transmission (IT) times and packet error rate. The authors suggest iterative algorithms for the sub-optimal solutions to the problem that solves a complex mathematical equation in each iteration, so it suffers from high runtime. However, algorithm runtime is as significant as total time minimization for low latency requirements.

This letter studies the minimum length scheduling problem for the optimization of power allocation, EH duration, and IT duration in RF-EH networks with short packets. We first propose a bi-level optimization based framework to derive an iterative algorithm for a near-optimal solution. To overcome the high runtime of the iterative algorithm, we also propose a low complexity optimization theory based deep learning framework, in which the output layer is simplified based on optimality analysis of the problem.

4.2 System Model and Assumptions

We consider a half duplex RF-EH network with a single antenna access point (AP) and N single antenna sources, denoted by $S_i, i = 1, 2, \ldots, N$. Time Division Multiple Access is employed, with the AP broadcasting signals in the downlink (DL) for the sources to harvest energy during τ_0 amount of time. Then, each source uses the harvested energy to send $D_i \geq 0$ amount of data to the AP in the uplink (UL) during τ_i amount of time. At the beginning of each frame, the AP obtains the DL and UL block fading channel gains [Chen et al., 2019, Nguyen et al., 2023], denoted by h_i and $g_i, i = 1, 2, \ldots, N$, respectively, and calculates the current schedule and informs the sources about it in a negligible amount of time. The AP can decide for a source S_i under deep fading not to transmit in that frame by setting $D_i = 0$.

The energy harvested at S_i is $E_i = \zeta_i P_A h_i \tau_0$, where $\zeta_i \in (0, 1)$ is the constant EH efficiency of S_i and P_A is constant transmit power of the AP, which is large enough to ignore the receiver noise component in EH. This model is valid if the input power of the EH circuit ranges in the linear regions of the rectifier and is widely adopted in the literature [Nguyen et al., 2023, Xie et al., 2023a, Vu et al., 2022].

The sources rely on rechargeable batteries, e.g., super-capacitors, with high self-discharge rates, so the energy harvested in a time frame cannot be stored for further use [Vu et al., 2022]. The energy storage of such batteries is low but assumed to be larger than the maximum amount of energy that can be harvested in a time frame. The continuous power model is applied for UL IT, meaning that the transmit power can take any value below a maximum level P^{max}. For IT, the sources use a portion, $\eta_i \in (0, 1]$, of their harvested energy. Thus, the average transmit power P_i of S_i is

$$P_i(\eta_i, \tau_0, \tau_i) = \frac{\eta_i E_i}{\tau_i} = \frac{\eta_i \zeta_i P_A h_i \tau_0}{\tau_i}. \tag{4.1}$$

There is no interference during IT. Finite block-length codes are used for which each source S_i encodes D_i data bits into a codeword block with a length of n. Thus, given packet error probability ϵ and packet length n, the UL rate for S_i is

$$R_i(\eta_i, \tau_0, \tau_i) \approx W \left[C(\rho_i) - \sqrt{\frac{V(\rho_i)}{\tau_i W}} Q^{-1}(\epsilon) \right] \tag{4.2}$$

where $\rho_i = \frac{g_i \eta_i \zeta_i P_A h_i \tau_0}{\tau_i W N_0}$ is SNR, $C(\rho_i) = \log(1 + \rho_i)$ is Shannon's channel capacity, N_0 is Additive White Gaussian Noise (AWGN) power spectral density at the AP, W is the channel bandwidth, $V = 1 - (1 + \rho_i)^{-2} \log_2(e)^2$ is the channel dispersion, and $Q(.)$ is the Gaussian Q function. $V \approx 1$ at high SNR values [Schiessl et al., 2015], which is a reasonable assumption as high SNRs are also required for ultra-reliability [Zhao et al., 2022].

4.3 Optimization Problem

This section formulates the minimum length scheduling problem with the objective of minimizing the total EH and IT durations as follows:

$$\min_{\substack{\tau_0, \tau_i, \eta_i, \\ i=1,2,\ldots,N}} \tau_0 + \sum_{i=1}^{N} \tau_i \tag{4.3a}$$

$$\text{s.t. } (1-\epsilon)\tau_i R_i(\eta_i, \tau_0, \tau_i) \geq D_i, i = 1, 2, \ldots, N, \tag{4.3b}$$

$$P_i(\eta_i, \tau_0, \tau_i) \leq P^{max}, \quad i = 1, 2, \ldots, N, \tag{4.3c}$$

$$\eta_i \leq 1, \qquad i = 1, 2, \ldots, N, \tag{4.3d}$$

$$\tau_0, \tau_i, \eta_i \geq 0, \qquad i = 1, 2, \ldots, N, \tag{4.3e}$$

The variables of the optimization problem are τ_0, EH duration; τ_i, IT duration of S_i; and η_i, exhausted portion of the harvested energy for S_i. Eq. (4.3b) ensures that S_i sends at least D_i bits to the AP. Eq. (4.3c) employs the maximum UL transmit power limit. Eq. (4.3d) limits the transmit power by harvested energy at that time frame. Eq. (4.3e) gives the non-negativity constraints.

Lemma 9. *Problem (4.3) is non-convex and non-linear.*

Proof. We prove the non-convexity of the problem by showing that the constraint given by Eq. (4.3c) does not represent a convex set. The eigenvalues of Hessian matrix of $P_i(\eta_i, \tau_0, \tau_i)$, given by Eq. (4.1), are

$$\lambda_i^1 = 0 \tag{4.4}$$

$$\lambda_i^2 = \zeta_i P_A h_i \left(\sqrt{(\tau_0^2 + \tau_i^2)(\eta_i^2 + \tau_i^2)} + \eta_i \tau_0 \right) / \tau_i^3 \tag{4.5}$$

$$\lambda_i^3 = \zeta_i P_A h_i \left(-\sqrt{(\tau_0^2 + \tau_i^2)(\eta_i^2 + \tau_i^2)} + \eta_i \tau_0 \right) / \tau_i^3. \tag{4.6}$$

$\lambda_i^2 > 0$, since $P_A, \tau_0 > 0$ and $\zeta_i, h_i, \eta_i, \tau_i > 0, \forall i, i = 1, \ldots, N$. $\lambda_i^3 < 0$, since $\sqrt{(\tau_0^2 + \tau_i^2)(\eta_i^2 + \tau_i^2)} > \tau_0 \eta_i, \forall i, i = 1, \ldots, N$. Hence, Hessian matrix of $P_i(\eta_i, \tau_0, \tau_i)$ is neither semidefinite positive nor semidefinite negative. P_i is neither convex nor concave function of (η_i, τ_0, τ_i). Consequently, Eq. (4.3c) does not represent a convex set. □

4.4 Bi-Level Optimization based Framework

We transform Problem (4.3) into bi-level optimization by decomposing it into N convex sub-problems regarding each S_i for fixed τ_0. The sub-problems are then coordinated by a master problem whose variable is τ_0. The optimal solution to the master problem is optimal for the original problem [Chiang et al., 2007].

Sub-problems: All of the sub-problems are in the same reduced form of Problem (4.3) for $N = 1$ and fixed $\tau_0 = \overline{\tau_0}$. We further define an auxiliary variable z

$$z = (1-\epsilon)W\tau_1\sqrt{\frac{1}{\tau_1 W}}Q^{-1}(\epsilon) \tag{4.7}$$

to rewrite the constraint given by Eq. (4.3b), i.e,

$$(1-\epsilon)W\tau_1\left[\log_2\left(1+\frac{\gamma_1\eta_1\overline{\tau_0}}{\tau_1}\right)-\sqrt{\frac{1}{\tau_1 W}}Q^{-1}(\epsilon)\right] \geq D_1, \tag{4.8}$$

as

$$(1-\epsilon)W\tau_1\log_2\left(1+\frac{\gamma_1\eta_1\overline{\tau_0}}{\tau_1}\right) - z \geq D_1 \tag{4.9}$$

where $\gamma_1 = \frac{\zeta_1 P_A h_1 g_1}{W N_0}$. Eq (4.7) can also be written as $\tau_1 = \beta z^2$ where

$$\beta = \frac{1}{W\left((1-\epsilon)Q^{-1}(\epsilon)\right)^2}. \tag{4.10}$$

Then, the sub-problems are given as follows:

$$\min_{\tau_1,\eta_1,z} \; \tau_1 \tag{4.11a}$$

$$\text{s.t. } \tau_1(1-\epsilon)W\log_2\left(1+\frac{\gamma_1\eta_1\overline{\tau_0}}{\tau_1}\right) \geq D_1 + z \tag{4.11b}$$

$$\tau_1 = \beta z^2 \tag{4.11c}$$

$$\eta_1\zeta_1 P_A h_1\overline{\tau_0}/\tau_1 \leq P^{max}, \tag{4.11d}$$

$$\eta_1 \leq 1 \tag{4.11e}$$

$$\tau_1, \eta_1, z \geq 0, \tag{4.11f}$$

Definition 2. *$\ddot{z}$, $\ddot{\tau}_1$, and $\ddot{\eta}_1$ are defined as the values of z, τ_1 and η_1, respectively, in the solution of Problem (4.11) when Eqs. (4.11b)-(4.11d) hold with equality. This means that S_1 transmits D_1 amount of data at P^{max}. The fixed EH duration, $\overline{\tau_0}$, must follow $\overline{\tau_0} \geq \ddot{\tau}_0 = \frac{P^{max}\ddot{\tau}_1}{\zeta_1 P_A h_1}$. A second order polynomial of z is formulated by Eqs. (4.11c) and (4.11d) into Eq. (4.11b). The real and positive solution of this polynomial is derived as*

$$\ddot{z} = \frac{\sqrt{4(1-\epsilon)\beta D_1 W\log_2\left(1+\frac{P^{max}g_1}{WN_0}\right)+1}+1}{2(1-\epsilon)\beta W\log_2\left(1+\frac{P^{max}g_1}{WN_0}\right)}. \tag{4.12}$$

By considering $z = \ddot{z}$, Eqs. (4.11d) and (4.11b), holding with equality, $\ddot{\tau}_1$ and $\ddot{\eta}_1$ are expressed as

$$\ddot{\tau}_1 = \frac{D_1 + \ddot{z}}{(1-\epsilon)W \log_2\left(1 + \frac{P^{max} g_1}{W N_0}\right)}, \tag{4.13}$$

$$\ddot{\eta}_1 = \frac{P^{max} \ddot{\tau}_1}{\zeta_1 P_A h_1 \overline{\tau_0}}. \tag{4.14}$$

Lemma 10. *Let us rewrite Eq. (4.11b) such that η_1 is a function of τ_1 and z, i.e. $\eta_1 \geq G(\tau_1, z) \triangleq \frac{\tau_1}{\overline{\tau_0}\gamma_1}(2^{\frac{D_1+z}{W\tau_1(1-\epsilon)}} - 1)$. $G(\tau_1, z)$ is increasing and convex function of z.*

Proof. We show the first and second derivatives of $G(\tau_1, z)$ with respect to z are positive as follows:

$$\frac{\delta G(\tau_1, z)}{\delta z} = \frac{\ln(2) 2^{\frac{D_1+z}{W\tau_1(1-\epsilon)}}}{(1-\epsilon)\gamma_1 \overline{\tau_0} W} > 0 \tag{4.15}$$

and

$$\frac{\delta^2 G(\tau_1, z)}{\delta z^2} = \frac{\ln^2(2) 2^{\frac{D_1+z}{W\tau_1(1-\epsilon)}}}{(1-\epsilon)^2 \gamma_1 \overline{\tau_0} W^2 \tau_1} > 0 \tag{4.16}$$

as $\gamma_1, \overline{\tau_0}, W > 0$ and $\epsilon < 1$. □

Theorem 4. *The optimal solution $(\overline{z}, \overline{\eta_1}, \overline{\tau_1})$ to Problem (4.11) is obtained as follows. For $\overline{\tau_0} \geq \ddot{\tau}_0$, $\overline{z} = \ddot{z}$, $\overline{\eta_1} = \ddot{\eta}_1$, and $\overline{\tau_1} = \ddot{\tau}_1$ by Eqs. (4.12)-(4.14). Otherwise, $\overline{\eta_1} = 1$, $\overline{z}$ is derived as a solution of the nonlinear equation $\beta \overline{z}^2 (1-\epsilon) W \log_2\left(1 + \frac{\gamma_1 \overline{\tau_0}}{\beta \overline{z}^2}\right) \geq D_1 + \overline{z}$ and $\overline{\tau_1} = \beta \overline{z}^2$.*

Proof. We prove the lemma via a graphical approach. Fig. 4.1 indicates the feasible region for Problem (4.11). As $G(\tau_1, z)$ is a convex and increasing function of z by Lemma 10, $G(\tau_1, z)$ curves for different z such as z_1, z_2, and z_3, are nonintersecting nested curves. To satisfy the minimum demand amount D_1, the solution must lie above the $G(\tau_1, z)$ curve. To satisfy Eq. (4.11c), the solution must be at the corresponding vertical dashed line.

The objective function τ_1 is independent from η_1 but dependent on z. For the minimum τ_1, we would pick the leftmost point in the feasible region. z value determines the location of the feasible region. Similarly, for the minimum τ_1, we would position the feasible region at the leftmost point by picking the lowest possible z.

When $\overline{\tau_0} \geq \ddot{\tau}_0$, i.e. the source can harvest enough energy to transmit at P_{max}, Eq. (4.11d) limits $G(\tau_1, z)$ to go left further (option 1). Then the solution is point A where $\overline{z} = \ddot{z}$, $\overline{\eta_1} = \ddot{\eta}_1$, and $\overline{\tau_1} = \ddot{\tau}_1$ by Eqs. (4.12)-(4.14).

Otherwise, i.e., $\overline{\tau_0} < \ddot{\tau}_0$, Eq. (4.11d) does not affect the feasible region (option 1). The energy causality constraint given by Eq. (4.11e) limits $G(\tau_1, z)$ moving further left. Due to Eq. (4.11e), a feasible solution must be under the $\eta = 1$ line. Therefore, the optimum solution is at the intersection of Eqs. (4.11b), (4.11c), and (4.11e), which is point B. $\square$

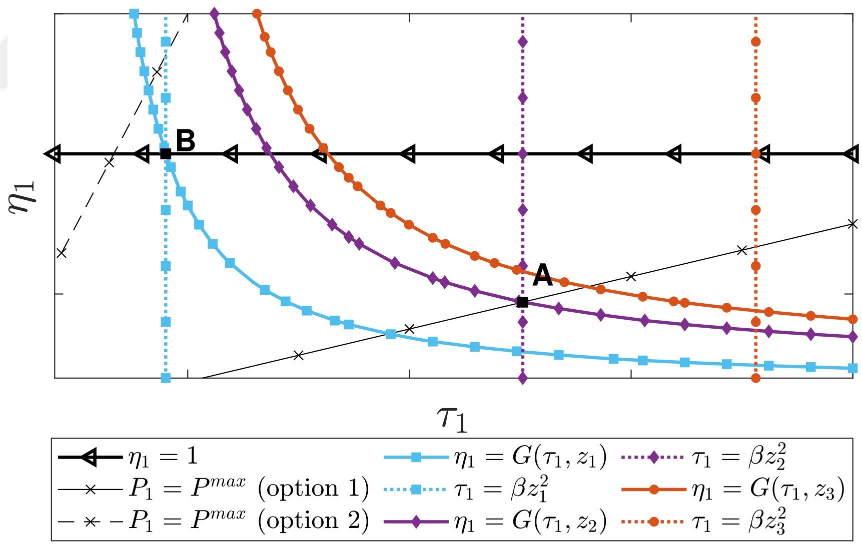

Figure 4.1: Graphical representation of the feasible region for Problem (4.11) for $z_1 < z_2 < z_3$.

Master Problem: Next, we prove that the objective of the master problem, i.e., the total EH and derived IT durations, is convex over EH time. This will enable us to search for optimal EH time with the golden search method.

Lemma 11. *$\overline{\tau_1}(\overline{\tau_0})$ is subdifferentiable at every $\overline{\tau_0} \in \textbf{dom}\overline{\tau_1}$.*

Proof. For $\overline{\tau_0} \neq \ddot{\tau_0}$, the derivative of the function exists. For $\overline{\tau_0} = \ddot{\tau_0}$, we show subdifferential of the function at $\ddot{\tau_0}$, $\partial\overline{\tau_1}(\ddot{\tau_0})$, exists. The sub-gradient vector v satisfies $v(x - \ddot{\tau_0}) \leq \overline{\tau_1}(x) - \overline{\tau_1}(\ddot{\tau_0})$ for all $x \in \mathbf{dom}\overline{\tau_1}$. If the EH time is greater than the required time for harvesting energy to transmit at P^{max}, i.e., $x \geq \ddot{\tau_0}$, sources are forced to transmit at P^{max} and IT duration is constant, i.e., $\overline{\tau_1}(x) = \overline{\tau_1}(\ddot{\tau_0})$. So $v(y - \ddot{\tau_0}) \leq 0$, then, $m \leq 0$. Otherwise, i.e., $x < \ddot{\tau_0}$, $v \leq \mu = \frac{\overline{\tau_1}(y) - \overline{\tau_1}(\ddot{\tau_0})}{x - \ddot{\tau_0}}$. $\overline{\tau_1}(x) - \overline{\tau_1}(\ddot{\tau_0}) > 0$ since $\overline{\tau_1}(x)$ is a decreasing function of x, then, $\mu < 0$. Thus, $\partial\overline{\tau_1}(\ddot{\tau_0}) = [\mu, 0]$. □

Theorem 5. *The objective function of the master problem, $g(\overline{\tau_0}) = \overline{\tau_0} + \sum_{i=1}^{N} \overline{\tau_i}(\overline{\tau_0})$, is convex over $\overline{\tau_0}$.*

Proof. We prove that $\overline{\tau_1}(\overline{\tau_0})$ is convex, then, $g(\overline{\tau_0})$ is also convex as $\overline{\tau_i}(\overline{\tau_0})$s are all in the same form, and the convexity is closed under sum. By following Theorem 2.4.1 in [Zalinescu, 2002], $\overline{\tau_1}(\overline{\tau_0})$ is convex since 1) $\overline{\tau_1}(\overline{\tau_0}) : (0, +\infty) \to (0, +\infty)$, is proper as $\mathbf{dom}\overline{\tau_1}$ is not an empty set; 2) $\mathbf{dom}\overline{\tau_1}$ is convex; 3) $\overline{\tau_1}(\overline{\tau_0})$ is subdifferentiable at every $\overline{\tau_0} \in \mathbf{dom}\overline{\tau_1}$ by Lemma 11. □

Based on the bi-level transformation, we can search for optimal $\overline{\tau_0}$ with golden section search method as in Algorithm 4. The golden section search method finds a near-optimal solution with sufficient accuracy by evaluating the objective function at two intermediate points, determined based on the golden ratio of a search interval, and updating the interval accordingly [Luenberger and Ye, 2008]. The upper and lower bounds of the search interval are set to $\max_{i\in\{1,\ldots,N\}} \ddot{\tau}_0^i$ and 0, respectively, where $\ddot{\tau}_0^i = \frac{P^{max}\ddot{\tau}_i}{\zeta_i P_A h_i}$ based on Definition 1 (Line 2). τ_0^λ and τ_0^μ are points in between lb and ub (Line 4). The objective function, $g(\overline{\tau_0}) = \overline{\tau_0} + \sum_i \overline{\tau_i}(\overline{\tau_0})$, is evaluated for $\overline{\tau_0} = \tau_0^\lambda$ and $\overline{\tau_0} = \tau_0^\mu$ (Line 5). If $g(\tau_0^\lambda) \leq g(\tau_0^\mu)$, then, ub is set to τ_0^μ (Line 6). Otherwise, lb is set to τ_0^λ (Line 7). The search continues until the difference between ub and lb is smaller than an error tolerance ε (Line 3). Finally, P_i, $\overline{\tau_i}(\overline{\tau_0})$, $g(\overline{\tau_0})$ are computed where $\overline{\tau_0} = ub$ for $i = 1, \ldots, N$ (Line 8).

Let C be the computational complexity to derive $\overline{\tau_i}$. In each iteration, $\overline{\tau_i}$ is calculated for $i = 1, 2, \ldots, N$. The complexity of golden section search is $\mathcal{O}(log_2(\frac{ub-lb}{\varepsilon}))$

[Luenberger and Ye, 2008]. Hence, the overall complexity of BOBA is $\mathcal{O}(CNlog_2(\frac{ub-lb}{\varepsilon}))$.

Algorithm 4 **Bi-Level Optimization based Algorithm (BOBA)**

Input: P^{max}, P_A, h_i, ζ_i, D_i, for $i = 1, \ldots, N$
Set $lb \leftarrow 0$ and $ub \leftarrow \max_{i\in\{1,\ldots,N\}} \ddot{\tau}_0^i$
while $ub - lb > \varepsilon$ **do**
  $\tau_0^\lambda = lb + 0.382(ub - lb)$ and $\tau_0^\mu = lb + 0.618(ub - lb)$
  Calculate $g(\tau_0^\lambda)$ and $g(\tau_0^\mu)$ based on $\overline{\tau_i}(\tau_0^\lambda)$ and $\overline{\tau_i}(\tau_0^\mu)$ for $i = 1, 2, \ldots, N$ by Thm. 4.
  if $g(\tau_0^\lambda) \leq g(\tau_0^\mu)$, **then** $ub \leftarrow \tau_0^\mu$.
  else $lb \leftarrow \tau_0^\lambda$
Return P_i, $\overline{\tau_i}(\overline{\tau_0})$, $g(\overline{\tau_0})$ where $\overline{\tau_0} = ub$ for $i = 1, \ldots, N$.

4.5 Optimization Theory based Deep Learning Framework

This section presents the optimization theory based deep learning framework for the minimum length scheduling. We propose a deep neural network (DNN) with a simplified output layer based on the optimality conditions of the problem, given in Theorem 6, rather than an output layer consisting of all variables of the problem.

Theorem 6. *In Problem (4.3), for given transmit powers P_i', where $P_i' \leq P^{max}$, of $S_i, i = 1, 2, \ldots, N$, the feasible time allocations $\tau_i', i = 1, 2, \ldots, N$, attaining the minimum schedule length is expressed by*

$$\tau_i' = \frac{(1-\epsilon)Wb^2 + (1-\epsilon)Wb\sqrt{b^2 + \frac{4D_iC(\rho_i')}{(1-\epsilon)W}} + 2D_iC(\rho_i')}{2(1-\epsilon)WC^2(\rho_i')} \tag{4.17}$$

$$\tau_0' = \max_i \left\{ \frac{P_i'\tau_i'}{\zeta_i P_A h_i} \right\} \tag{4.18}$$

for $i = 1, 2, \ldots, N$ where $b = \sqrt{V(\rho_i')/W}Q^{-1}(\epsilon)$.

Proof. Let $\rho_i' = g_iP_i/WN_0$ be the SNR for the given transmit power P_i',, where $P_i' \leq P^{max}$, $i = 1, 2, \ldots, N$. Then, minimum IT times are obtained by satisfying the data requirement constraint in Eq. (4.3b) with equality, i.e.,

$$(1-\epsilon)W\tau_i' \left[C(\rho_i') - \sqrt{\frac{V(\rho_i')}{\tau_i' W}} Q^{-1}(\epsilon)\right] = D_i. \tag{4.19}$$

This is a second-order polynomial function of τ_i' where all the polynomial coefficients are positive numbers. There are two possible solutions. The solution, which always results in real and positive τ_i', is obtained as in Eq. (4.17).

To satisfy the individual energy demands of sources, $(P_i'\tau_i')/(\zeta_i P_A h_i)$ amount of EH time must be allocated individually for each source. Then, the feasible EH time τ_0' for the whole network is the maximum of all individually required EH times as in Eq. (4.18). □

Fig. 4.2 presents the optimization theory based deep learning framework, which includes a multi-input, multi-output, fully connected, and feed-forward DNN architecture. The deep learning framework without considering the optimality conditions for Problem (4.3) would define a non-linear mapping from the DL and UL channel gains to optimal transmit powers and schedule lengths. When we incorporate the optimization theory into the deep learning framework, we simplify the deep learning architecture representing Problem (4.3) by reducing the output set to the transmit powers. Hence, for the proposed DNN, the inputs are channel gains h_i, g_i; whereas the outputs are the transmit powers P_i of each S_i, $i = 1, \ldots, N$. A customized activation function $P^{max}\sigma(x)$, where $\sigma(x)$ is the sigmoid function, is defined in the output layer, to ensure the constraint in Eq. (4.3c). Then, this power allocation is mapped to the optimal EH duration τ_0, and IT duration τ_i of each user S_i, $i = 1, \ldots, N$ based on Eqs. (4.17) and (4.18). This mapping is designed as a second output layer consisting of $N+1$ nodes. There are five hidden layers of the size $16N$, $8N$, $4N$, $2N$, and N. The number of layers is set to five via grid search by evaluating validation loss for the different numbers of layers. Each hidden layer uses ReLU activation function. We employ unsupervised learning to train the DNN predicting optimal P_i, $i = 1, 2, \ldots, N$, by incorporating Eqs. (4.17), (4.18) and Eq. (4.3a) as a loss function. We name the DNN as US-NET.

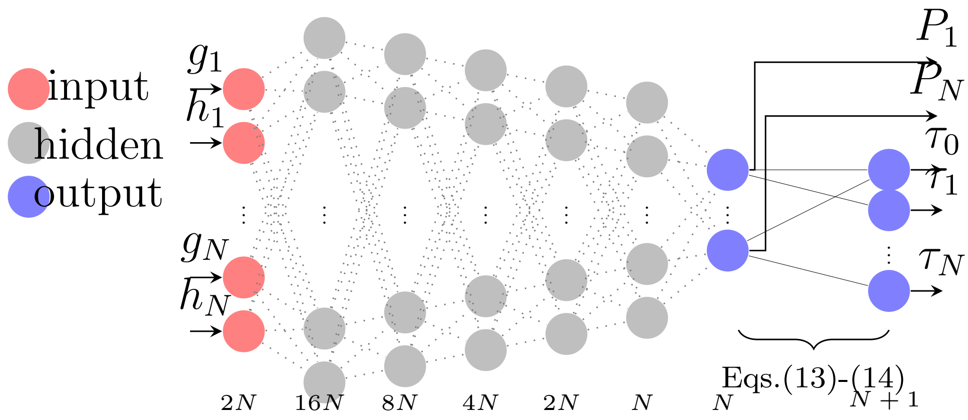

Figure 4.2: The proposed deep neural network architecture

The computational complexity of DNNs is commonly assessed by floating point operations (FLOPs) [Nguyen et al., 2023]. The inference of power allocations requires $404N^2$ FLOPs. The complexity for mapping the powers to time allocations is $\mathcal{O}(N)$.

4.6 Performance Evaluation

In this section, the proposed approaches, BOBA and US-NET, are compared with the benchmark block coordinate descent (BCD) algorithm [Chen et al., 2019], and harvest-then-transmit (HTT) protocol [Ju and Zhang, 2014]. BCD aims to reach the minimum length schedule by jointly optimizing EH and IT durations with a packet error rate lower than a threshold, which is set to ϵ. It optimizes the packet error rate for a given schedule length in the outer loop; whereas it calculates the schedule length for a given error rate in the inner loop. HTT divides unit time block T into $\alpha_0 T$ for EH and $\alpha_i T$ for IT of each source, where $\sum_{i=0}^{N} \alpha_i = 1$, α_i's are optimized for throughput maximization, and T is set to $10\mu s$. HTT and BCD do not consider power allocation with UL transmit power limitation. We enforce the P^{max} limitation on HTT and BCD for a fair comparison. The allocated EH and IT durations, by either HTT or BCD, may not be enough for every S_i to send D_i amount of information. For such sources, the additional schedule length for the remaining data amount is calculated by the corresponding approach.

In an indoor environment, sources are uniformly distributed within a circular area of 1m radius where the AP is located at the center. The simulation parameters are chosen as $W = 1$ MHz, $N_0 = -110$ dBm, $\epsilon = 10^{-5}$, $\varepsilon = 10^{-8}$, $\zeta_i = 0.5 \forall i$, $D_i = 50$ bits $\forall i$, $P_{AP} = 2$ W, and $P^{max} = 1$ mW. The channel attenuation is determined as follows. The large-scale channel fading is modeled as $PL(d) = PL(d_0) + 10 \upsilon log(d/d_0) + Z$, where d is the distance between the source and the AP, $PL(d)$ is the path loss at a distance d in dB, $PL(d_0) = 31.7$ dB, is the path loss at reference distance $d_0 = 1$m, $\upsilon = 2$ is the path loss exponent, and Z is a Gaussian random variable with zero mean and standard deviation $\sigma_Z = 2$. The small-scale channel fading is modeled by Rayleigh fading with scale parameter Ω set to the mean power level obtained by $PL(d)$. Under the given parameters, SNR values are greater than 7dB in all channel realizations in agreement with the high SNR assumption.

Simulations are performed in a laptop with Windows 64-bit OS, 8GB RAM, and Intel i7-7600U dual-core processor. $12,000$ independent random network realizations are generated for each different network size. Generated data is divided into the train, validation, and test sets, with sizes of $10,000$; $1,000$; and $1,000$, respectively. Adam optimizer with batch size 32 and learning rate 10^{-4} are utilized to optimize the network weights for US-NET. The performance of all the algorithms is measured over the same test set.

Fig. 4.3a depicts the schedule length for increasing number of sources from 2 to 12. BOBA reduces the schedule length up to 52% and 32% compared to HTT and BCD, respectively. US-NET performs closely to BOBA with at most 6% gap.

Fig. 4.3b shows the schedule length for varying P^{max} in 5-source network. BOBA and US-NET outperform HTT and BCD, especially at lower P^{max}, e.g., 44% and 35% at $P^{max} = 1$mW, respectively, as they consider P^{max} while adjusting schedule length.

Fig. 4.3c indicates the schedule length for varying ϵ in 5-source network. The optimality gaps of HTT, BCD, and US-NET decrease by 6%, 4%, and 0.2% when

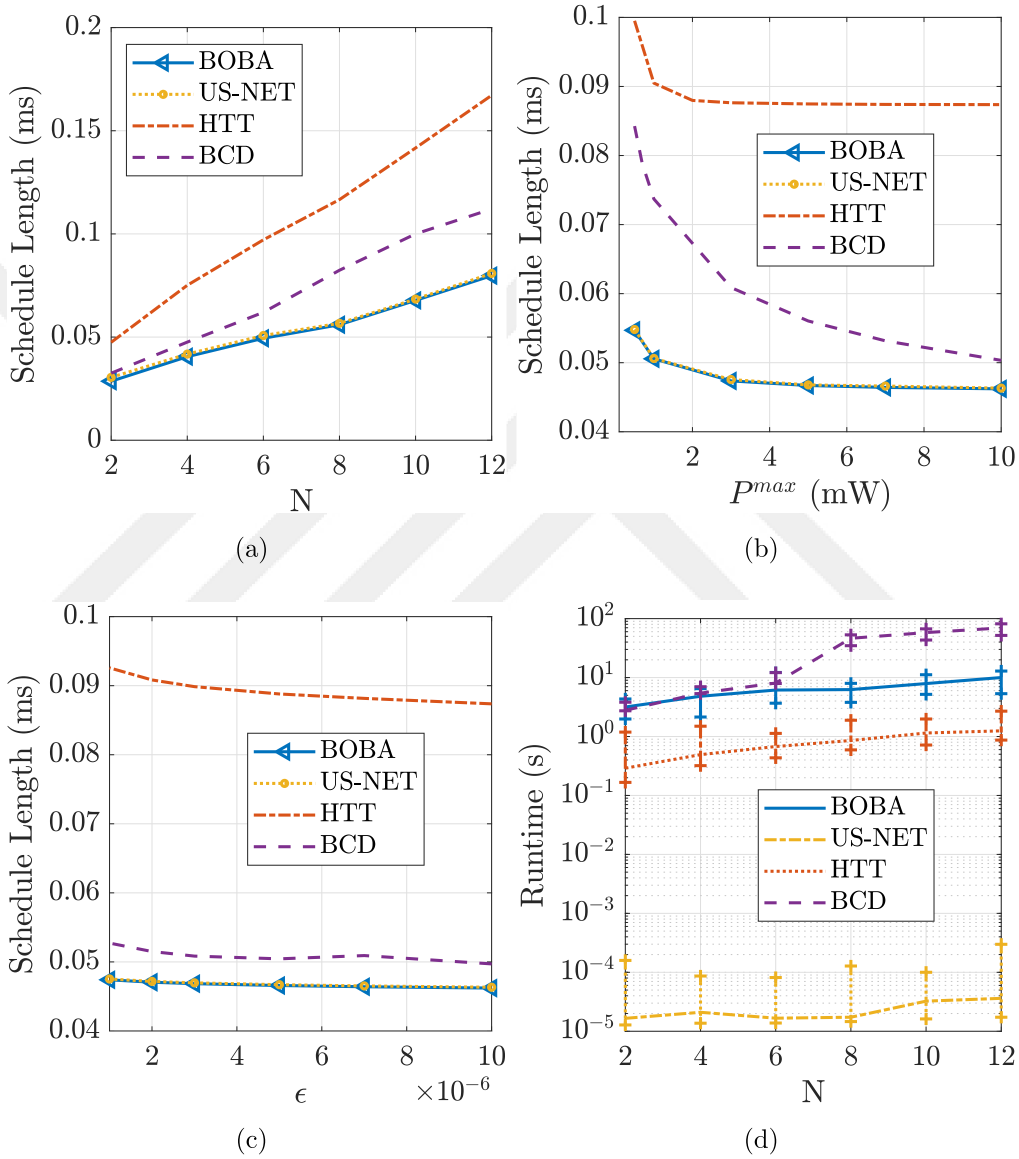

Figure 4.3: (a) Schedule length vs. number of sources, (b) Schedule length vs. UL transmit power limit in 5-source network, (c) Schedule length vs. error rate in 5-source network, and (d) Runtime vs. number of sources.

ϵ increases from 10^{-6} to 10^{-5}. The optimum schedule length is slightly higher for lower ϵ, e.g., 2.6% higher for $\epsilon = 10^{-6}$ than $\epsilon = 10^{-5}$, since lower ϵ causes lower R_i.

Fig. 4.3d presents the average MATLAB runtime of all algorithms for increasing number of sources from 2 to 12. The vertical bars indicate the minimum and maximum runtimes for the given number of sources. HTT, BCD, and BOBA resulting in a very high runtime indicates that computing schedule lengths with an iterative algorithm at the beginning of each time frame takes considerable time. BCD has the highest runtime since it iterates for both error rate and time allocations.

4.7 Conclusion

For the minimum length scheduling problem for net-zero-energy networks, we propose a bi-level optimization-based framework and low-complexity optimization theory based deep learning framework. The former searches for optimal EH duration by calculating the schedule length for a given EH time in each iteration, whereas the latter applies a DNN architecture in which output layer is simplified based on the optimality analysis of the problem. The proposed approaches outperform state-of-art algorithms regarding schedule length, whereas the deep learning approach also provides low runtimes.

Chapter 5

DEEP LEARNING BASED LOW COMPLEXITY RELAY SELECTION FOR WIRELESS POWERED COOPERATIVE COMMUNICATION NETWORKS

5.1 Introduction

Wireless Powered Communication Networks (WPCNs) promise information transmission without a fixed power supply for applications where replacing batteries is costly or even not possible [Lu et al., 2015]. Wireless Powered Cooperative Communication Networks (WPCCNs) employ relays in WPCNs to assist sources for information or energy transfer, which leads to a dramatic increase in reception reliability, energy efficiency, system capacity and network coverage [Chen et al., 2018].

In WPCCNs, the relay selection problem is studied for both half-duplex [Chen et al., 2015, Sui et al., 2018, Onalan et al., 2020] and full-duplex [Kazmi et al., 2020] scenarios with the objective of energy efficiency[Kazmi et al., 2020], lower outage probability[Chen et al., 2015, Sui et al., 2018], throughput maximization [Chen et al., 2015, Sui et al., 2018, Kazmi et al., 2020], and minimum length scheduling [Onalan et al., 2020]. These studies propose iterative algorithms to obtain optimal or suboptimal relay selections. The iterative algorithms that solve a complex mathematical equation in each iteration suffer from high run-time. However, algorithms with high runtime may not be practical for time-critical applications.

Machine Learning (ML) techniques provide robust, low-complexity, and close-to-optimal solutions for many extremely complex scenarios in wireless communications [Kato et al., 2020]. Thus, ML-based solutions have also proliferated for the relay selection in WPCCNs [Si et al., 2021, Zhang et al., 2020, Nguyen et al., 2021, Nguyen et al., 2023, Su et al., 2019, Han et al., 2022]. In[Si et al., 2021], Support Vector Machines (SVMs) are utilized for relay selection problem with the objective of outage minimization in device-to-device multi-hop links under interference. [Zhang et al., 2020] compares SVM and Deep Neural Network (DNN) based relay selection schemes in two-way Simultaneous Information and Power Transfer (SWIPT) for maximum throughput. DNNs are also applied for relay selection problem of single-source-multiple-relay cognitive IoT networks with the objective of throughput maximization [Nguyen et al., 2021]. Deep Reinforcement Learning is applied for relay selection in underwater acoustic sensor networks with energy harvesting (EH) relays for long-term cumulative uplink capacity [Han et al., 2022]. Very recently, cooperative beamforming relay selection empowered by convolutional DNN based channel allocation has been proposed for throughput maximization in single-source-multiple-relay networks with short packet transmissions [Nguyen et al., 2023]. Although the aforementioned works benefit from the ML algorithms to tackle complex problems, none of them applies ML for either minimum length scheduling problem, which is critical for delay-constrained applications, or multiple-relay-multiple-source scenarios, where the problem is more complex due to the joint consideration of all source relay pairs.

This paper considers multiple-source-multiple-relay WPCCN, where relays and sources harvest energy from the radio frequency (RF) signals broadcast by an access point (AP) for the information transmission (IT) from the sources to the AP. We formulate relay selection, scheduling, and power control problem with the objective of minimum schedule length and constraints on demand, energy, and maximum transmit power. A two-step solution strategy is applied, for which we first obtain minimum schedule length and power allocation for a given relay selection by [Onalan et al., 2020], then search for the best relay selection with a DNN. The goal of this paper is to find the optimum relay selection to minimize the total schedule length with a low complexity DNN resulting in low runtime. The major contributions of the paper are listed as follows:

- We formulate the relay selection problem in the two-step solution strategy as a novel multi-class classification problem, where the inputs are channel gains and derived values based on the optimality conditions of the problem, and the outputs are the classes representing all possible relay selection options for each source. We, then, propose a feed-forward DNN architecture for the solution of the classification problem.

- We implement several conventional supervised ML algorithms such as K-Nearest Neighbour (KNN), SVM, Decision Tree (DT), and Random Forest (RF) for benchmarking.

- Simulation results highlight the superiority of DNNs against all other ML algorithms and three state-of-art iterative heuristic algorithms in terms of closeness-to-optimality and low complexity.

The rest of the paper is organized as follows. Section 5.2 describes the system model and the assumptions. Section 5.3 formulates the relay selection, scheduling, and power allocation problem. Section 5.4 presents the DNN-based solution to the problem. Section 5.5 evaluates the performance of the proposed DNN against the benchmark algorithms. Section 5.6 concludes the paper.

5.2 System Model and Assumptions

We consider a half duplex WPCCN containing one AP, N sources, denoted by S_i, $i = 1, 2, \ldots, N$, and K decode-and-forward (DF) relays, denoted by R_j, $j = 1, 2, \ldots K$. The AP, all the sources, and relays are equipped with a single antenna and operate in the same frequency band.

Harvest-then-Cooperate protocol[Chen et al., 2015] is applied as a medium access protocol. In each transmission frame, each source S_i needs to send $D_{S_i} > 0$ amount of data to the AP for $i = 1, 2, \ldots, N$ with the help of a single or no relay. The relays can assist multiple sources and must convey all the information they receive from the sources to the AP. At the beginning of each frame, the AP informs the sources about the current schedule and relay selection in a fixed and negligible time. Then, both relays and sources harvest energy from the signals broadcast by AP during τ_0

amount of time. With the harvested energy, each source S_i communicates directly to the AP or cooperates with a relay R_j to send information to the AP during $\tau_{S_i}^{R_j}$ for $i = 1, 2, \ldots, N$ and $j = 0, 1, 2, \ldots K$, where R_0 refers to AP. Finally, each selected relay R_j conveys the information gathered from the sources to the AP in duration $\tau_{R_j}^{AP}$ for $j = 1, 2, \ldots K$.

The AP has an unlimited power source. However, sources and relays only have rechargeable batteries with low energy storage and high self-discharge rate, e.g., super-capacitors [Kaus et al., 2010]. They cannot store the harvested energy for further use. They have to replenish energy at the beginning of each transmission frame for IT in that frame.

We assume block fading channels. Let h_X^Y and g_X^Y be the channel gains between X and Y for DL and UL, respectively, where $X, Y \in \{AP, S_i, R_j\}$, $i = 1, 2, \ldots, N$ and $j = 1, 2, \ldots K$ (e.g., $h_{AP}^{S_i}$ is the DL channel gain between AP and S_i). All the channel gains are assumed to be known by the AP at the beginning of each time block, similar to the previous works, e.g., [Kazmi et al., 2020, Nguyen et al., 2023]. The energy spent to obtain channel gains at the AP is negligible.

Transmit power of AP, P_A, is assumed to be large enough to ignore noise component during EH phase. All the sources and relays have constant harvesting efficiency denoted by $\zeta_{S_i} \in (0, 1)$ and $\zeta_{R_j} \in (0, 1)$, respectively. This model is valid if the EH circuit is designed such that the EH efficiency is flat over desired receive power range [Choi et al., 2018] and is widely used in the literature [Si et al., 2021, Nguyen et al., 2021, Nguyen et al., 2023]. Hence, the energy harvested at S_i and R_j, for $i = 1, \ldots, N$ and $j = 1, \ldots, K$, can be expressed as $E_{S_i} = \zeta_{S_i} \tau_0 P_A h_{AP}^{S_i}$ and $E_{R_j} = \zeta_{R_j} \tau_0 P_A h_{AP}^{R_j}$, respectively.

We consider a continuous power model where the transmit power takes any value below a maximum level P^{max}. The transmit power is further limited by the amount of the harvested energy. The required energy for decoding the received message at relays is negligible compared to the energy consumption for IT [Gu and Aissa, 2015]. Thus, the average transmit power of S_i and R_j are $P_{S_i}^{R_j} = \nu_{S_i}^{R_j} E_{S_i} / \tau_{S_i}^{R_j}$ and $P_{R_j}^{AP} = \nu_{R_j}^{AP} E_{R_j} / \tau_{R_j}^{AP}$, respectively, where $\nu_{S_i}^{R_j} [\nu_{R_j}^{AP}] \in (0, 1)$

is the amount of energy exhausted at $S_i[R_j]$ during IT.

We ignore interference as all sources and relays use separate time slots for IT. We assume AWGN channel with bandwidth W and power spectral density N_0. Then, the signal-to-noise ratio (SNR) in S_i to R_j for $i = 1, \ldots, N$ and $j = 0, \ldots, K$, and R_j to the AP for $j = 1, \ldots, K$ links are respectively given as

$$\gamma_{S_i}^{R_j} = \frac{P_{S_i}^{R_j} g_{S_i}^{R_j}}{WN_0} = \frac{\nu_{S_i}\zeta_{S_i}\tau_0 P_A h_{AP}^{S_i} g_{S_i}^{R_j}}{\tau_{S_i}^{R_j} WN_0} \tag{5.1}$$

$$\gamma_{R_j}^{AP} = \frac{P_{R_j}^{AP} g_{R_j}^{AP}}{WN_0} = \frac{\nu_{R_j}\zeta_{R_j}\tau_0 P_A h_{AP}^{R_j} g_{R_j}^{AP}}{\tau_{R_j}^{AP} WN_0} \tag{5.2}$$

We use the continuous transmission rate model and Shannon's channel capacity formula for AWGN channels to determine the maximum achievable rate. Hence, the instantaneous UL transmission rates from S_i to R_j and from R_j to AP are given by

$$T_{S_i}^{R_j} = W \log_2(1 + \gamma_{S_i}^{R_j}), \tag{5.3}$$

$$T_{R_j}^{AP} = W \log_2(1 + \gamma_{R_j}^{AP}). \tag{5.4}$$

.

5.3 Optimization Problem

This section, first, presents the mathematical formulation of the relay selection, scheduling, and power control problem, and then, describes the solution strategy for the formulated problem. The optimality conditions of the problem are also analyzed to be exploited for the design of DNN-based solution in the next sections.

5.3.1 Formulation

For a multiple-source-multiple-relay half duplex WPCCN, the relay selection, scheduling, and power control problem with the objective of total time minimization subject to demand, energy, and power constraints is formulated in [Onalan et al., 2020] as follows:

$$\min \qquad \tau_0 + \sum_{i=1}^{N}\sum_{j=0}^{K} \tau_{S_i}^{R_j} + \sum_{j=1}^{K} \tau_{R_i}^{AP} \tag{5.5a}$$

$$\text{s.t.} \quad \sum_{j=0}^{K} b_i^j = 1, \qquad i = 1, \dots, N, \tag{5.5b}$$

$$\frac{\nu_{S_i}^{R_j} \zeta_{S_i} \tau_0 P_A h_{AP}^{S_i}}{\tau_{S_i}^{R_j}} \leq P^{max} b_i^j, \ i = 1, \dots, N, \quad j = 0, \dots, K, \tag{5.5c}$$

$$\frac{\nu_{R_j}^{AP} \zeta_{R_j} \tau_0 P_A h_{AP}^{R_j}}{\tau_{R_j}^{AP}} \leq \min \left\{ P^{max}, P^{max} \sum_{i=1}^{N} b_i^j \right\}, \quad j = 1, \dots, K, \tag{5.5d}$$

$$\tau_{S_i}^{R_j} W \log_2(1 + \gamma_{S_i}^{R_j}) \geq D_{S_i} b_i^j, \quad i = 1, \dots, N, \ j = 0, \dots, K, \tag{5.5e}$$

$$\tau_{R_j}^{AP} W \log_2(1 + \gamma_{R_j}^{AP}) \geq \sum_{i=1}^{N} D_{S_i} b_i^j, \quad j = 1, \dots, K, \tag{5.5f}$$

$$\nu_{S_i}, \nu_{R_j} \in (0, 1) \quad i = 1, \dots, N, \ j = 0, \dots, K \tag{5.5g}$$

$$\tau_0, \tau_{R_j}^{AP}, P_{R_j}^{AP}, \tau_{S_i}^{R_j}, P_{S_i}^{R_j} \geq 0, \quad i = 1, \dots, N, \quad j = 0, \dots, K, \tag{5.5h}$$

$$b_i^j \in \{0, 1\}, \quad i = 1, \dots, N, \ j = 0, \dots, K. \tag{5.5i}$$

The variables of the optimization problem are τ_0, EH duration; $\tau_{S_i}^{R_j}$, IT duration from the i^{th} source to the j^{th} relay; $\tau_{R_j}^{AP}$, IT duration from the j^{th} relay to the AP; $\nu_{S_i}^{R_j}$, ratio of the harvested energy spent for IT at S_i; $\nu_{R_j}^{AP}$, ratio of the harvested energy spent for IT at R_j; and b_i^j, the relay selection parameter which is equal to 1 if R_j is selected for S_i, and 0 otherwise.

The objective of the optimization problem is to minimize the duration of the schedule for EH and IT. Eq. (5.5b) guarantees that each source cooperates with one and only one relay. Remember that a relay can be chosen for more than one source. Eqs. (5.5c) and (5.5d) determine the maximum allowable transmit power of the sources and relays, respectively. If R_j is not selected for S_i, $\nu_{S_i}^{R_j}$ so $P_{S_i}^{R_j}$ is forced to be zero in Eq. (5.5c). If R_j is not selected for any source, then $\nu_{R_j}^{AP}$ so $P_{R_j}^{AP}$ is set to zero by Eq. (5.5d). Demand constraint Eq. (5.5e) requires that each source S_i

conveys a certain amount D_{S_i} of data to the AP. Eq. (5.5f) enforces relays to convey all data they gather from sources to the AP. Eq. (5.5g) defines the range of $\nu_{S_i}^{R_j}$ and $\nu_{R_j}^{AP}$ to adjust the UL transmit powers. Lastly, Eq. (5.5h) and (5.5i) represent non-negativity and integrality constraints, respectively.

The formulated problem is a non-convex Mixed-Integer Non-Linear Programming (MINLP) problem and proved to be NP-hard [Onalan et al., 2020].

5.3.2 Solution Strategy

We first reformulate Problem (5.5) for a given relay selection. When relay selection variables b_i^j's are fixed, Problem (5.5) turns into the scheduling and power control sub-problem for WPCN with multiple source-destination pairs. In our previous studies, we have provided the optimal solution, and close-optimal low-complexity DNN-based solution to this problem [Onalan et al., 2020, Onalan et al., 2022]. We, then, search for the best relay selection with the low-complexity deep learning algorithm, presented in Section 5.4.

Note that this work obtains the optimal solution of the scheduling and power control sub-problem with the Power Constrained Multiple User Time Minimization (POWMU) algorithm proposed in [Onalan et al., 2020] for the fair comparison of benchmark relay selection algorithms also using POWMU in Section 5.5.

5.3.3 Optimality Conditions

For 1-source-1-relay network, under the moderate and high AWGN, the necessary condition on relay selection R_1 at source S_1 is given in [Onalan et al., 2020] as

$$\min\left(g_{S_1}^{R_1} h_{AP}^{S_1}, g_{R_1}^{AP} h_{AP}^{R_1}\right) > g_{S_1}^{AP} h_{AP}^{S_1}. \tag{5.6}$$

This means cooperating with the relay, when Eq. (5.6) is satisfied, results in lower schedule length.

Let us consider each source-relay pair as a single-source-single-relay network. For each $S_i - R_j$ pair, based on Eq. (5.6), total of NK necessary conditions are written as $\min\left(g_{S_i}^{R_j} h_{AP}^{S_i}, g_{R_j}^{AP} h_{AP}^{R_j}\right) > g_{S_j}^{AP} h_{AP}^{S_i}$. We, then, define vector $\boldsymbol{\gamma} \in \mathbb{R}^{N(K+1)\times 1}$ with the elements of these necessary conditions, min $\left(g_{S_i}^{R_j} h_{AP}^{S_i}, g_{R_j}^{AP} h_{AP}^{R_j}\right)$ for $i = 1, 2, \ldots, N$, $j = 1, 2, \ldots, K$ and $g_{S_j}^{AP} h_{AP}^{S_i}$ for $i = 1, 2, \ldots, N$. $\boldsymbol{\gamma}$ will be used as input vector for DNN based solution in Section 5.4.

5.4 Deep Neural Network based Low Complexity Relay Selection

This section presents the DNN framework for the relay selection problem. The relay selection problem is formulated as a classification problem with $(K+1)^N$ classes representing $K+1$ possible relay selection options for N different sources as follows:

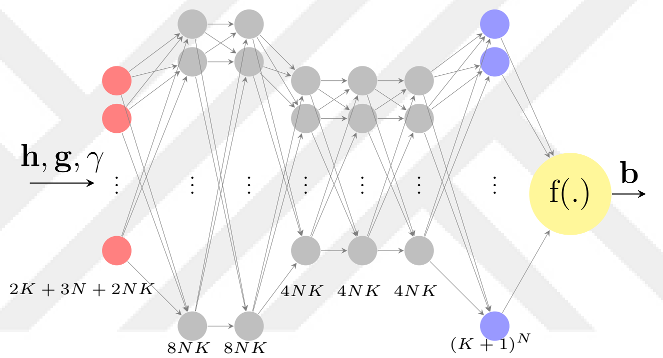

Figure 5.1: The proposed DNN architecture

$$\mathcal{P} : \{\mathbf{h}, \mathbf{g}, \boldsymbol{\gamma}\} \rightarrow \{\mathbf{b}\}$$

where $\mathbf{h} \in \mathbb{R}^{(N+K)\times 1}$ is the input vector whose elements are the DL channel gains $h_{AP}^{S_i}$, $h_{AP}^{R_j}$ for $i = 1, 2, \ldots, N$ and $j = 1, 2, \ldots K$; $\mathbf{g} \in \mathbb{R}^{(K+N(K+1))\times 1}$ is another input vector whose elements are the UL channel gains $g_{S_i}^{R_j}$, $g_{R_j}^{AP}$ for $i = 1, 2, \ldots, N$ and $j = 0, 1, 2, \ldots K$; $\mathbf{b} \in \mathbb{R}^{N\times 1}$ is the output vector whose elements represent the selected relay for each source S_i for $i = 1, 2, \ldots, N$. For instance, $b = [1, 2]$ in a 2-source-2-relay network means that R_1 is selected for S_1 and R_2 is selected for S_2.

This formalization allows us to design multi-input, multi-output DNN architecture, called REL-NET, for the low-complexity solution of the relay selection problem. Next, we introduce the architecture, data generation, and training processes of the proposed DNN in Sections 5.4.1-5.4.3. Finally, the benchmark ML algorithms are presented in Section 5.4.4.

5.4.1 DNN Architecture

Figure 5.1 depicts the purposed fully connected deep neural network architecture with five hidden layers. $\mathbf{h}$,$\mathbf{g}$, and γ are the inputs of the proposed DNN. The number of inputs is $2K + 3N + 2NK$. The five hidden layers are of the size $8KN$,$8KN$,$4KN$,$4KN$, and $4KN$. The output layer consists of $(K + 1)^N$ nodes representing each class. We utilize tanh activation function in each hidden layer. The output layer produces the probabilities corresponding to each class represented by an output node. We apply softmax function, $f(.)$, after the output layer to find the resulting class.

5.4.2 Data Generation

DL and UL channel gains, $\mathbf{h}$ and $\mathbf{g}$, are generated as follows: Sources are uniformly distributed in a circular quadrant between radius $3 - 4$ m. The AP is located at the center of the circle. Relays are deterministically positioned between the sources and the AP at a distance of 2 m from the AP. Large scale channel statistics are formulated as $PL(d) = PL(d_0) - 10\upsilon \log_{10}(d/d_0) + Z$, where $PL(d_0)$ is the free space path loss at unit distance d_0 in dB, d is the distance between the transmitter and receiver, $PL(d)$ is the path loss at a distance d in dB, υ is the path-loss exponent, and Z is a zero-mean Gaussian random variable with standard deviation σ_Z. For small-scale statistics, the Rayleigh fading model is used with scale parameter Ω set to the mean power level determined by $PL(d)$. For generated $\mathbf{h}$ and $\mathbf{g}$, $\boldsymbol{\gamma}$, the input vector representing the elements of the necessary condition on relay selection, is constructed.

5.4.3 Training

The truth labels for the supervised training process are the optimal relay selection obtained by Branch-and-Bound based Algorithm (BBA) [Onalan et al., 2020]. BBA searches for the optimal solution by dividing the entire solution space into smaller sub-spaces. This division, also called branching, is performed by assigning a value to one of the relay selection variables b_i^j's. Then, the resulting sub-space is checked against lower and upper bounds in the optimal solution to observe whether a better solution than the incumbent solution can be obtained. If not, this sub-space is not further divided into new sub-spaces,i.e., pruning. The branching continues until b_i^j's are set for all sources. After the relay selection for all sources is completed, the corresponding schedule length is calculated by POWMU.

For the training of REL-NET, log-loss function and Adam optimizer with batch size 200 and learning rate 10^{-4} is utilized. The hyperparameters are selected via grid search. $500,000$ independent random network realizations are generated as described in the previous section for the training of each different network size. Generated data is divided into the train, validation, and test sets, with sizes of $480,000$, $10,000$, and $10,000$, respectively.

5.4.4 Benchmark ML Algorithms

We employ various supervised ML algorithms, including KNN, SVM, DT, and RF as benchmarks to compare their performance with DNNs. The input features and output classes are the same as REL-NET. We use scikit-learn libraries for the implementation of the algorithms. The default parameters are used unless stated otherwise. For DT, the minimum number of samples in a node is 20. For RF, the number of forests is $(K+1)^N$. For KNN, the number of neighbors is set to 20. The same train, validation, and test sets with REL-NET are employed.

5.5 Performance Evaluation

This section compares the performances of the proposed DNN solution, REL-NET, with benchmark ML algorithms presented in Section 5.4.4, and the state-of-art heuristic algorithms Opportunistic Relaying (OR)[Chen et al., 2015], BBA, One Branch Heuristic (OBH), Relaxed Problem Based Heuristic (RPH), and Relay Selection and Time Minimization Algorithm (RSTMA) [Onalan et al., 2020]. OR picks

R_j with

$$\arg\max_j \min\left(g_{S_i}^{R_j} h_{AP}^{S_i}, g_{R_j}^{AP} h_{AP}^{R_j}\right)$$

for each source S_i, for $i = 1, \ldots, N$. BBA is the optimal algorithm that is used to obtain truth labels in the training process of ML algorithms. OBH applies a branch-and-bound strategy similar to BBA but only follows the branch with the maximum b_i^j instead of all. RPH solves the convex relaxation of the problem and picks the relay R_j with $\max_{j\in\{0,\ldots,K\}} b_i^j$ for source S_i, for $i = 1, \ldots, N$. RSTMA starts with an initial relay selection obtained by OR strategy for each source independently. Then, it iteratively improves the solution by changing the source-relay pairs.

Simulations are performed in Windows 64-bit OS, 8GB RAM, and Intel i7-7600U dual-core processor. The performance of all the algorithms is measured over the test data set generated as described in Section 5.4.2. The simulation results are presented as an average of the performance over $10,000$ independent random network realizations.

We consider an indoor environment operating at a center frequency of $f_c = 915$ with the following simulation parameters: $W = 1$ MHz, $N_0 = -90$ dBm, $\zeta_{S_i} = \zeta_{R_j} = 50\%$ $\forall i, j$, $PL(d_0) = 31.67$ dB, $\sigma_Z = 2$ dB, and $\upsilon = 2$, $P_{AP} = 4$ W, $P^{max} = 10$ mW, $D_{Si} = 50$ bits $\forall i$. Without loss of generality, D_{Si}, ζ_{S_i}, and ζ_{R_j} values are selected as same for simpler implementation.

Figure 5.2 indicates the gain provided input vector $\boldsymbol{\gamma}$ in terms of training loss, i.e., log-loss, and validation score, i.e., accuracy. Adding $\boldsymbol{\gamma}$ into the feature set provides a faster training process and lower loss compared to the feature set with only channel gains $\mathbf{h}, \mathbf{g}$.

Table 5.1 compares the macro (M) and weighted (W) precision, recall, f1-score, and accuracy of REL-NET against all ML and iterative algorithms for 4-user-2-relay-network. REL-NET outperforms all other algorithms in terms of all metrics. Other ML algorithms, especially RF, have competitive results for small networks, e.g., $K = 2, N = 2$, but their performance degrades with increasing network size, e.g., $K = 2, N = 4$. OBH is competitive with REL-NET while outperforming

Table 5.1: Precision, recall, F1, and accuracy of the ML Algorithms and benchmark iterative heuristics

	K=2 N=4 #Classes=81						
	Precision		**Recall**		**F1**		**Acc.**
	M	**W**	**M**	**W**	**M**	**W**	
KNN	0.31	0.33	0.29	0.32	0.29	0.32	0.32
SVM	0.54	0.55	0.52	0.54	0.53	0.4	0.54
DT	0.3	0.31	0.29	0.3	0.29	0.3	0.3
RF	0.61	0.61	0.61	0.61	0.61	0.61	0.61
REL-NET	0.85	0.85	0.84	0.85	0.84	0.85	0.85
OR	0.39	0.41	0.26	0.36	0.27	0.33	0.36
RSTMA	0.45	0.49	0.33	0.49	0.33	0.42	0.49
RPH	0.74	0.76	0.77	0.76	0.76	0.76	0.76
OBH	0.81	0.84	0.84	0.83	0.83	0.83	0.83

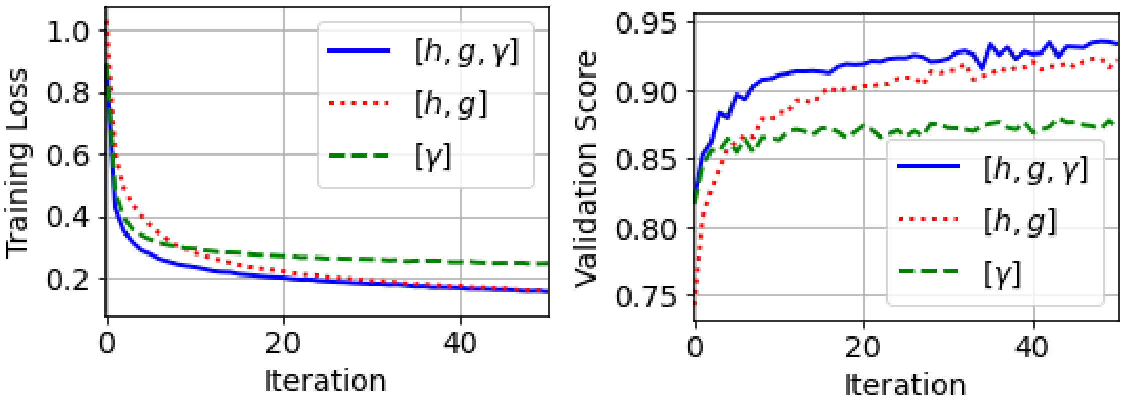

(a) (b)

Figure 5.2: (a) Training loss and (b) validation score for 2-source-2-relay network for different input features.

other iterative heuristic algorithms, whose performance is also very close to REL-NET. None of the ML algorithms are trained to differentiate false positives and false negatives; whereas precision and recall values are close to each other in all iterative

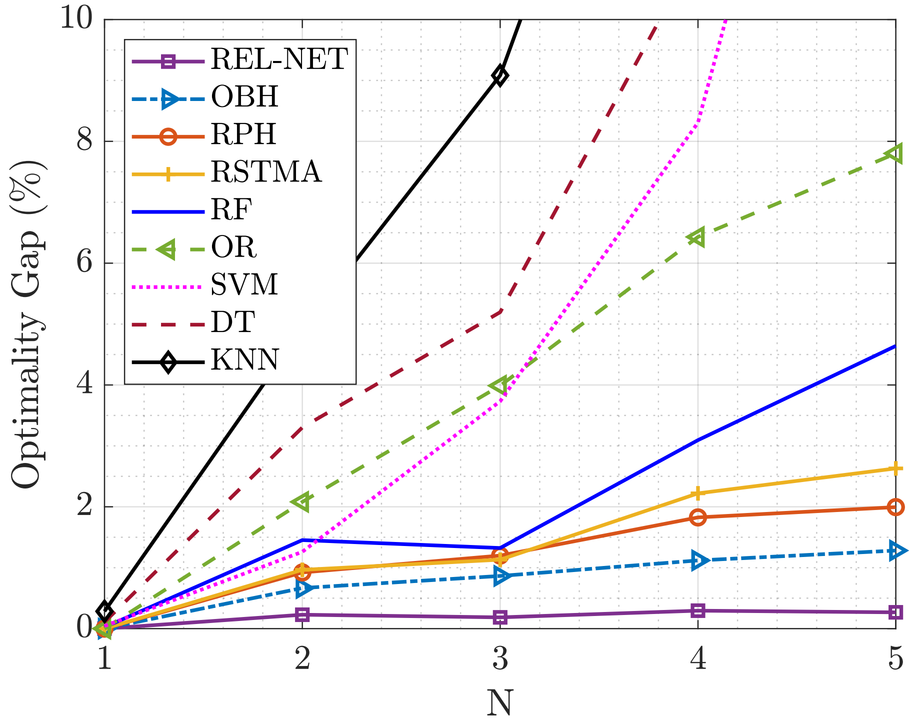

Figure 5.3: Optimality gap in 2-relay network for a different number of sources.

and ML algorithms. This can be attributed to the problem definition.

Figure 5.3 depicts the optimality gap of all the algorithms in a 2-relay network for an increasing number of sources from 1 to 5. The optimality gap is the ratio of the difference between the schedule length obtained by an algorithm and the optimum schedule length to the optimum schedule length. The optimum schedule length is obtained by BBA. The proposed solution, REL-NET, provides the closest solution to the optimum. For $N = 3$, the optimality gap of REL-NET is 0.18%; whereas the optimality gap of benchmark algorithms is between 0.86-9%. Optimality gap of KNN, DT, and SVM exponentially increases. Among the conventional ML algorithms, only RF could outperform state-of-art OR protocol.

Figure 5.4 presents the optimality gap of all the algorithms in a 2-source network for an increasing number of relays from 2 to 10. The proposed solution, REL-NET, provides the closest solution to the optimum. OBH and RSTMA perform closely to REL-NET, especially at higher K. Optimality gap of KNN, DT, RF, and SVM rapidly increases with the increasing number of relays so the classes. As the number of relays increases, there becomes one available relay for each source. Then, the problem is closer to finding the individual best relay selection for each source for which OR and RPH can perform well. This is why the optimality gap of OR and RPH decreases at $K > 8$.

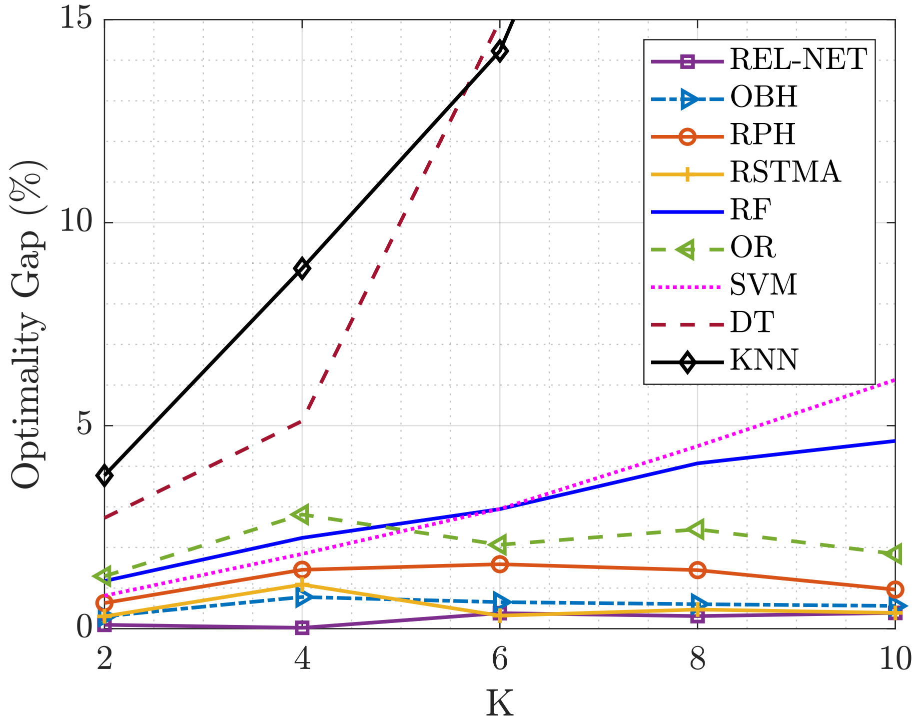

Figure 5.4: Optimality gap in 2-source network for a different number of relays.

Figure 5.5 shows the runtime performance of the algorithms for different number of sources ranging from 1 to 5. For a fair comparison, MATLAB implementations of all the algorithms are used for runtime evaluation. Note that the DNN training is offline, so the training times are not considered here. REL-NET is up to 4071, 569, and 2.33 times faster than OBH, RPH, and RSTMA, respectively. Although the runtime of RSTMA is lower than REL-NET in small-size networks, it is higher for larger networks as the required iterations in RSTMA increase with the network size. OR is the quickest relay selection method with a performance of up to 2.38 times faster than REL-NET.

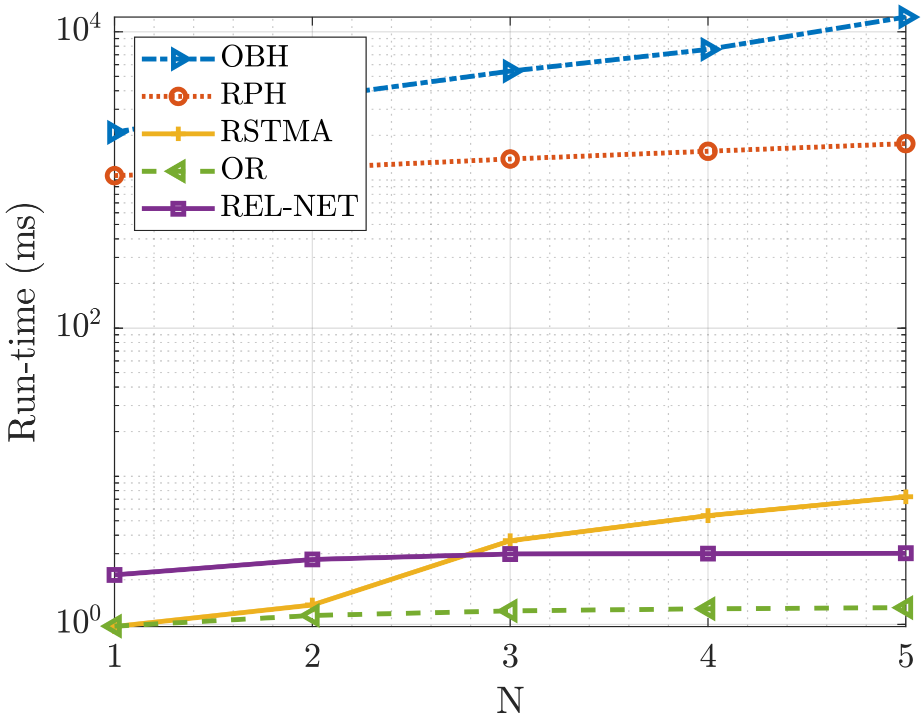

Figure 5.5: Runtime performance in 2-relay network for a different number of sources.

5.6 Conclusion

This paper proposes a low complexity DNN-based solution for the relay selection problem with the objective of minimum schedule length in multi-source-multi-relay half-duplex WPCCNs. The relay selection problem is considered as a classification problem where the inputs are the channel gains and the parameters derived from these gains based on the optimality conditions of the problem, and the output classes represent relay selections for each source. To solve this classification problem, a feed-forward DNN, called REL-NET, is designed. REL-NET is trained offline with supervised learning, for which the optimal solutions are obtained by a branch-and-bound-based optimal algorithm. REL-NET outperforms all benchmark algorithms in terms of precision, recall, f1-score, accuracy, and optimality gap in schedule length. In a 3-user-2-relay network, the optimality gap of REL-NET is only 0.18% whereas this gap is 0.86-9% for benchmark algorithms. The runtime performance of REL-NET is up to 4071, 569, and 2.33 times lower than three state-of-art iterative heuristic algorithms. Therefore, REL-NET would especially be preferred for its lower complexity without compromising optimality. Although the OR strategy is 2.38 times faster than REL-NET, it has the worst performance in the optimality gap, e.g., 4% in the 3-user-2-relay network, amongst REL-NET and all other iterative algorithms.

Chapter 6

TEACHER-STUDENT LEARNING BASED LOW COMPLEXITY RELAY SELECTION IN WIRELESS POWERED COMMUNICATIONS

6.1 Introduction

Energy Harvesting (EH) is a promising alternative to fixed power supplies (e.g., batteries) for energy-constrained network applications such as Internet-of-Things (IoT) [Ashraf et al., 2021]. In EH networks, information sources scavenge energy from their surroundings to send/receive packets, which can enable the net-zero energy objective of 6G mobile networks [Viswanathan and Mogensen, 2020]. IEEE 802.11 study group has been investigating the use cases and feasibility of wireless-powered IoT over next-generation WiFi [IEEE 802.11 AMP TIG/SG, 2023].

Radio Frequency (RF) signals are preferred over other energy sources such as vibration and sun due to their independence from climate conditions, accessibility, and more predictable and controllable nature [Ashraf et al., 2021]. RF-EH network design follows two main protocols: Simultaneous Information and Power Transfer (SWIPT), in which power and information are sent simultaneously, and Wireless Powered Communication Networks (WPCN), in which power and information are sent consecutively in downlink (DL) and uplink (UL) [Lu et al., 2015]. Both SWIPT and WPCN are studied under different conditions and designed for various objective functions such as maximum throughput, minimum schedule length, and energy efficiency. Further, relays are considered to improve network performance in terms of these objectives. Adding relays into networks leads to relay selection problem.

The relay selection problem is studied in SWIPT networks with both amplify and forward [Gupta et al., 2019] and decode and forward relays [Zheng et al., 2023].

[Gupta et al., 2019] jointly optimizes relay selection, subcarrier pairing, user allocation, and power allocation to improve the energy efficiency of multiple-source-multiple-relay multi-carrier networks. An iterative algorithm based on tractable quasi-concave form by applying a string of convex transformations is proposed. [Zheng et al., 2023] jointly optimizes relay selection, power allocation, beamforming, and signal splitting to maximize the end-to-end throughput of single-source-multiple-relay networks. Again, an iterative algorithm is proposed based on decoupling the non-convex variables into different sub-problems. As iterative algorithms suffer from high runtimes, sub-optimal relay selection schemes, based on channel characteristics of source-to-relay and/or relay-to-destination links, are also studied in both works.

The relay selection problem is investigated in both half-duplex [Onalan et al., 2020][Xie et al., 2023b] and full-duplex [Kazmi et al., 2020][Kazmi et al., 2021] WPCN under different objectives such as minimum length scheduling [Onalan et al., 2020, Kazmi et al., 2020], maximum throughput [Kazmi et al., 2021], age-of-information minimization [Xie et al., 2023b]. [Onalan et al., 2020][Kazmi et al., 2020] and [Kazmi et al., 2021] formulate joint relay selection, scheduling, and power allocation problems in multiple-source-multiple-relay networks. They first solve scheduling and power control problem for fixed relay selection, and then, search for the optimum relay selection with iterative algorithms. [Xie et al., 2023b] considers single-source-multiple-relay IoT system; selects a fixed number of all possible relays that received the status update from the source at the earliest; and then jointly optimizes the number of relays and the packet lengths at the source and relays by using a gradient-based two-step search algorithm. All proposed iterative algorithms that solve a complex mathematical equation in each iteration suffer from high run-time. However, algorithms with high runtime may not be practical for time-critical applications.

Deep Neural Networks (DNNs) and Deep Reinforcement Learning (DRL) have recently been applied to relay selection problems in EH networks to provide low complexity, high accuracy, and robust solutions [Wang et al., 2021, Han et al., 2022, Nguyen et al., 2021, Zhang et al., 2020, Nguyen et al., 2023]. [Wang et al., 2021] proposes a distributed actor-critic reinforcement algorithm running for each source separately to maximize the total data delivery ratio. [Han et al., 2022] applies deep deterministic policy gradient (DDPG) and deep Q network (DQN) algorithms for joint relay selection and power allocation problem with the objective of cumulative throughput maximization in single-source-multiple-relay networks. [Nguyen et al., 2021] and [Zhang et al., 2020] study relay selection problem for SWIPT with the objective of maximum throughput in single-source-multiple-relay and two-way relaying networks, respectively. In [Nguyen et al., 2021], DNNs are used to predict the achievable throughput, and an iterative algorithm performs relay selection based on these predicted throughputs. In [Zhang et al., 2020], the relay selection problem is defined as a classification problem and solved by DNNs. [Nguyen et al., 2023] formulates joint relay selection and beamforming problems to maximize throughput. For the solution, Convolutional Neural Networks with multiscale-accumulation connections are proposed for throughput prediction; whereas the relay selection is performed by iterative algorithms based on the predicted throughputs. Although the deep learning approaches solving sub-problems decrease complexity in [Nguyen et al., 2021, Nguyen et al., 2023], the iterative algorithms are still needed to choose relays. The deep learning algorithms can be extended to relay selection problems. Further, the aforementioned work considers single-source-multiple-relay networks. However, the relay selection problem in multiple source-destination networks requires a separate study since individually optimum relays do not guarantee the best relay selection for the entire network. Only [Onalan and Coleri, 2023], applies deep learning for the low-complexity solution of the classification problem over relay selection for multiple-source-multiple-relay pairs. However, it assumes a less realistic linear EH model and has scalability issues for large network sizes due to the exponentially increasing number of classes with network size.

Knowledge distillation (KD) techniques [Gou et al., 2021] are proposed to compress large deep learning models [Tang et al., 2021] or employ domain-specific knowledge to deep learning frameworks [Zheng et al., 2022, Qi et al., 2023]. KD transfers knowledge from a complex network, a.k.a teacher network, to a simple network, a.k.a student network, to improve the performance of the simple network close to the complex network. Although KD is commonly applied in speech and image processing, it has limited applications in wireless communications. [Tang et al., 2021] employs KD to provide low-complexity CSI estimation in MIMO communication. [Zheng et al., 2022] applies KD on DRL to harness network domain knowledge to improve the robustness of and trust on DRL. [Qi et al., 2023] uses KD within federated learning to overcome the heterogeneity of local models to improve modulation classification tasks.

This paper studies multiple-source-multiple-relay WPCCN, where both sources and relays have EH capabilities. In our system model, by using the harvested energy, each source needs to send information via a selected relay or directly to the AP; whereas each relay must convey all gathered information from sources to the AP. We aim to obtain low-complexity solutions for optimal relay selection, power control, and scheduling for energy harvesting and information transmission under non-linear EH conditions. The major contributions of the paper are listed as follows:

- We extend the joint relay selection, scheduling, and power control problem formulated based on the linear EH model in [Onalan et al., 2020] to non-linear EH conditions. Non-linearity in energy conversion model changes the required EH duration for demanded IT, so it changes the optimum solution for all variables such as relay selection, time, and power allocations. The formulated problem is a non-convex mixed integer non-linear problem (MINLP) and NP-hard. We follow the solution strategy proposed in [Onalan et al., 2020], which starts from a simpler sub-problem of scheduling and power control solved by a bi-level transformation-based iterative algorithm, and then searches for the optimal relay selection via branch-and-bound based algorithm. We adapt these algorithms to non-linear EH conditions. These algorithms will be used for performance comparisons and training of the proposed deep learning frameworks.

- We define the relay selection problem as a classification problem and propose two novel Convolutional Neural Network (CNN) based architectures for low complexity solutions. The inputs of both architectures are the channel gains.

The outputs are relay selection variables represented by different classes. The first architecture uses convolutional blocks and benefits from skip connections [Tong et al., 2017, He et al., 2016, Huang et al., 2017] between layers. The second architecture replaces several convolutional blocks with inception blocks [Szegedy et al., 2015] to lower the trainable parameter size without sacrificing accuracy for memory-constrained applications.

- To reduce the complexity even more, we employ knowledge distillation techniques, specifically teacher-student learning. To the best of our knowledge, we are the first to apply teacher-student learning for low-complexity resource allocation and optimization in wireless communication.

- To benefit from teacher-student learning at most, we search for the best student network architecture with a novel dichotomous search-based algorithm. This search adaptively selects the number of trainable parameters, indicating the complexity of the architecture, of the CNN-based model by evaluating the trade-off between complexity and validation loss in each iteration. For the given number of trainable parameters, the student network architecture is designed, in terms of the number of layers and nodes at each layer, by a novel runtime efficient sequential search instead of grid searching all possible layer and node combinations.

- We illustrate the superior performance of the proposed deep learning frameworks compared to the iterative benchmark algorithms in terms of schedule length and complexity via extensive simulations.

The rest of the paper is organized as follows. Section 6.2 describes the system model. In Section 6.3, the optimization problem is formulated, and the solution strategy is discussed. Section 6.4 formulates and solves the scheduling and power control problem for a given relay selection. For the relay selection problem, Section 6.5 presents the proposed CNN-based models and teacher-student learning approach. Section 6.6 presents the simulation results. Finally, Section 6.7 concludes the paper.

6.2 System Model

Fig.1 depicts the considered multiple-source-multiple-relay half-duplex WPCCN, where sources send information to the AP in the uplink by exhausting the harvested energy in the downlink with or without the help of a relay. Both sources and relays do not have any embedded energy supplies, so they have to replenish energy by broadcast RF signal by AP for IT. The WPCCN contains one AP, N EH sources, denoted by S_i, $i = 1, 2, \ldots, N$, and K EH decode-and-forward (DF) relays, denoted by R_j, $j = 1, 2, \ldots K$.

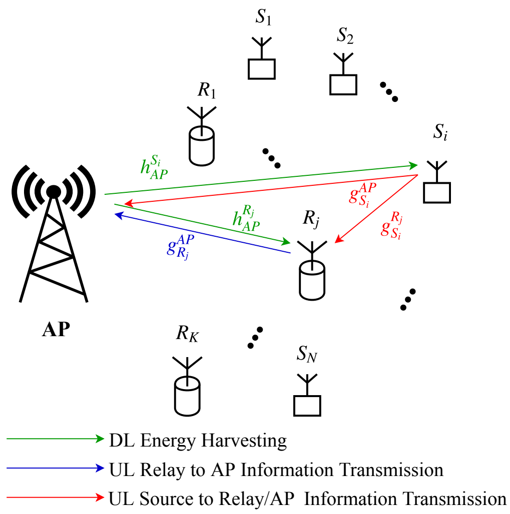

Figure 6.1: System Model

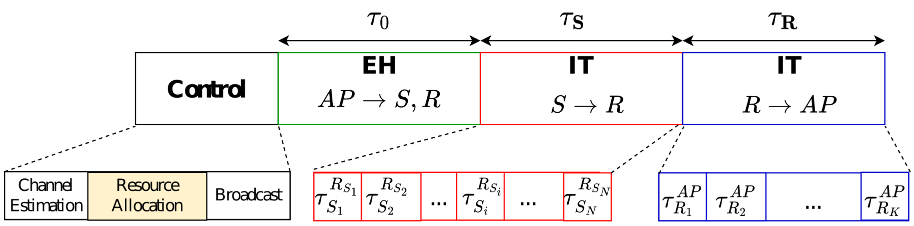

Figure 6.2: Time Frame

6.2.1 Channel Model

We consider block-fading channels between X and Y where $X, Y \in \{AP, S_i, R_j\}$, $i = 1, 2, \ldots, N$ and $j = 1, 2, \ldots K$, and the channel gains remain constant within each time block but vary independently among different blocks. The DL and UL channel gains between X and Y are denoted by h_X^Y and g_X^Y, respectively. For instance, $h_{AP}^{S_i}$ is the DL channel gain between AP and S_i. We assume that the AP perfectly knows all the channel gains, similar to the previous works, e.g., [Kazmi et al., 2020, Kazmi et al., 2021, Onalan et al., 2020, Xie et al., 2023b, Nguyen et al., 2023, Onalan and Coleri, 2023]. With this assumption, we focus on the relay selection problem and obtain the performance limits of the investigated network [Onalan et al., 2020].

6.2.2 Tranmission Model

TDMA protocol is used as a medium access control protocol. Fig. 6.2 depicts the time division structure. A time block is divided into 4-time slots for control, EH, IT of sources, and IT of relays. In a time block, each source S_i needs to send $D_{S_i} > 0$ amount of data to the AP for $i = 1, 2, \ldots, N$.

In the control slot, the sources estimate the channels via pilot signals by the AP and feed the channel gain information back to the AP. Compared to the time and energy cost of IT, the time and energy spent for channel estimation can be considered negligible for a low mobility network [Li et al., 2019]. Then, based on the channel gains, the AP runs the proposed algorithms to optimize the resource allocation. As resource allocation problems usually have high complexity, e.g. NP-Hard, the time spent on resource allocation may not be negligible. To complete operations in a time-block within channel coherence time, low-complexity resource allocation algorithms are required. Finally, the AP broadcasts the information on allocated resources to all the relays and sources in a negligible amount of time.

In EH slot, the relays and sources harvest energy from the AP during τ_0 amount of time. The sources and relays possess rechargeable batteries with low energy storage and high self discharge rate, e.g. super-capacitors [Kaus et al., 2010]. Therefore, the harvested energy can be used within the time block but cannot be stored for further use.

In the first IT slot, each source communicates directly to the AP or a selected relay with the harvested energy. Then, in the second IT slot, the selected relays convey the gathered information from sources to the AP. IT time slots are divided into sub-slots corresponding to each source and relay. Assume that the j^{th} relay is selected by the i^{th} source for cooperation. Then, a sub-slot is allocated for the IT from source S_i to relay R_j with duration $\tau_{S_i}^{R_j}$ and another sub-slot is allocated for the IT from R_j to AP with duration $\tau_{R_j}^{AP}$ for $i = 1, 2, \ldots, N$ and $j = 0, 1, 2, \ldots K$, where R_0 refers to AP. If the i^{th} source prefers direct communication with the AP, information transfer is completed in the first IT block in $\tau_{S_i}^{R_0}$ amount of time and $\tau_{R_0}^{AP}$ is obviously zero.

Note that each source can use a single relay for IT. However, the relays can assist multiple sources and must convey all the information they receive from the sources to the AP.

6.2.3 Downlink Energy Harvesting

The AP is assumed to have an unlimited power source. The transmission power of the AP is assumed to be constant and denoted by P_A. We assume that P_A is large enough to ignore AWGN noise component during EH phase.

The relays and sources harvest energy from the AP during τ_0 amount of time. We apply a practical non-linear EH model [Boshkovska et al., 2015]. Thus, the energy harvested at the i^{th} source and j^{th} relay, for $i = 1, \ldots, N$ and $j = 1, \ldots, K$, can, respectively, be expressed as

$$E_{S_i} = \frac{\Psi_{S_i} - M_{S_i}\Omega_{S_i}}{1 - \Omega_{S_i}}\tau_0 \tag{6.1}$$

$$E_{R_j} = \frac{\Psi_{R_j} - M_{R_j}\Omega_{R_j}}{1 - \Omega_{R_j}}\tau_0 \tag{6.2}$$

where

$$\Omega_{S_i} = \frac{1}{1 + exp(a_{S_i} b_{S_i})} \tag{6.3}$$

$$\Omega_{R_j} = \frac{1}{1 + exp(a_{R_j} b_{R_j})} \tag{6.4}$$

$$\Psi_{S_i} = \frac{M_{S_i}}{1 + \exp(-a_{S_i}(h_{AP}^{S_i} P_A - b_{S_i}))} \tag{6.5}$$

$$\Psi_{R_j} = \frac{M_{R_j}}{1 + \exp\left(-a_{R_j}(h_{AP}^{R_j} P_A - b_{R_j})\right)} \tag{6.6}$$

and $a_{S_i}, a_{R_j}, b_{S_i}, b_{R_j}, M_{S_i}$, and M_{R_j} are constant parameters characterizing non-linear behaviour of EH circuit.

6.2.4 Uplink Information Transfer

We consider continuous power model, where the average transmit power $P_{S_i}^{R_j}$ and $P_{R_j}^{AP}$ of S_i and R_j takes any value below a maximum level P^{max}[Onalan et al., 2020, Kazmi et al., 2021]. $P_{S_i}^{R_j}$ and $P_{R_j}^{AP}$ are also limited by the amount of the harvested energy given by Eqs. (6.1) and (6.2). The required energy for decoding the received message at relays is negligible compared to the energy consumption for IT. Thus, $P_{S_i}^{R_j} \leq E_{S_i}/\tau_{S_i}^{R_j}$ and $P_{R_j}^{AP} \leq E_{R_j}/\tau_{R_j}^{AP}$.

The maximum achievable rate during IT is formulated based on continuous transmission rate model and Shannon's channel capacity formula for AWGN channels. There is no interference during IT as all sources and relays use separate time slots. Then, the instantaneous UL transmission rates $T_{S_i}^{R_j}$ from S_i to R_j and $T_{R_j}^{AP}$ from R_j to AP are given by

$$T_{S_i}^{R_j} = W \log_2 \left(1 + \frac{P_{S_i}^{R_j} g_{S_i}^{R_j}}{W N_0}\right) \tag{6.7}$$

$$T_{R_j}^{AP} = W \log_2 \left(1 + \frac{P_{R_j}^{AP} g_{R_j}^{AP}}{W N_0}\right). \tag{6.8}$$

6.3 Problem Formulation and Solution Strategy

The relay selection, scheduling, and power control problem with the objective of minimizing schedule length subject to demand, energy, and power constraints is formulated similar to the optimization problem in [Onalan et al., 2020] with linear

EH model as follows:

$$\min \quad \tau_0 + \sum_{i=1}^{N}\sum_{j=0}^{K}\tau_{S_i}^{R_j} + \sum_{j=1}^{K}\tau_{R_j}^{AP} \tag{6.9a}$$

$$\text{s.t.} \quad \sum_{j=0}^{K} b_i^j = 1, \qquad i = 1,\dots,N, \tag{6.9b}$$

$$P_{S_i}^{R_j} \leq P^{max} b_i^j, \quad i = 1,\dots,N,\ j = 0,\dots,K, \tag{6.9c}$$

$$P_{R_j}^{AP} \leq \min\left\{P^{max}, P^{max}\sum_{i=1}^{N} b_i^j\right\}, \quad j = 0,\dots,K, \tag{6.9d}$$

$$P_{S_i}^{R_j}\tau_{S_i}^{R_j} \leq \frac{\Psi_{S_i} - M_{S_i}\Omega_{S_i}}{1-\Omega_{S_i}}\tau_0, \qquad i = 1,\dots,N, \quad j = 0,\dots,K, \tag{6.9e}$$

$$P_{R_j}^{AP}\tau_{R_j}^{AP} \leq \frac{\Psi_{R_j} - M_{R_j}\Omega_{R_j}}{1-\Omega_{R_j}}\tau_0, \qquad j = 1,\dots,K, \tag{6.9f}$$

$$\tau_{S_i}^{R_j} W \log_2\left(1 + \frac{P_{S_i}^{R_j} g_{S_i}^{R_j}}{WN_0}\right) \geq D_{S_i} b_i^j, \quad i = 1,\dots,N,\ j = 0,\dots,K, \tag{6.9g}$$

$$\tau_{R_j}^{AP} W \log_2\left(1 + \frac{P_{R_j}^{AP} g_{R_j}^{AP}}{WN_0}\right) \geq \sum_{i=1}^{N} D_{S_i} b_i^j, \quad j = 0,\dots,K, \tag{6.9h}$$

$$\tau_0, \tau_{R_j}^{AP}, P_{R_j}^{AP}, \tau_{S_i}^{R_j}, P_{S_i}^{R_j} \geq 0, \quad i = 1,\dots,N, \quad j = 1,\dots,K, \tag{6.9i}$$

$$b_i^j \in \{0,1\}, \quad i = 1,\dots,N,\ j = 1,\dots,K. \tag{6.9j}$$

The variables of the optimization problem are τ_0, EH duration; $\tau_{S_i}^{R_j}$, IT duration from the i^{th} source to the j^{th} relay; $\tau_{R_j}^{AP}$, IT duration from the j^{th} relay to the AP; $P_{S_i}^{R_j}$, transmit power of the i^{th} source when it transmits to the j^{th} relay; $P_{R_j}^{AP}$, transmit power of the j^{th} relay when it transmits to the AP; and b_i^j, the relay selection parameter that takes value 1 if the j^{th} relay is selected for the i^{th} source and 0 otherwise, for $i = 1,\dots,N$ and $j = 0,\dots,K$.

The objective of the optimization problem is to minimize the total duration for EH and IT. Eq. (6.9b) ensures that one and only one relay is selected for each source, allowing for the possibility of a relay being selected for multiple sources. The maximum allowable transmit power of the sources and relays are set by Eqs. (6.9c) and (6.9d), respectively. Eq. (6.9c) forces $P_{S_i}^{R_j}$ to be zero when R_j is not selected for S_i. Similarly, Eq. (6.9d) sets $P_{R_j}^{AP}$ to zero when R_j is not selected for any source. Eqs. (6.9e) and (6.9f) are energy causality constraints limiting $P_{S_i}^{R_j}$ and $P_{R_j}^{AP}$ by the harvested energy amount. Demand constraint Eq. (6.9g) requires that each source S_i conveys a D_{S_i} amount of data to the AP or the selected relay. The demand constraint Eq. (6.9h) guarantees that relays convey all data they gather from sources to the AP. Lastly, Eq. (6.9i) and (6.9j) represent non-negativity and integrality constraints, respectively.

Problem (6.9) is a non-convex MINLP as all equations except Eqs. (6.9b)-(6.9d) are non-linear and Eqs. (6.9e)-(6.9h) are non-convex. The problem is NP-hard as proven in [Onalan et al., 2020].

We follow the solution strategy in [Onalan et al., 2020]. The reduced form of Problem (6.9) is formulated for a given relay selection. When the relay selection is fixed, the total schedule length can be minimized with respect to constraints for energy causality, demand requirement, and maximum transmit power. The chosen relays act as sources since they must convey the gathered messages from sources to the AP. On the other hand, the selected relays determine the destination of each source. If no relay is selected for a source, AP is the destination. Thus, a scheduling and power control problem is formulated for WPCN with multiple source-destination pairs and an AP as an energy source. The solution to the reduced problem has been well-studied for the linear EH model. An iterative optimal algorithm has been proposed based on bi-level transformation [Onalan et al., 2020], which is named *POWer constrained Multiple User time minimization Algorithm* (POWMU). Non-linearity in EH affects the required EH length to satisfy the data demanded of sources, thus, it changes the optimum solution of the scheduling and power control problem. We adapt POWMU algorithm to the non-linear EH model considered in this work in Section 6.4.

After calculating the minimum schedule length corresponding to a relay selection, the best relay selection can be obtained by searching over all source-relay combinations. To find the optimum relay selection, [Onalan et al., 2020] suggests a branch-and-bound algorithm (BBA), which we also adapt to the non-linear EH model. BBA branches on relay selection variables and solves the scheduling and power control problem when the selection is completed. To prevent the exhaustive search on all possible combinations, the algorithm uses bounding techniques to prune the BB-tree nodes that cannot provide better feasible points than the ones obtained at the previous nodes. For pruning, we develop lower and upper-bound generation techniques specific to our problem. However, at the worst case, BBA has exponential complexity. Although two BB-based heuristic approaches with lower runtimes had been proposed in [Onalan et al., 2020], these heuristics still iteratively solve complex mathematical equations and suffer from complexity. To provide a low-complexity solution to the relay selection problem, this work proposes novel CNN architectures and knowledge distillation techniques in Section 6.5.

6.4 Scheduling and Power Control under Non-Linear EH

This section presents the reduced form of Problem (6.9) for the given relay selection. The selected relays are considered sources since they must send information to the AP by exhausting the harvested energy. Let L be the number of selected relays. Then, the resulting number of sources becomes $N' = N + L$. The selected relays are also the destinations of the sources. Accordingly, the scheduling and power control problem in multiple-source-multiple-destination WPCN under non-linear EH conditions is formulated as follows:

$$\begin{aligned}
\min \quad & \tau_0 + \sum_{i=1}^{N'} \tau_{S_i} && (6.10a)\\
\text{s.t.} \quad & P_{S_i}\tau_{S_i} \leq \frac{\Psi_{S_i} - M_{S_i}\Omega_{S_i}}{1-\Omega_{S_i}}\tau_0, \quad i = 1, 2, \ldots, N', && (6.10b)\\
& \tau_{S_i} W \log_2\left(1 + \frac{P_{S_i} g_{S_i}}{W N_0}\right) \geq D_{S_i},\ i = 1, 2, \ldots, N', && (6.10c)\\
& P_{S_i} \leq P^{max}, \qquad i = 1, 2, \ldots, N', && (6.10d)
\end{aligned}$$

$$\tau_0, \tau_{S_i}, P_{S_i} \geq 0, \qquad i = 1, 2, \ldots, N', \tag{6.10e}$$

where g_{S_i} is the UL channel gain between S_i and its destination; P_{S_i} is the transmit power of S_i; and τ_{S_i} is the IT time from S_i to its destination for $i = 1, \ldots, N'$. The variables of Problem (6.10) are P_{S_i}, τ_{S_i} and τ_0. Problem (6.10) aims to minimize the total duration for EH and IT. Eqs. (6.10b), (6.10c), (6.10d), and (6.10e) represent the constraints for energy causality, demand requirement, maximum transmit power, and non-negativity respectively.

The objective function given in Eq.(6.10a) is convex over τ_0 [Onalan et al., 2020]. Thus, the optimal τ_0 can be searched via bisection search whose iterations solve N' subproblems calculating the minimum IT length of each source S_i for the given EH length. The sub-problems are formulated for $N' = 1$ and fixed $\tau_0 = \overline{\tau_0}$, as follows:

$$\min \quad \tau_{S_1} \tag{6.11a}$$

$$\text{s.t.} \quad P_{S_1}\tau_{S_1} \leq \frac{\Psi_{S_1} - M_{S_1}\Omega_{S_1}}{1 - \Omega_{S_1}}\overline{\tau_0}, \tag{6.11b}$$

$$\tau_{S_1} W \log_2\left(1 + \frac{P_{S_1} g_{S_1}}{W N_0}\right) \geq D_{S_1}, \tag{6.11c}$$

$$P_{S_1} \leq P^{max}, \tag{6.11d}$$

$$\tau_{S_1}, P_{S_1} \geq 0, \tag{6.11e}$$

The objective of the subproblems is minimizing τ_{S_1} for the fixed $\tau_0 = \overline{\tau_0}$ where Eqs. (6.11b), (6.11c), and (6.11d) represent energy causality, data causality and maximum allowed transmit power constraints, respectively. Problem (6.11) is non-convex due to the non-convexity of Eqs. (6.11b) and (6.11c). Next, we provide the solution to Problem (6.11).

Lemma 12. *Let $\overline{\tau_{S_1}}$ be the optimal solution to Problem (6.11). The optimal IT duration $\overline{\tau_{S_1}}$ is expressed by*

$$\overline{\tau_{S_1}} = \frac{D_{S_1}}{W \log_2\left(1 + \frac{P^{max} g_{S_1}}{W N_0}\right)} \tag{6.12}$$

if

$$\overline{\tau_0} \geq \ddot{\tau}_0 = \frac{P^{max}\overline{\tau_{S_1}}(1 - \Omega_{S_1})}{\Psi_{S_1} - M_{S_1}\Omega_{S_1}}. \tag{6.13}$$

Otherwise, $\overline{\tau_{S_1}}$ *is derived as a solution of the nonlinear equation*

$$\overline{\tau_0} = \frac{\overline{\tau_{S_1}}}{\gamma_{S_1}} \left(2^{\frac{D_{S_1}}{W\overline{\tau_{S_1}}}} - 1 \right), \tag{6.14}$$

where

$$\gamma_{S_1} = \frac{g_{S_1}(\Psi_{S_1} - M_{S_1}\Omega_{S_1})}{WN_0(1 - \Omega_{S_1})}. \tag{6.15}$$

Proof. The proof follows the proof of Lemma 3 in [Onalan et al., 2020]. Different from [Onalan et al., 2020], Eqs. (6.13) and (6.15) are formulated considering non-linear EH conditions. □

Lemma 13. *The upper and lower bounds for the optimum* τ_0 *of Problem (6.10) is expressed respectively by*

$$\tau_0^{ub} = \max_{i \in \{1,\ldots,N'\}} \frac{P^{max}\overline{\tau_{S_i}}(1 - \Omega_{S_i})}{\Psi_{S_i} - M_{S_i}\Omega_{S_i}} \tag{6.16}$$

and

$$\tau_0^{lb} = \max_{i \in \{1,\ldots,N'\}} \frac{D_{S_i} \ln(2)}{W\alpha_{S_i}\gamma_{S_i}} \left(2^{\alpha_{S_i}/\ln(2)} - 1 \right) \tag{6.17}$$

where $\gamma_{S_i} = \frac{g_{S_i}(\Psi_{S_i} - M_{S_i}\Omega_{S_i})}{WN_0(1-\Omega_{S_i})}$, $\alpha_{S_i} = \mathbb{L}_0\left(\frac{\gamma_{S_i}-1}{e}\right) + 1$, *and* $\mathbb{L}_0(.)$ *is the Lambert W-function in 0 branch.*

Proof. The upper bound is the maximum of the solutions of the networks where S_i is the single source and transmitting at P^{max}, i.e., Eqs. (6.10b)-(6.10d) hold with equality, for $i = 1, \ldots, N'$. The lower bound is the maximum of the optimal solutions of the networks where S_i is the single source, for $i = 1, \ldots, N'$. The proof follows the proof of Lemma 5 and 6 in [Onalan et al., 2020] by updating equations with nonlinear EH formulations. □

Algorithm 5 Non-linear EH Power Constrained Multiple User Time Minimization Algorithm (NL-POWMU)

1: **Input:** P^{max}, P_A, γ_{S_i}, α_{S_i}, Ψ_{S_i}, Ω_{S_i}, M_{S_i},D_{S_i}, for $i = 1, \ldots, N'$

2: **Output:** τ_0, τ_{S_i}, P_{S_i} for $i = 1, \ldots, N'$

3: Compute τ_0^{ub} and τ_0^{lb} by Lemma 13

4: **while** $\tau_0^{ub} - \tau_0^{lb} > 2\epsilon$ **do**

5: $\quad \tau_0^{'} = \frac{lb+ub}{2}$

6: $\quad$ **if** $\frac{dg(\overline{\tau_0})}{d(\overline{\tau_0})}|_{\overline{\tau_0}=\tau_0^{'}} \geq 0$, **then** $\tau_0^{ub} \leftarrow \tau_0^{'}$.

7: $\quad$ **if** $\frac{dg(\overline{\tau_0})}{d(\overline{\tau_0})}|_{\overline{\tau_0}=\tau_0^{'}} \leq 0$, **then** $\tau_0^{lb} \leftarrow \tau_0^{'}$.

8: Evaluate and return $\tau_0 = \tau_0^{'}$, $\tau_{S_i} = \overline{\tau_{S_i}}(\tau_0')$ and P_{S_i}, for $i = 1, \ldots, N'$

Algorithm 5 presents the optimal algorithm NL-POWMU. Initially, the algorithm sets the lower (τ_0^{lb}) and upper (τ_0^{ub}) bounds on τ_0 using Lemma 13 (Line 3). The algorithm, then, applies the bisection search on τ_0 based on the convexity of the objective function over τ_0 (Lines 4-7). This search aims to iteratively converge to the optimal solution by evaluating the slope of the objective function at the midpoint of an EH time interval and shrinking the interval accordingly. In each iteration, the current solution, $\tau_0^{'}$, is set to the mean of the τ_0^{lb} and τ_0^{ub} (Line 5). The objective function is denoted by $g(\overline{\tau_0}) = \overline{\tau_0} + \sum_{i\in\{1,\ldots,N'\}} \overline{\tau_{S_i}}(\overline{\tau_0})$. If the first derivative of $g(\overline{\tau_0})$ calculated at $\tau_0^{'}$ is non-negative, indicating an increasing trend at that point, the upper bound τ_0^{ub} is updated to $\tau_0^{'}$ (Line 6). Conversely, if the derivative is non-positive, indicating a decreasing trend at that point, the lower bound τ_0^{lb} is updated to $\tau_0^{'}$ (Line 7). This iterative process continues until the difference between τ_0^{ub} and τ_0^{lb} becomes smaller than a predefined small constant 2ϵ, where $\epsilon > 0$ is used to control the solution's accuracy (Line 4). If the derivative becomes 0, indicating the discovery of the optimal solution, both τ_0^{ub} and τ_0^{lb} are set to $\tau_0^{'}$, so the algorithm terminates. The last computed value of $\tau_0^{'}$ is set as the optimal EH time. Subsequently, the algorithm evaluates and returns the optimal IT times $\overline{\tau_{S_i}}(\tau_0')$ for $\tau_0^{'}$ and power allocation P_{S_i} for $i = 1, \ldots, N'$ (Line 8).

6.5 Teacher-Student Learning based Relay Selection Framework

This section presents the deep learning framework for the relay selection problem. The conventional approach to obtain source-relay pairs without deep learning is to resort to an iterative optimization algorithm at the beginning of each time block at the AP, which leads to substantial runtimes. In our deep-learning-based design, the AP can predict optimal relay selections with high accuracy and low complexity, thanks to the well-trained deep-learning architecture based on vast amounts of data enabling the generalization of patterns and relationships in the problem.

The relay selection problem is formulated as a classification problem with $(K+1)$ classes representing $(K+1)$ possible relay selection options for each source as follows:

$$\mathcal{P} : \{\mathbf{h}, \mathbf{g}\} \rightarrow \{\mathbf{b}\}$$

where $\mathbf{h} \in \mathbb{R}^{(N+K)\times 1}$ is the input vector whose elements are the DL channel gains $h_{AP}^{S_i}$, $h_{AP}^{R_j}$ for $i = 1, 2, \ldots, N$ and $j = 1, 2, \ldots K$; $\mathbf{g} \in \mathbb{R}^{(K+N(K+1))\times 1}$ is another input vector whose elements are the UL channel gains $g_{S_i}^{R_j}$, $g_{R_j}^{AP}$ for $i = 1, 2, \ldots, N$ and $j = 0, 1, 2, \ldots K$; $\mathbf{b} \in \mathbb{R}^{(K+1)\times N}$ is the output vector where $\mathbf{b}_{ij}$, the element at j^{th} row and i^{th} column, takes value 1 if R_j is selected for S_i for $j = 0, 1, 2, \ldots, K$ and $i = 1, 2, \ldots, N$, and 0 otherwise. For instance, in a 2-source-2-relay network, the case where R_1 is selected for S_1 and no relay is selected for S_2 is mapped to

$$\mathbf{b} = \begin{bmatrix} 0 & 1 \\ 1 & 0 \\ 0 & 0 \end{bmatrix}$$

This representation allows us to design a deep learning architecture to obtain the approximation function $\mathcal{P}$ for a low-complexity solution to the relay selection problem.

Fig. 6.3a depicts the training process of the proposed deep learning architecture. The architecture learns the approximation function $\mathcal{P}$ offline and supervised. The optimal relay selections are obtained via BBA [Onalan et al., 2020]. The training process iteratively improves the deep learning model by updating weights and biases

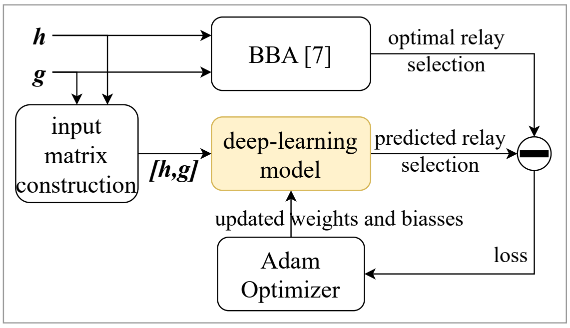

(a)

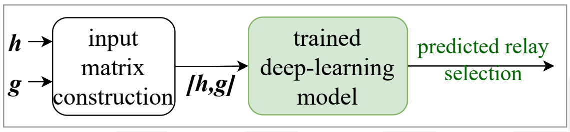

(b)

Figure 6.3: a) Training and b) Prediction processes of deep learning model

with the Adaptive Moment Estimation (Adam) [Kingma and Ba, 2014] to minimize the loss function. We employ cross-entropy loss function

$$\mathcal{CEL}(\mathbf{b}', \mathbf{b}) = \frac{1}{N}\sum_{i=1}^{N}\sum_{j=0}^{K}\mathbf{b_{ji}}\log\left(\frac{\exp\left(\mathbf{b}'_{\mathbf{ji}}\right)}{\sum_{j=0}^{K}\exp\left(\mathbf{b}'_{\mathbf{ji}}\right)}\right) \tag{6.18}$$

between the optimal relay selections $\mathbf{b}$ and predicted ones $\mathbf{b}'$ to observe how well classification model performs, where $\mathbf{b}'_{ji} \in \mathbb{R}$ are unnormalized outputs, i.e. logits, of the deep learning model for $j = 0, 1, 2, \ldots, K$ and $i = 1, 2, \ldots, N$. The cross-entropy loss $\mathcal{L}(\mathbf{b}', \mathbf{b})$ captures the divergence between the probability distribution of the predicted and optimal relay selections.

After the completion of the training, the resulting deep learning model with optimized weights and biases is used to predict relay selections online at the beginning of each time block at the AP in a single step, as shown in Fig. 6.3b. The prediction step predominantly comprises the multiplication and addition of weights and biases, thereby resulting in a significant reduction in runtime. As a result, the computational complexity becomes the burden of offline training instead of online prediction.

In deep-learning architecture design, we prefer CNNs due to the following advantages [Goodfellow et al., 2016]:

1. **Sparse interactions:** CNNs exhibit sparse interactions achieved by using smaller kernels than the input. Deep CNNs can efficiently capture intricate interactions with deeper layers, indirectly engaging with broader input segments through simple building blocks characterized by sparse interactions. Due to the sparsity, CNNs require fewer parameters which enhances memory efficiency and statistical efficiency while decreasing computational workload.

2. **Parameter sharing:** CNNs employ parameter sharing through convolution, where each kernel element is used across input positions, enabling a single parameter set to be learned for all locations. Although this doesn't impact forward propagation runtime, convolution operation substantially enhances memory efficiency and statistical efficacy compared to dense matrix multiplications.

3. **Spatial relationships:** The parameter sharing enables a single set of learned parameters to be applied to different spatial locations, capturing shared common patterns and spatial relationships efficiently. In the relay selection problem, the relation between DL and UL channel gains in both the source-to-relay and relay-to-AP links needs to be learned. A pattern resulting in S_1 to select R_j in one network realization can be repeated for S_N to select R_j in another network realization. As channel gains of different sources are located at different locations of the input matrix, observing spatial relations is critical.

We employ 2D convolution blocks to include the larger area in convolution operation to discover similar patterns between the source-relay pairs. Therefore, we transform 1D input vectors to the closest size rectangular matrix where the empty elements are filled by zero padding in the input matrix construction step, as shown in Fig 6.3.

We, first, design a deep learning architecture consisting of 2D convolutional blocks and skip connections, which is called *Skip connected Convolutional NETwork*

(SC-NET). The details of SC-NET are presented in Section 6.5.1. We, then, propose another deep learning architecture by replacing 2D convolutional blocks with the ones running in multiple flows for memory-constrained applications. Such blocks are called *inception blocks*, so the proposed architecture is named as *SKip INception NETwork* (SKIN-NET), and described in detail in Section 6.5.2. We, finally, further compress the SC-NET by reducing the number of layers and nodes in the architecture for even lower computational complexity. The compressed architecture is called MINI-SC-NET. Obviously, a lower number of parameters limits the learning capacity of the network and results in lower accuracy. To overcome such learning limitations, we propose to apply teacher-student learning where a bigger teacher network, SC-NET, is employed to train the smaller student network, which is called STU-SC-NET, in addition to the truth labels. The details on teacher-student learning are given in Section 6.5.3.

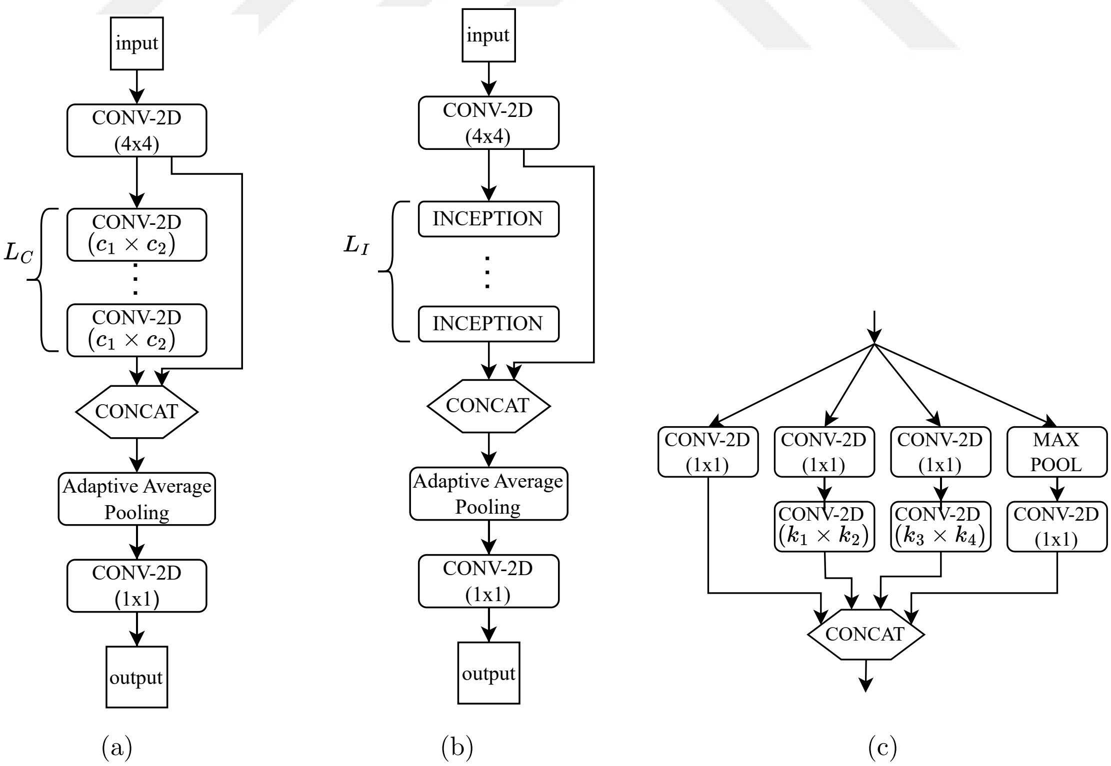

Figure 6.4: a) Proposed Network Architecture with convolution blocks b) Proposed Network Architecture with inception blocks c) Details of inception block

6.5.1 SC-NET Architecture

Fig. 6.4a presents the deep learning architecture of SC-NET. SC-NET applies a 2D convolution block (CONV-2D) in the first and the last layers with kernel sizes 4x4 and 1x1, respectively. After the first convolution block, there are again L_C 2D convolution blocks with kernel size c_1xc_2. L_C, c_1, and c_2 are optimized during the training process based on the performance of the architecture on the validation set. ReLU activation function is applied for all convolutional layers to introduce non-linearity. Further, batch normalization is applied after all convolutional layers for faster and more stable training.

SC-NETs benefit from skip connections which are shortcuts connecting the output of one layer to the input of another layer that is not adjacent to it. In deep CNNs, skip connections are helpful in dealing with diluted information or vanishing gradients passing through multiple layers by allowing information to bypass several layers [Tong et al., 2017]. The skip connection between two non-adjacent layers can be performed by addition[He et al., 2016] or concatenation[Huang et al., 2017]. We prefer concatenation to combine features from different layers and enhance feature reusability. In SC-NET, the output of the first layer is concatenated to the last layer before the adaptive average pooling.

After concatenation, SC-NET employs adaptive average pooling. In general, the pooling layer downsamples its inputs; hence it reduces the number of trainable parameters and provides lower complexity [Goodfellow et al., 2016]. The downsampling also prevents overfitting and leads to generalizable and robust results. Adaptive average pooling adapts the necessary kernel size to generate an output of the given dimensionality from the given input[van Wyk and Bosman, 2019] and performs downsampling by returning the average value of the inputs within the kernel. We prefer adaptive average pooling to fit the desired output vector dimension easily while increasing compression and robustness.

6.5.2 SKIN-NET Architecture

Fig. 6.4c presents the deep learning architecture of SKIN-NET. Similar to SC-NET, SKIN-NET also employs 2D convolution blocks with kernel sizes 4x4 and 1x1 in the first and the last layers, adaptive average pooling, and a skip connection from the output of the first layer to the last layer before the adaptive average pooling.

SKIN-NET replaces L_C convolution blocks of SC-NET with L_I inception blocks. The inception blocks run multiple flows, including convolutional blocks, in parallel to capture more diversified features [Szegedy et al., 2015]. They are preferred especially for memory constraint applications since they can achieve similar performance with lower network parameters. In our architecture, an inception block includes four parallel flows whose outputs are concatenated at the end. All lines apply 2D convolution with 1x1 kernel size. The fourth line uses max-pooling before the convolution. The second and third lines apply another convolution with kernel size $k_1 \times k_2$ and $k_3 \times k_4$. Kernel sizes must be optimized based on network size to reach optimum performance. Batch normalization is again applied after all inception layers for faster and more stable training.

6.5.3 Teacher-Student Learning

This section presents teacher-student learning to reduce the complexity of SC-NET. A compact architecture can be reached by decreasing L_C and the number of nodes in each convolutional layer. However, standalone training of such a smaller network would be incapable of reaching the accuracy of SC-NET. Therefore, we benefit from the expertise of SC-NET to train the smaller student network, called STU-SC-NET. Teacher-student learning transfers knowledge from a well-performing teacher network to a smaller or less powerful student network, using techniques like soft target guidance and distillation [Gou et al., 2021]. This approach allows the student model to learn from the teacher's expertise and improve its performance.

Teacher-student learning both benefits from the hard-coded truth labels $\mathbf{b}$ and the soft outputs of SC-NET, denoted by $\mathbf{b}'$, to train STU-SC-NET. The difference between the truth labels $\mathbf{b}$, and the predicted outcomes of STU-SC-NET,$\mathbf{b}''$, where $\mathbf{b}''_{ji} \in \mathbb{R}$ are unnormalized outputs, i.e. logits, of the student model for $j = 0, 1, 2, \ldots, K$ and $i = 1, 2, \ldots, N$, is measured by cross-entropy loss $\mathcal{CEL}$ similar to the training of SC-NET and SKIN-NET. Kullback-Leibler-Divergence is applied between the soft outputs of SC-NET, $\mathbf{b}'$ and the predicted outcomes of STU-SC-NET $\mathbf{b}''$ as given by

$$\mathcal{KLD}(\mathbf{b}'', \mathbf{w}) = \frac{1}{N} \sum_{i=1}^{N} \sum_{j=0}^{K} \mathbf{w_{ji}} \log \left(\frac{\mathbf{w_{ji}}}{\mathbf{b''_{ji}}} \right). \tag{6.19}$$

Then, the overall training loss function is the weighted average of two loss values and expressed as

$$\mathcal{L}(\mathbf{b}'', \mathbf{b}, \mathbf{w}) = \lambda_1 \mathcal{CEL}(\mathbf{b}'', \mathbf{b}) + \lambda_2 \mathcal{KLD}(\mathbf{b}'', \mathbf{w}), \tag{6.20}$$

where λ_1 and λ_2 are constant weight values. $\mathcal{L}(\mathbf{b}'', \mathbf{b}, \mathbf{w})$ enables knowledge transfer from teacher SC-NET to student STU-SC-NET by incorporating $\mathcal{KLD}(\mathbf{b}'', \mathbf{w})$.

Algorithm 6 describes Dichotomous based Architecture Search Algorithm (DASA) for STU-SC-NET, which determines the architecture of STU-SC-NET by iteratively shrinking the number of trainable parameters, denoted by Ω^{STU}. The inputs of DASA are truth labels, $\mathbf{b}$; soft outputs of SC-NET, $\mathbf{w}$; a set of available number of nodes, $\mathcal{M}$; the number of trainable parameters of SC-NET, Ω^{SC}; the number of layers of SC-NET, L_C^{SC}; and the set consisting of number of nodes in each layer, M^{SC}. Dichotomous search operated in an interval determined by an upper bound (ub) and a lower bound (lb), which are initially set to Ω^{SC} and 0, respectively (Line 3). The number of layers L_C^{STU} and nodes in each layer M^{STU} of STU-SC-NET is initialized the same as SC-NET's (Line 4). In each iteration, Dichotomous search sets Ω^{STU} to the middle point of the interval (Line 6) and calls *SEQuential Parameter Search Algorithm* (Seq-PSA), presented in Algorithm 7, to determine the number of layers and nodes in each layer, for given $\mathcal{M}$ to reach Ω^{STU} (Line 7). Seq-PSA constructs a CNN architecture with L_C^{STU} layers and M_k^{STU} nodes at each layer, where $M_k^{STU} \in \mathcal{M}, k = 1, 2, \ldots, L_C^{STU}$ and $0 < L_C^{STU} \leq L_C^{SC}$. Then, the architecture is trained via teacher-student learning (Lines 8-13). The training ends with a validation loss value v^{STU}, which is calculated by cross-entropy loss formulation given

Algorithm 6 **Dichotomous based Architecture Search Algorithm (DASA) for STU-SC-NET**

```
Input: b, w, M, Ω^SC, L_C^SC, M^SC
Output: Trained STU-SC-NET
ub ← Ω^SC and lb ← 0
L_C^STU ← L_C^SC, M^STU ← M^SC
repeat
    Ω^STU = [(ub + lb)/2]
    Call Seq-PSA for given M and Ω^STU and update L_C^STU, M^STU, Ω^STU
    repeat
        Forward propagate STU-SC-NET and obtain b″
        Calculate loss by Eq (6.20)
        Backward propagation via Adam optimizer
        Update weights and biases of STU-SC-NET
    until training converges.
    if v^STU ¡ v^th then
        update ub ← Ω^STU
    else
        update lb ← Ω^STU
until ub − lb < ϵ
```

by Eq.6.18. If v^{STU} is lower than the threshold v^{th}, ub is updated as Ω^{STU} to shrink the architecture further (Lined 14-15). Otherwise, lb is set to Ω^{STU} to enlarge the architecture to fit the desired validation loss range (Lined 16-17). Iterations of dichotomous search continue until the difference between ub and lb is negligible (Line 18).

Algorithm 7 Sequential Parameter Search Algorithm (Seq-PSA)

1: Input: L_C^{STU}, M^{STU}, Ω^{STU}, and $\mathcal{M}$
2: Output: updated L_C^{STU}, M^{STU}, and Ω^{STU}
3: $\Omega^{STU'} \leftarrow 0$ and $k \leftarrow L_C^{STU}$
4: **repeat**
5: Calculate $\mathbf{\Omega}_m$, $\forall m \in \mathcal{M}$ at layer k
6: $M_k^{STU} \leftarrow \arg\min_m |\Omega^{STU} - \mathbf{\Omega}|$
7: $\Omega^{STU'} \leftarrow \arg\min_{\mathbf{\Omega}_m} |\Omega^{STU} - \mathbf{\Omega}|$
8: $k \leftarrow k - 1$
9: **until** $|\Omega^{STU} - \Omega^{STU'}| < \Omega^{STU} \times 0.01$ and $k > 0$
10: $\Omega^{STU} \leftarrow \Omega^{STU'}$

Algorithm 7 presents Seq-PSA to efficiently update L_C^{STU} and M^{STU}, for given L_C^{STU}, M^{STU}, Ω^{STU}, and $\mathcal{M}$. Since the commonly used grid search method is intractable and computationally expensive for such parameter search [Bao and Liu, 2006, Yang et al., 2019]; we apply a method that sequentially adjusts the number of nodes from the last layer to the first layer of the architecture. The current value of the number of trainable parameters, denoted by $\Omega^{STU'}$, is initialized as 0; whereas k, the layer whose number of nodes are being adjusted in the current iteration, is initialized as the last layer (Line 3). For the current layer k, Seq-PSA tries all possible $m \in \mathcal{M}$ for M_k^{STU} and calculates the resulting number of trainable parameters Ω_m (Line 5). m providing the closest Ω_m to Ω^{STU} is selected for layer k (Line 6). The closest Ω_m to Ω^{STU} determines the value of $\Omega^{STU'}$ (Line 7). Note that $\mathcal{M}$ always contains 0, and picking $m = 0$ means removing the layer from the architecture. Seq-PSA continues by adjusting the number of nodes at the previous layer (Line 8) until either all layers are adjusted, or the current $\Omega^{STU'}$ is close enough to target Ω^{STU} (Line 9). At the end, Ω^{STU} is set to $\Omega^{STU'}$ (Line 10).

6.6 Performance Evaluation

The goal of this section is to analyze the performance of the proposed deep learning approaches in terms of training and validation loss performances, architecture sizes, and runtime complexities, and compare their performance to the optimal solution by BBA and the state-of-art sub-optimal algorithms Opportunistic Relaying (OR)[Chen et al., 2015], One Branch Heuristic (OBH) [Onalan et al., 2020], the state-of-art deep learning framework called REL-NET [Onalan and Coleri, 2023]. BBA is the optimal algorithm we used to obtain truth labels during training. OBH applies a branch-and-bound strategy similar to BBA but follows a single branch, where the solution of the relaxed problem results in the maximum b_i^j, instead of all. OR picks R_j with $\arg\max_j \min\left(g_{S_i}^{R_j} h_{AP}^{S_i}, g_{R_j}^{AP} h_{AP}^{R_j}\right)$ for each source S_i, for $i = 1, \ldots, N$. REL-NET is a feed-forward DNN that treats the relay selection problem as a classification problem where each possible source-relay pair is represented by a class resulting in $(K+1)^N$ classes in total. We further use the same compact architecture of STU-SC-NET trained only by truth labels as SC-NET, called MINI-SC-NET, as a benchmark approach to indicate the benefit of teacher-student learning.

6.6.1 Data Generation

DL and UL channel gains, $\mathbf{h}$ and $\mathbf{g}$, are generated as follows: Sources are uniformly distributed in a circular quadrant between radius $3-4$ m. The AP is located at the center of the circle. Relays are positioned between the sources and the AP at a distance of 2 m from the AP and with an equal distance from each other. Large scale channel statistics are formulated as $PL(d) = PL(d_0) - 10\upsilon \log_{10}(d/d_0) + Z$, where $PL(d_0)$ is the free space path loss at unit distance d_0 in dB, d is the distance between the transmitter and receiver, $PL(d)$ is the path loss at a distance d in dB, υ is the path-loss exponent, and Z is a zero-mean Gaussian random variable with standard deviation σ_Z. For small-scale statistics, the Rayleigh fading model is used

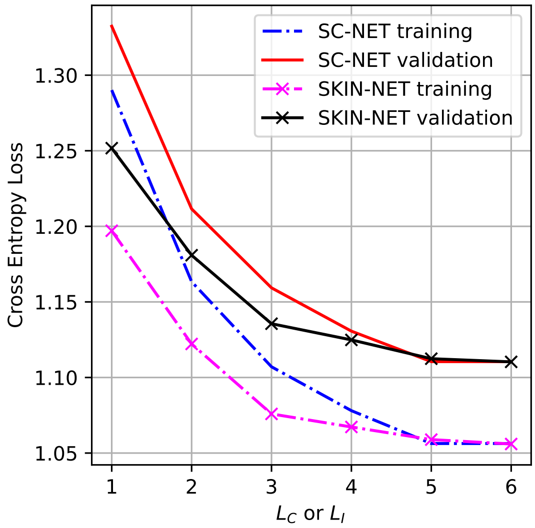

(a)

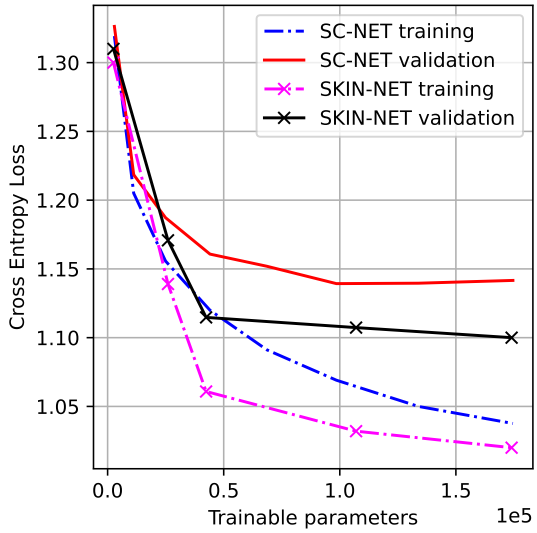

(b)

Figure 6.5: Cross Entropy Loss vs. a) number of layers b) number of trainable parameters in a 3-source-2-relay network.

with scale parameter Ω set to the mean power level determined by $PL(d)$.

700, 000 independent random network realizations are generated for each different network size. Generated data is divided into the train, validation, and test sets, with sizes of 689, 000; 10, 000; and 1, 000, respectively. The performance of all the algorithms is measured over the test data set. The simulation results are presented as an average of the performance over 1, 000 independent random network realizations of the test set.

We consider the following simulation parameters: $a_k = 150$, $b_k = 0.014$, $M_k = 0.024$, $W = 1$ MHz, $N_0 = -90$ dBm, $PL(d_0) = 31.67$ dB, $\sigma_Z = 2$ dB, and $\upsilon = 2$, $P_{AP} = 4$ W, $P^{max} = 10$ mW, $D_{Si} = 50$ bits $\forall i$. Without loss of generality, D_{Si} values are selected the same for simpler implementation.

6.6.2 Deep Learning Performance

For the proposed deep learning approaches, this section presents the training and validation loss performances, the proposed architecture sizes, and runtime complexities. The proposed architectures are implemented in PyTorch. Their weights are optimized by Adam optimizer with batch size 128 and learning rate of 10^{-3}. The hyperparameters such as kernel size and number of layers are fine-tuned via grid search unless otherwise stated. Training is performed on an NVIDIA TITAN XP graphics processing unit (GPU). Testing is performed on Windows 64-bit OS, 8GB RAM, and Intel i7-7600U dual-core processor. We consider the following algorithm parameters for architecture search: $\mathcal{M} = \{64, 32, 24, 16, 8, 2, 0\}$, and $\epsilon = 300$.

Fig. 6.5a depicts the training and validation loss for SC-NET and SKIN-NET as the number of layers, L_C or L_I, increases from 1 to 6 while the number of trainable parameters is fixed in a 3-source-2-relay network. We compare SC-NET and SKIN-NET to observe the impact of convolution and inception blocks on the loss performance. The increasing number of layers improves the cross-entropy loss until $L_C = 5$ or $L_I = 5$. SKIN-NET provides lower loss values with fewer layers. Lower validation losses with the same complexity underpin the success of inception-based architectures. Note that STU-SC-NET employs a different training loss due to the nature of teacher-student learning, so it is not directly comparable with SC-NET and SKIN-NET in terms of loss values.

Fig. 6.5b depicts the training and validation loss for SC-NET and SKIN-NET as the number of trainable parameters increases in a 3-source-2-relay network. The increasing number of parameters improves the cross-entropy loss until 100,000 parameters. The lower validation and training cross-entropy is achieved by SKIN-NET due to inception blocks based on which one can create deeper architectures with the same number of trainable parameters compared to SC-NET.

Tables 6.1 and 6.2 present the fine-tuned hyperparameters for SC-NET and SKIN-NET, respectively. SKIN-NET possesses 7.35 times less parameters, making it advantageous for memory-constraint applications compared to SC-NET. However, SKIN-NET's parallel flows increase its runtime by three times compared to SC-NET. Note that the runtime tradeoff between SC-NET and SKIN-NET varies depending on the implementation of the algorithms. In this case, Pytorch implementation ignores parallel flows in SKIN-NET. With implementations prioritizing parallel processing, SKIN-NET may result in lower runtimes [Pal et al., 2019]. Note that the runtimes presented in these tables only consider the testing phase of the relay selection.

Table 6.1: SC-NET Parameters

N	K	input size	L_C	Number of nodes per layer	kernel (c_1xc_2)	Trainable parameters	Runtime (ms)
1	2	2x4	5	16,64,64,32,32,16,10	2x2	36,457	0.11
2	2	3x4	5	16,64,64,32,32,16,10	3x2	55,131	0.12
3	2	4x4	5	16,64,64,32,32,16,10	3x3	86,391	0.14
4	2	5x4	5	16,64,64,32,32,16,10	4x4	166,543	0.21
5	2	6x4	5	16,64,64,32,32,16,10	5x4	272,945	0.24

Table 6.2: SKIN-NET Parameters

N	K	input size	L_I	Number of nodes per layer	kernel $(k_1xk_2), (k_3xk_4)$	Trainable parameters	Runtime (ms)
1	2	2x4	5	32,64,64,32,24,16	4x4,2x2	24,261	0.3
2	2	3x4	5	32,64,64,32,24,16	4x4,3x2	25,517	0.33
3	2	4x4	5	32,64,64,32,24,16	4x4,3x3	27,401	0.41
4	2	5x4	5	32,64,64,32,24,16	4x4,4x4	31,797	0.47
5	2	6x4	5	32,64,64,32,24,16	4x4,5x5	37,449	0.59

Figs. 6.6a and 6.6b respectively present the training and validation losses for STU-SC-NET throughout the iterations of DASA given in Algorithm 6 in a 3-source-2-relay network. In first six iterations, DASA shrinked the architecture size. Since the validation loss exceeds the determined threshold, 1.5, in the sixth iteration, DASA enlarged the architecture for the next step. At the last step, the architecture size reduced one last time and DASA stoped. The training and validation losses worsen as the number of trainable parameters, as expected. However, the decreased

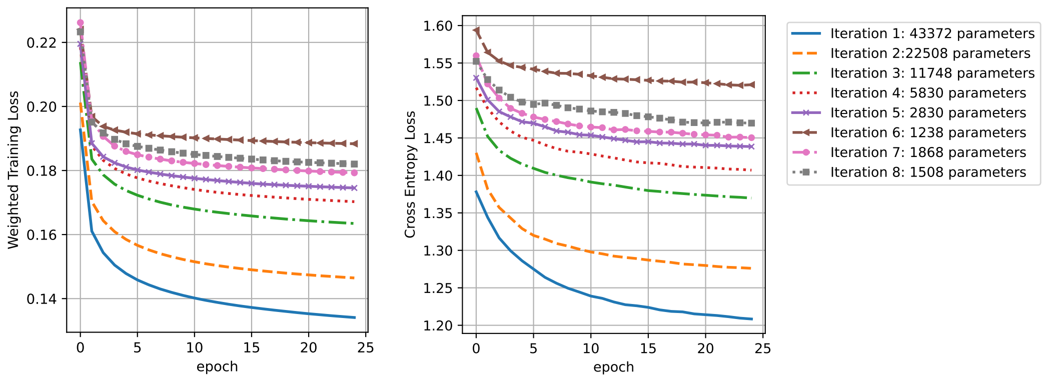

(a) (b)

Figure 6.6: a) Training and b) Validation Losses throughout the iterations of DASA given in Algorithm 6 in a 3-source-2-relay network.

number of parameters indicates decreased runtime since the complexity of CNNs is commonly scaled by the number of parameters. DASA aims to find the best tradeoff between the loss value and parameter size. DASA decides on architecture with 1508 trainable parameters in 8 iterations with validation cross-entropy loss lower than 1.5.

Table 6.3 presents the hyperparameters for STU-SC-NET determined by DASA. The comparison with Tables 6.1 and 6.2 indicates a significant reduction in terms of the number of trainable parameters and runtimes provided by STU-SC-NET. STU-SC-NET provides up to 16 times lower runtime than SC-NET and up to 29 times less trainable parameters than SKIN-NET. Note that the runtimes presented in the table only consider the testing phase of the relay selection step.

6.6.3 Benchmark Comparison

This section compares the performances of the proposed deep learning architectures SC-NET, SKIN-NET, and STU-SC-NET, with the aforementioned benchmark algorithms.

Fig. 6.7a depicts the schedule length as the number of sources varies from 1 to 5 in a 2-relay network. Cooperating with relays significantly improves the sched-

Table 6.3: STU-SC-NET Parameters

N	K	input size	L_C	Number of nodes per layer	kernel (c_1xc_2)	Trainable parameters	Runtime (ms)
1	2	2x4	1	8,8,8,10	2x2	833	0.011
2	2	3x4	1	8,8,8,10	2x2	923	0.011
3	2	4x4	1	8,8,8,10	2x2	1508	0.012
4	2	5x4	1	8,8,8,10	2x2	2507	0.013
5	2	6x4	1	8,8,8,10	2x2	6,881	0.015

ule length, e.g., 95% for N=2. BBA is the optimal algorithm providing always the minimum schedule length. SC-NET outperforms all other sub-optimal approaches, which SKIN-NET follows. MINI-SC-NET is the worst-performing deep learning-based approach as it has a small architecture. STU-SC-NET performs up to 9% better than MINI-SC-NET, indicating the improvement provided by a teacher network during training. The optimality gap of SC-NET, SKIN-NET, OBH, REL-NET, STU-SC-NET, MINI-SC-NET, and OR are 20%, 22% 23%, 24%, 27%, and 34%, in a 4-source-2-relay network, respectively.

Fig. 6.7b shows the runtimes of the proposed and benchmark algorithms as the number of sources varies from 1 to 5 in a 2-relay network. The runtime of MINI-SC-NET is omitted as it overlaps with STU-SC-NET due to the same size architecture. BBA and OBH have three orders of magnitude higher runtimes than all other approaches. OR has the lowest runtime. Due to its parallel architecture, SKIN-NET requires more runtime than other deep learning approaches. STU-SC-NET has the lowest runtime among deep learning approaches as it has the smallest architecture. OBH, SKIN-NET, SC-NET, REL-NET, STU-SC-NET provides up to 20, 44360, 70997, 92916, 99328 times lower runtime than BBA.

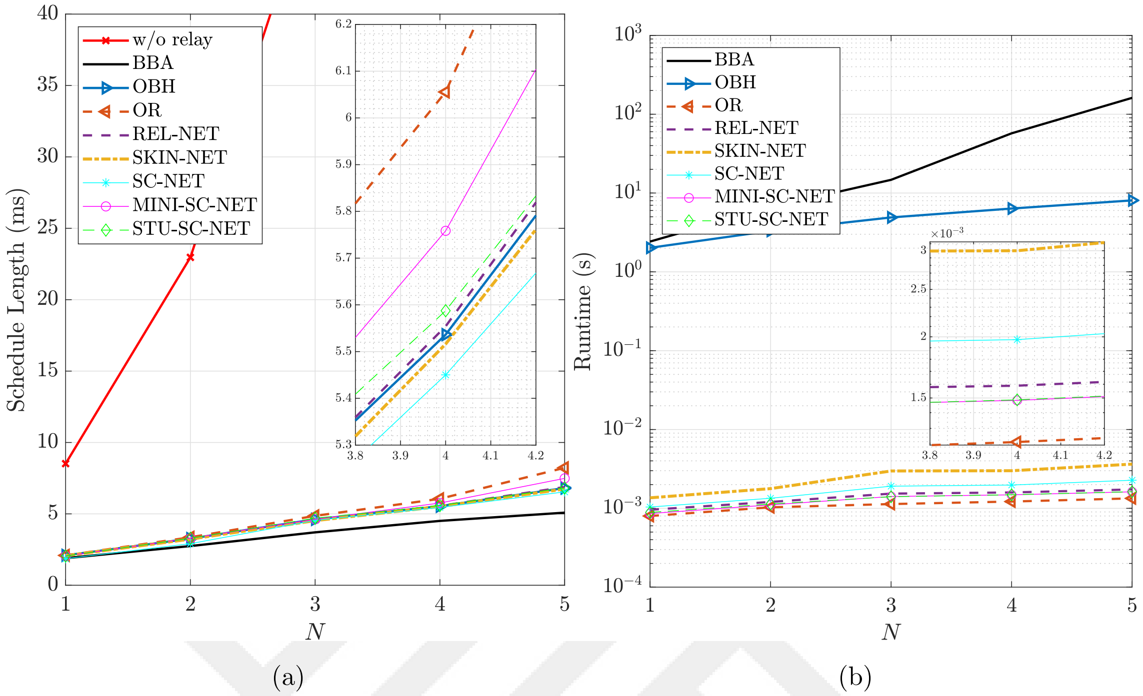

Figure 6.7: a) Schedule length b) Runtime vs. the number of sources in a 2-relay network.

6.7 Conclusion

We study the joint relay selection, scheduling, and power control problem for multiple-source-multiple-relay WPCCN with a non-linear EH model. The objective of the problem is to minimize the schedule length; whereas the problem has constraints on data demand, energy causality, and maximum UL transmit power. The problem is non-convex MINLP and NP-hard. Given the relay selection, a bisection searched-based algorithm solves the scheduling and power control problem. For the low-complexity solution to the remaining relay selection problem, this work proposes a CNN-based solution, called SC-NET. We extend the CNN-based solution with inception blocks, called SKIN-NET, to decrease trainable parameter size without loosing accuracy for memory-constraint applications. We finally apply teacher-student learning, to decrease the runtime complexity further. The student network is called STU-SC-NET. To find the optimum compact architecture for STU-SC-NET, a dichotomous search-based algorithm is proposed. We demonstrate via numerical simulations that our proposed approaches exhibit better performance than the state-of-art iterative algorithms. SC-NET can be preferred for the lowest optimality gap with low runtime. SKIN-NET can be preferred for memory constraint applications as its parameter size is significantly less than SC-NET. STU-SC-NET can be preferred for the lowest runtime with high accuracy.

Chapter 7

CONCLUSION

This thesis proposes deep learning based approaches for the low complexity solutions to the resource allocation and optimization problems in WPCNs. In particular, the joint relay selection, scheduling, and power control problem in multiple-source-multiple-relay WPCCNs are studied under the systems with the linear and non-linear EH models; and finite and infinite packet length regimes.

Chapter 2 presents the novel joint relay selection, scheduling, and power control problem for multiple-source-multiple-relay network and optimization theory-based solution of the problem. The objective of the problem is minimizing the total duration of wireless power and information transfer; whereas the constraints are energy causality, data demand, and maximum allowed transmit power. The formulated problem is non-convex mixed-integer non-linear programming problem, and proven to be NP-hard. We first formulate a sub-problem on scheduling and power control for a given relay selection. We propose an efficient optimal algorithm based on a bi-level optimization over power transfer time allocation. Then, for optimal relay selection, we present optimal exponential-time Branch-and-Bound (BB) based algorithm where the nodes are pruned with problem specific lower and upper bounds. We also provide two BB-based heuristic approaches limiting the number of branches generated from a BB-node, and a relay criterion based lower complexity heuristic algorithm. The proposed algorithms are demonstrated to outperform conventional harvest-then-cooperate approaches in terms of schedule length for various network settings.

Chapter 3 presents the deep learning-based framework for a low-complexity solution to the minimum length scheduling problem in half-duplex WPCNs. The objective of the problem is to minimize the duration of the schedule for energy harvesting (EH) and information transmission (IT), subject to the data demand, energy causality, and maximum transmit power constraints. Multi-input multi-output feed-forward deep neural network (DNN) architecture is considered, where the inputs are channel state information and two parameters derived from the optimality conditions of the problem; and outputs are the transmit powers, EH and IT lengths. To ensure the feasibility of the DNN outputs, we design a final layer which maps the estimated transmit powers to the feasible EH and IT lengths. The DNN is trained offline with both supervised and unsupervised techniques. Simulation results indicate that the proposed DNN-based approaches are faster than the benchmark iterative algorithms. These approaches also outperform benchmark sub-optimal algorithms in terms of accuracy and robustness against varying network conditions.

Chapter 4 formulates the scheduling and power control problem for short packet communications. The problem is nonlinear and non-convex, so hard to solve. To obtain a near-optimal solution, a bi-level optimization-based framework is proposed with the master problem searching for optimal EH duration iteratively and subproblems of calculating the schedule length for a given EH time in each iteration. Then, we propose a low complexity optimization theory based deep learning framework based on the simplification of the deep learning architecture by using optimality conditions. The proposed approaches outperform state-of-art algorithms in terms of schedule length. The optimization theory based deep learning approach further decreases the complexity significantly.

Chapter 5 proposes a low complexity solution based on deep learning to solve the relay selection problem with the objective of minimum schedule length in multi-source-multi-relay WPCCNs. We formulate the relay selection problem as a novel multi-class classification problem whose classes represent all possible relay selection combinations for all sources. To solve this classification problem, a feed-forward deep neural network (DNN) architecture is designed. The inputs are the channel gains and parameters derived from these gains based on the optimality conditions of the problem. The output is the relay selection for all sources represented by a class. Conventional supervised Machine Learning (ML) algorithms, including Decision Tree, Random Forest, Support Vector Machine, and K-Nearest Neighbour, are also implemented for benchmark comparisons. The proposed network outperforms the benchmark ML algorithms and previous iterative heuristic algorithms regarding precision, recall, f1-score, accuracy, and optimality gap in schedule length with lower runtime.

Chapter 6 focuses on the joint relay selection, scheduling, and power control problem in multiple-source-multiple-relay RF-EH networks under nonlinear EH conditions. The joint optimization problem is solved in two folds. First, the optimal solution to the scheduling and power control problem is obtained for the given relay selection. Second, the relay selection problem is formulated as a classification problem, for which two convolutional neural network (CNN) based architectures are proposed. In both architectures, the inputs are channel gains; whereas the outputs are the selected relays represented by a specific class. While the first architecture employs conventional 2D convolution blocks; the second architecture replaces them with inception blocks, to decrease trainable parameter size without sacrificing accuracy for memory-constraint applications. Both architectures benefit from skip connections between layers to enhance feature reusability. We also apply teacher-student learning, where the teacher network is larger, and the student is a smaller size CNN-based architecture distilling the teacher's knowledge to decrease the runtime complexity further. To determine the best architecture for the student network, a novel dichotomous search based algorithm is employed. This search iteratively decreases the number of trainable parameters of the student network and selects the number of layers and nodes at each layer for a given number of trainable parameters with a novel sequential parameter search algorithm. Our simulation results demonstrate that the proposed solutions provide lower complexity than the state-of-art iterative approaches without compromising optimality.

In a nutshell, this thesis highlights the performance improvement brought by relays to WPCNs and promising solution strategies by deep learning approaches for resource allocation and optimization problems in WPCNs.

The future work of this thesis is in two directions: i) extensions for the optimization problem formulation and ii) improvements on the deep learning models. For the former, the problem formulations can be extended for other energy sources than RF signals in EH and for erroneous channel state information (CSI) instead of perfectly known CSI assumption. For the latter, end-to-end training approach can be applied to deep learning models currently trained separately for scheduling and power control, and relay selection subproblems. The training step currently has computational complexity and cost, so it must be optimized for a sustainable system in the future. In particular, more effective synthetic data generation for training, time and cost-efficient training processes, and more effective loss functions can be studied. Further, deep reinforcement learning algorithms can be useful for problems in more changing environmental conditions, e.g., energy harvesting models.

BIBLIOGRAPHY

[Akhtar and Rehmani, 2017] Akhtar, F. and Rehmani, M. H. (2017). Energy harvesting for self-sustainable wireless body area networks. *IT Professional*, 19(2):32–40.

[Alcaraz López et al., 2018] Alcaraz López, O. L., Fernández, E. M. G., Souza, R. D., and Alves, H. (2018). Ultra-reliable cooperative short-packet communications with wireless energy transfer. *IEEE Sensors Journal*, 18(5):2161–2177.

[Ammar and Reynolds, 2018] Ammar, A. and Reynolds, D. (2018). Energy harvesting networks: Energy versus data cooperation. *IEEE Communications Letters*, 22(10):2128–2131.

[Ashraf et al., 2021] Ashraf, N., Sheikh, S. A., Khan, S. A., Shayea, I., and Jalal, M. (2021). Simultaneous Wireless Information and Power Transfer With Cooperative Relaying for Next-Generation Wireless Networks: A Review. *IEEE Access*, 9.

[Baidas et al., 2019] Baidas, M. W., Bahbahani, Z., El-Sharkawi, N., Shehada, H., and Alsusa, E. (2019). Joint relay selection and energy-efficient power allocation in downlink multi-cell noma networks. In *2019 IEEE Wireless Communications and Networking Conference (WCNC)*, pages 1–8.

[Balatsoukas-Stimming and Studer, 2019] Balatsoukas-Stimming, A. and Studer, C. (2019). Deep unfolding for communications systems: A survey and some new directions. In *2019 IEEE International Workshop on Signal Processing Systems (SiPS)*, pages 266–271.

[Bao and Liu, 2006] Bao, Y. and Liu, Z. (2006). A fast grid search method in support vector regression forecasting time series. In Corchado, E., Yin, H., Botti, V., and Fyfe, C., editors, *Intelligent Data Engineering and Automated Learning – IDEAL 2006*, pages 504–511, Berlin, Heidelberg. Springer Berlin Heidelberg.

[Belotti et al., 2012] Belotti, P., Kirches, C., Leyffer, S., Linderoth, J., Luedtke, J., and Mahajan, A. (2012). Mixed-integer nonlinear optimization. Technical report, Argonne National Laboratory.

[Boshkovska et al., 2015] Boshkovska, E., Ng, D. W. K., Zlatanov, N., and Schober, R. (2015). Practical non-linear energy harvesting model and resource allocation for swipt systems. *IEEE Communications Letters*, 19(12):2082–2085.

[Chen et al., 2015] Chen, H., Li, Y., Rebelatto, J. L., Uchoa-Filho, B. F., and Vucetic, B. (2015). Harvest-then-cooperate: Wireless-powered cooperative communications. *IEEE Transactions on Signal Processing*, 63(7):1700–1711.

[Chen et al., 2018] Chen, H., Zhai, C., Li, Y., and Vucetic, B. (2018). Cooperative strategies for wireless-powered communications: An overview. *IEEE Wireless Communications*, 25(4):112–119.

[Chen et al., 2019] Chen, J., Zhang, L., Liang, Y., Kang, X., and Zhang, R. (2019). Resource allocation for wireless-powered iot networks with short packet communication. *IEEE Transactions on Wireless Communications*, 18(2):1447–1461.

[Chen and Tellambura, 2005] Chen, Y. and Tellambura, C. (2005). Performance analysis of maximum ratio transmission with imperfect channel estimation. *IEEE Communications Letters*, 9(4):322–324.

[Chi et al., 2017] Chi, K., Zhu, Y., Li, Y., Huang, L., and Xia, M. (2017). Minimization of transmission completion time in wireless powered communication networks. *IEEE Internet of Things Journal*, 4(5):1671–1683.

[Chiang et al., 2007] Chiang, M., Low, S. H., Calderbank, A. R., and Doyle, J. C. (2007). Layering as optimization decomposition: A mathematical theory of network architectures. *Proceedings of the IEEE*, 95(1):255–312.

[Choi et al., 2018] Choi, K. W., Rosyady, P. A., Ginting, L., Aziz, A. A., Setiawan, D., and Kim, D. I. (2018). Theory and experiment for wireless-powered sensor networks: How to keep sensors alive. *IEEE Transactions on Wireless Communications*, 17(1):430–444.

[Cui et al., 2018] Cui, W., Shen, K., and Yu, W. (2018). Spatial Deep Learning for Wireless Scheduling. In *2018 IEEE Global Communications Conference (GLOBECOM)*, pages 1–6.

[Cui et al., 2020] Cui, W., Shen, K., and Yu, W. (2020). Deep learning for robust power control for wireless networks. In *ICASSP 2020 - 2020 IEEE International Conference on Acoustics, Speech and Signal Processing (ICASSP)*, pages 8554–8558.

[Ding et al., 2014] Ding, Z., Krikidis, I., Sharif, B. S., and Poor, H. V. (2014). Wireless information and power transfer in cooperative networks with spatially random relays. *IEEE Transactions on Wireless Communications*, 13(8):4440–4453.

[Durisi et al., 2016] Durisi, G., Koch, T., and Popovski, P. (2016). Toward massive, ultrareliable, and low-latency wireless communication with short packets. *Proceedings of the IEEE*, 104(9):1711–1726.

[Elsayed and Erol-Kantarci, 2019] Elsayed, M. and Erol-Kantarci, M. (2019). AI-Enabled Future Wireless Networks: Challenges, Opportunities, and Open Issues. *IEEE Vehicular Technology Magazine*, 14(3):70–77.

[Elsayed and Erol-Kantarci, 2019] Elsayed, M. and Erol-Kantarci, M. (2019). Ai-enabled future wireless networks: Challenges, opportunities, and open issues. *IEEE Vehicular Technology Magazine*, 14(3):70–77.

[Goodfellow et al., 2016] Goodfellow, I., Bengio, Y., and Courville, A. (2016). *Deep Learning*. MIT Press. `http://www.deeplearningbook.org`.

[Gou et al., 2021] Gou, J., Yu, B., Maybank, S. J., and Tao, D. (2021). Knowledge distillation: A survey. *Int. J. Comput. Vision*, 129(6):1789–1819.

[Grant and Boyd, 2014] Grant, M. and Boyd, S. (2014). CVX: Matlab software for disciplined convex programming, version 2.1.

[Grover and Sahai, 2010] Grover, P. and Sahai, A. (2010). Shannon meets tesla: Wireless information and power transfer. In *2010 IEEE International Symposium on Information Theory*. IEEE.

[Gu and Aissa, 2015] Gu, Y. and Aissa, S. (2015). RF-based energy harvesting in decode-and-forward relaying systems: Ergodic and outage capacities. *IEEE Transactions on Wireless Communications*, 14(11):6425–6434.

[Gu et al., 2018] Gu, Y., Chen, H., Li, Y., Liang, Y.-C., and Vucetic, B. (2018). Distributed multi-relay selection in accumulate-then-forward energy harvesting relay networks. *IEEE Transactions on Green Communications and Networking*, 2(1):74–86.

[Gu et al., 2015] Gu, Y., Chen, H., Li, Y., and Vucetic, B. (2015). An adaptive transmission protocol for wireless-powered cooperative communications. In *2015 IEEE International Conference on Communications (ICC)*. IEEE.

[Gupta et al., 2019] Gupta, A., Singh, K., and Sellathurai, M. (2019). Time-Switching EH-Based Joint Relay Selection and Resource Allocation Algorithms for Multi-User Multi-Carrier AF Relay Networks. *IEEE Transactions on Green Communications and Networking*, 3(2).

[Hadzi-Velkov et al., 2017a] Hadzi-Velkov, Z., Nikoloska, I., Chingoska, H., and Zlatanov, N. (2017a). Opportunistic scheduling in wireless powered communication networks. *IEEE Transactions on Wireless Communications*, 16(6):4106–4119.

[Hadzi-Velkov et al., 2017b] Hadzi-Velkov, Z., Nikoloska, I., Chingoska, H., and Zlatanov, N. (2017b). Opportunistic scheduling in wireless powered communication networks. *IEEE Transactions on Wireless Communications*, 16(6):4106–4119.

[Hameed et al., 2021] Hameed, I., Tuan, P. V., and Koo, I. (2021). Deep learning–based energy beamforming with transmit power control in wireless powered communication networks. *IEEE Access*, 9:142795–142803.

[Han et al., 2022] Han, S., Li, L., Li, X., Liu, Z., Yan, L., and Zhang, T. (2022). Joint relay selection and power allocation for time-varying energy harvesting-driven uasns: A stratified reinforcement learning approach. *IEEE Sensors Journal*, 22(20):20063–20072.

[He et al., 2019] He, C., Liang, J., Qian, G., Guo, C., and Feng, D. (2019). Optimal time allocation in multi-cell wireless powered communication networks. *IEEE Access*, 7:26519–26526.

[He et al., 2016] He, K., Zhang, X., Ren, S., and Sun, J. (2016). Deep residual learning for image recognition. In *2016 IEEE Conference on Computer Vision and Pattern Recognition (CVPR)*, pages 770–778.

[Hillier and Lieberman, 2010] Hillier, F. S. and Lieberman, G. J. (2010). *Introduction to Operations Research, 9th Ed.* McGrawHill, New York.

[Hou and Kumar, 2012] Hou, I.-H. and Kumar, P. R. (2012). Real-time communication over unreliable wireless links: a theory and its applications. *IEEE Wireless Communications*, 19(1):48–59.

[Huang et al., 2017] Huang, G., Liu, Z., Van Der Maaten, L., and Weinberger, K. Q. (2017). Densely connected convolutional networks. In *Proceedings of the IEEE conference on computer vision and pattern recognition*, pages 4700–4708.

[Iqbal et al., 2020] Iqbal, M. S., Sadi, Y., and Coleri, S. (2020). Minimum length scheduling for full duplex time-critical wireless powered communication networks. *IEEE Transactions on Wireless Communications*, 19(9):5993–6006.

[Iqbal et al., 2022a] Iqbal, M. S., Sadi, Y., and Coleri, S. (2022a). Minimum length scheduling for discrete-rate full-duplex wireless powered communication networks. *IEEE Transactions on Wireless Communications*, 21(1):135–148.

[Iqbal et al., 2022b] Iqbal, M. S., Sadi, Y., and Coleri, S. (2022b). Minimum length scheduling for discrete-rate full-duplex wireless powered communication networks. *IEEE Transactions on Wireless Communications*, 21(1):135–148.

[Ju and Zhang, 2014] Ju, H. and Zhang, R. (2014). Throughput maximization in wireless powered communication networks. *IEEE Transactions on Wireless Communications*, 13(1):418–428.

[Kang et al., 2015] Kang, X., Ho, C. K., and Sun, S. (2015). Full-duplex wireless-powered communication network with energy causality. *IEEE Transactions on Wireless Communications*, 14(10):5539–5551.

[Kato et al., 2020] Kato, N., Mao, B., Tang, F., Kawamoto, Y., and Liu, J. (2020). Ten challenges in advancing machine learning technologies toward 6g. *IEEE Wireless Communications*, 27(3):96–103.

[Kaus et al., 2010] Kaus, M., Kowal, J., and Sauer, D. U. (2010). Modelling the effects of charge redistribution during self-discharge of supercapacitors. *Electrochimica Acta*, 55(25):7516 – 7523.

[Kazmi et al., 2020] Kazmi, S. A. A., Iqbal, M. S., and Coleri, S. (2020). Total transmission time minimization through relay selection for full-duplex wireless powered cooperative communication networks. In Grieco, L. A., Boggia, G., Piro, G., Jararweh, Y., and Campolo, C., editors, *Ad-Hoc, Mobile, and Wireless Networks*, pages 257–268, Cham. Springer International Publishing.

[Kazmi et al., 2021] Kazmi, S. A. A., Iqbal, M. S., and Coleri, S. (2021). Relay Selection and Throughput Maximization for Full Duplex Wireless Powered Cooperative Communication Networks. In *2021 IEEE 32nd Annual International Symposium on Personal, Indoor and Mobile Radio Communications (PIMRC)*.

[Ke et al., 2010] Ke, F., Feng, S., and Zhuang, H. (2010). Relay selection and power allocation for cooperative network based on energy pricing. *IEEE Communications Letters*, 14(5):396–398.

[Khan and Coleri, 2021] Khan, N. and Coleri, S. (2021). Deep neural network based minimum length scheduling in wireless powered communication networks. In *2021 IEEE Globecom Workshops (GC Wkshps)*, pages 1–6.

[Khan et al., 2017] Khan, T. A., Heath, R. W., and Popovski, P. (2017). Wirelessly powered communication networks with short packets. *IEEE Transactions on Communications*, 65(12):5529–5543.

[Kim et al., 2018] Kim, H., Lee, H., Duan, L., and Lee, I. (2018). Sum-rate maximization methods for wirelessly powered communication networks in interference channels. *IEEE Transactions on Wireless Communications*, 17(10):6464–6474.

[Kingma and Ba, 2014] Kingma, D. P. and Ba, J. (2014). Adam: A method for stochastic optimization. *arXiv preprint arXiv:1412.6980*.

[Krikidis, 2014] Krikidis, I. (2014). Simultaneous information and energy transfer in large-scale networks with/without relaying. *IEEE Transactions on Communications*, 62(3):900–912.

[Le et al., 2008] Le, T., Mayaram, K., and Fiez, T. (2008). Efficient far-field radio frequency energy harvesting for passively powered sensor networks. *IEEE Journal of Solid-State Circuits*, 43(5):1287–1302.

[Lee et al., 2021] Lee, W., Lee, K., Choi, H.-H., and Leung, V. C. M. (2021). Deep learning for swipt: Optimization of transmit-harvest-respond in wireless-powered interference channel. *IEEE Transactions on Wireless Communications*, 20(8):5018–5033.

[Li et al., 2019] Li, X., Zhou, X., Sun, C., and Ng, D. W. K. (2019). Online policies for throughput maximization of energy-constrained wireless-powered communication systems. *IEEE Transactions on Wireless Communications*, 18(3):1463–1476.

[Liang et al., 2020] Liang, F., Shen, C., Yu, W., and Wu, F. (2020). Towards Optimal Power Control via Ensembling Deep Neural Networks. *IEEE Transactions on Communications*, 68(3):1760–1776.

[Liu et al., 2017] Liu, J., Xiong, K., Fan, P., and Zhong, Z. (2017). Rf energy harvesting wireless powered sensor networks for smart cities. *IEEE Access*, 5:9348–9358.

[Liu et al., 2014] Liu, L., Zhang, R., and Chua, K.-C. (2014). Multi-antenna wireless powered communication with energy beamforming. *IEEE Transactions on Communications*, 62(12):4349–4361.

[Lu et al., 2015] Lu, X., Wang, P., Niyato, D., Kim, D. I., and Han, Z. (2015). Wireless networks with RF energy harvesting: A contemporary survey. *IEEE Communications Surveys & Tutorials*, 17(2):757–789.

[Luenberger and Ye, 2008] Luenberger, D. G. and Ye, Y. (2008). *Linear and Nonlinear Programming*. Springer New York, NY.

[Luo et al., 2016] Luo, Y., Zhang, J., and Letaief, K. B. (2016). Transmit power minimization for wireless networks with energy harvesting relays. *IEEE Transactions on Communications*, 64(3):987–1000.

[López et al., 2017] López, O. L. A., Alves, H., Souza, R. D., and Fernández, E. M. G. (2017). Ultrareliable short-packet communications with wireless energy transfer. *IEEE Signal Processing Letters*, 24(4):387–391.

[Mishra et al., 2017] Mishra, D., De, S., and Krishnaswamy, D. (2017). Dilemma at RF energy harvesting relay: Downlink energy relaying or uplink information transfer? *IEEE Transactions on Wireless Communications*, 16(8):4939–4955.

[Morsi et al., 2015] Morsi, R., Michalopoulos, D. S., and Schober, R. (2015). Multiuser scheduling schemes for simultaneous wireless information and power transfer over fading channels. *IEEE Transactions on Wireless Communications*, 14(4):1967–1982.

[Nasir et al., 2015] Nasir, A. A., Zhou, X., Durrani, S., and Kennedy, R. A. (2015). Wireless-powered relays in cooperative communications: Time-switching relaying protocols and throughput analysis. *IEEE Transactions on Communications*, 63(5):1607–1622.

[Nguyen et al., 2023] Nguyen, T.-V., Nguyen, V.-D., da Costa, D. B., Huynh-The, T., Hu, R. Q., and An, B. (2023). Short-packet communications in multihop networks with wet: Performance analysis and deep learning-aided optimization. *IEEE Transactions on Wireless Communications*, 22(1):439–456.

[Nguyen et al., 2021] Nguyen, T.-V., Tran, T.-N., Shim, K., Huynh-The, T., and An, B. (2021). A deep-neural-network-based relay selection scheme in wireless-powered cognitive iot networks. *IEEE Internet of Things Journal*, 8(9):7423–7436.

[Nosratinia et al., 2004] Nosratinia, A., Hunter, T., and Hedayat, A. (2004). Cooperative communication in wireless networks. *IEEE Communications Magazine*, 42(10):74–80.

[Onalan and Coleri, 2023] Onalan, A. G. and Coleri, S. (2023). Deep learning based low complexity relay selection for wireless powered cooperative communication networks. In *2023 International Balkan Conference on Communications and Networking (BalkanCom)*, pages 1–6.

[Onalan et al., 2022] Onalan, A. G., Kopru, B., and Coleri, S. (2022). Deep learning based minimum length scheduling for half duplex wireless powered communication networks. In *2022 IEEE 33rd Annual International Symposium on Personal, Indoor and Mobile Radio Communications (PIMRC)*, pages 939–944.

[Onalan et al., 2020] Onalan, A. G., Salik, E. D., and Coleri, S. (2020). Relay selection, scheduling, and power control in wireless-powered cooperative communication networks. *IEEE Transactions on Wireless Communications*, 19(11):7181–7195.

[Pal et al., 2019] Pal, S., Ebrahimi, E., Zulfiqar, A., Fu, Y., Zhang, V., Migacz, S., Nellans, D., and Gupta, P. (2019). Optimizing multi-gpu parallelization strategies for deep learning training. *IEEE Micro*, 39(5):91–101.

[Perera et al., 2018] Perera, T. D. P., Jayakody, D. N. K., Sharma, S. K., Chatzinotas, S., and Li, J. (2018). Simultaneous wireless information and power transfer (SWIPT): Recent advances and future challenges. *IEEE Communications Surveys & Tutorials*, 20(1):264–302.

[Qi et al., 2023] Qi, P., Zhou, X., Ding, Y., Zhang, Z., Zheng, S., and Li, Z. (2023). Fedbkd: Heterogenous federated learning via bidirectional knowledge distillation for modulation classification in iot-edge system. *IEEE Journal of Selected Topics in Signal Processing*, 17(1):189–204.

[IEEE 802.11 AMP TIG/SG, 2023] IEEE 802.11 AMP TIG/SG (2023). Technical report on support of amp iot devices in wlan. Technical report, IEEE.

[Sadi and Coleri Ergen, 2014] Sadi, Y. and Coleri Ergen, S. (2014). Minimum length scheduling with packet traffic demands in wireless ad hoc networks. *IEEE Transactions on Wireless Communications*, 13(7):3738–3751.

[Saif et al., 2021] Saif, A., Dimyati, K., Noordin, K. A., G C, D., Shah, N. S. M., Abdullah, Q., and Mohamad, M. (2021). An efficient energy harvesting and optimal clustering technique for sustainable postdisaster emergency communication systems. *IEEE Access*, 9:78188–78202.

[Salik et al., 2019] Salik, E. D., Gurur Onalan, A., and Ergen, S. C. (2019). Minimum length scheduling for power constrained harvest-then-transmit communication networks. In *2019 IEEE 30th Annual International Symposium on Personal, Indoor and Mobile Radio Communications (PIMRC)*, pages 1–6.

[Schiessl et al., 2015] Schiessl, S., Gross, J., and Al-Zubaidy, H. (2015). Delay analysis for wireless fading channels with finite blocklength channel coding. In *Proceedings of the 18th ACM International Conference on Modeling, Analysis and Simulation of Wireless and Mobile Systems*, MSWiM '15, page 13–22, New York, NY, USA. Association for Computing Machinery.

[Sengupta et al., 2018] Sengupta, A. S., Satpathy, S., Mohanty, S. P., Baral, D., and Bhattacharyya, B. K. (2018). Supercapacitors outperform conventional batteries [energy and security]. *IEEE Consumer Electronics Magazine*, 7(5):50–53.

[Seo et al., 2021] Seo, S., Arik, S., Yoon, J., Zhang, X., Sohn, K., and Pfister, T. (2021). Controlling neural networks with rule representations. In *Advances in Neural Information Processing Systems*, volume 34, pages 11196–11207. Curran Associates, Inc.

[Si et al., 2021] Si, G., Dou, Z., Lin, Y., and Wang, M. (2021). A relay selection algorithm in energy harvesting ad-hoc networks with interference constraints. In *2021 IEEE 94th Vehicular Technology Conference (VTC2021-Fall)*, pages 1–5.

[Su et al., 2019] Su, Y., Lu, X., Zhao, Y., Huang, L., and Du, X. (2019). Cooperative communications with relay selection based on deep reinforcement learning in wireless sensor networks. *IEEE Sensors Journal*, 19(20):9561–9569.

[Sui et al., 2018] Sui, D., Hu, F., Zhou, W., Shao, M., and Chen, M. (2018). Relay selection for radio frequency energy-harvesting wireless body area network with buffer. *IEEE Internet of Things Journal*, 5(2):1100–1107.

[Szegedy et al., 2015] Szegedy, C., Liu, W., Jia, Y., Sermanet, P., Reed, S., Anguelov, D., Erhan, D., Vanhoucke, V., and Rabinovich, A. (2015). Going deeper with convolutions. In *2015 IEEE Conference on Computer Vision and Pattern Recognition (CVPR)*, pages 1–9.

[Tang et al., 2021] Tang, H., Guo, J., Matthaiou, M., Wen, C.-K., and Jin, S. (2021). Knowledge-distillation-aided lightweight neural network for massive mimo csi feedback. In *2021 IEEE 94th Vehicular Technology Conference (VTC2021-Fall)*, pages 1–5.

[Tong et al., 2017] Tong, T., Li, G., Liu, X., and Gao, Q. (2017). Image super-resolution using dense skip connections. In *Proceedings of the IEEE International Conference on Computer Vision (ICCV)*.

[Trench, 2013] Trench, W. F. (2013). *Introduction to Real Analysis*. Faculty Authored and Edited Books & CDs.7.

[van Wyk and Bosman, 2019] van Wyk, G. J. and Bosman, A. S. (2019). Evolutionary neural architecture search for image restoration. In *2019 International Joint Conference on Neural Networks (IJCNN)*, pages 1–8.

[Vandendorpe et al., 2009] Vandendorpe, L., Louveaux, J., Oguz, O., and Zaidi, A. (2009). Rate-optimized power allocation for df-relayed ofdm transmission under sum and individual power constraints. *EURASIP Journal on Wireless Communications and Networking*, 2009(1):1–11.

[Varshney, 2008] Varshney, L. R. (2008). Transporting information and energy simultaneously. In *2008 IEEE International Symposium on Information Theory*. IEEE.

[Viswanathan and Mogensen, 2020] Viswanathan, H. and Mogensen, P. E. (2020). Communications in the 6g era. *IEEE Access*, 8:57063–57074.

[Vu et al., 2022] Vu, T.-H., Nguyen, T.-V., Nguyen, T.-T., and Kim, S. (2022). Performance analysis and deep learning design of wireless powered cognitive noma iot short-packet communications with imperfect csi and sic. *IEEE Internet of Things Journal*, 9(13):10464–10479.

[Wang et al., 2018] Wang, F., Guo, S., Yang, Y., and Xiao, B. (2018). Relay selection and power allocation for cooperative communication networks with energy harvesting. *IEEE Systems Journal*, 12(1):735–746.

[Wang et al., 2021] Wang, T., Wu, S., Wang, Z., Jiang, Y., Ma, T., and Yang, Z. (2021). A Multi-Featured Actor-Critic Relay Selection Scheme for Large-Scale Energy Harvesting WSNs. *IEEE Wireless Communications Letters*, 10(1).

[Xie et al., 2023a] Xie, J., Chang, Z., Guo, X., and Hämäläinen, T. (2023a). Energy efficient resource allocation for wireless powered uav wireless communication system with short packet. *IEEE Transactions on Green Communications and Networking*, 7(1):101–113.

[Xie et al., 2013] Xie, L., Shi, Y., Hou, Y. T., and Lou, A. (2013). Wireless power transfer and applications to sensor networks. *IEEE Wireless Communications*, 20(4):140–145.

[Xie et al., 2023b] Xie, M., Jia, X., Yin, J., Wang, Q., and Zhou, M. (2023b). Age of Information for Partial Earliest Relay Aided Short Packet Status Update with Energy Harvesting. *IEEE Transactions on Wireless Communications.*

[Yang et al., 2019] Yang, Y., Che, J., Deng, C., and Li, L. (2019). Sequential grid approach based support vector regression for short-term electric load forecasting. *Applied Energy*, 238:1010–1021.

[Yu et al., 2019] Yu, Z., Chi, K., Zheng, K., Li, Y., and Cheng, Z. (2019). Transmit power allocation of energy transmitters for throughput maximisation in wireless powered communication networks. *IET Communications*, 13(9):1200–1206.

[Zalinescu, 2002] Zalinescu, C. (2002). *Convex Analysis in General Vector Spaces*. World Scientific, River Edge, N.J.

[Zappone et al., 2019] Zappone, A., Di Renzo, M., Debbah, M., Lam, T. T., and Qian, X. (2019). Model-aided wireless artificial intelligence: Embedding expert knowledge in deep neural networks for wireless system optimization. *IEEE Vehicular Technology Magazine*, 14(3):60–69.

[Zhang et al., 2016] Zhang, D., Chen, Z., Zhou, H., Chen, L., and Shen, X. (2016). Energy-balanced cooperative transmission based on relay selection and power control in energy harvesting wireless sensor network. *Computer Networks*, 104:189 – 197.

[Zhang and Ho, 2013] Zhang, R. and Ho, C. K. (2013). MIMO broadcasting for simultaneous wireless information and power transfer. *IEEE Transactions on Wireless Communications*, 12(5):1989–2001.

[Zhang et al., 2020] Zhang, Z., Lu, Y., Huang, Y., and Zhang, P. (2020). Neural network-based relay selection in two-way swipt-enabled cognitive radio networks. *IEEE Transactions on Vehicular Technology*, 69(6):6264–6274.

[Zhao et al., 2022] Zhao, H., Xu, B., Wang, Q., Huang, H., and Zhang, X. (2022). Unsupervised learning for energy efficient power allocation in ultra-reliable and low-latency communications. In *2022 IEEE 96th Vehicular Technology Conference (VTC2022-Fall)*, pages 1–5.

[Zhao et al., 2016] Zhao, Y., Li, Q., Huang, L., Feng, S., Han, T., and Zhang, J. (2016). Wireless information and power transfer on cooperative multi-path relay channels. In *2016 IEEE/CIC International Conference on Communications in China (ICCC)*, pages 1–6.

[Zheng et al., 2016] Zheng, T., Gidlund, M., and Åkerberg, J. (2016). Wirarb: A new mac protocol for time critical industrial wireless sensor network applications. *IEEE Sensors Journal*, 16(7):2127–2139.

[Zheng et al., 2023] Zheng, Y., Hu, J., and Yang, K. (2023). SWIPT aided Co-operative Communications with Energy Harvesting based Selective-Decode-and-Forward Protocol: Benefiting from Channel Aging Effect. *IEEE Transactions on Green Communications and Networking*.

[Zheng et al., 2022] Zheng, Y., Lin, L., Zhang, T., Chen, H., Duan, Q., Xu, Y., and Wang, X. (2022). Enabling robust drl-driven networking systems via teacher-student learning. *IEEE Journal on Selected Areas in Communications*, 40(1):376–392.